THE

LONDON, EDINBURGH, AND DUBLIN

PHILOSOPHICAL MAGAZINE

AND

JOURNAL OF SCIENCE.

[SEVENTH SERIES.]

SUPPLEMENT, NOVEMBER 1937.

LXXVI. *The Diffraction of Electromagnetic Waves from an Electrical Point Source round a Finitely Conducting Sphere, with Applications to Radiotelegraphy and the Theory of the Rainbow* *.—Part II.

By BALTH. VAN DER POL *and* H. BREMMER, *Natuurkundig Laboratorium der N. V. Philips' Gloeilampenfabrieken, Eindhoven, Holland* †.

9. *The Secondary Field considered as the Superposition of an Infinity of Waves originating after* 1, 2, 3 . . . . *Reflections.*

IN Part I. of this paper the diffraction round a sphere of waves originating from a point source was considered starting with the harmonic series (1). Thereupon a transformation of this series was affected with the aid of a contour integral, resulting in a series which converges rather rapidly in the shadow region, while the convergence in the "lit" part of space is not appropriate for numerical evaluation. As in many physical applications a knowledge of the wave-field in the "lit" part of space is of importance, we now proceed to an entirely different attack on the problem; while again starting

* Part I. of the present paper appeared in the Phil. Mag. xxiv. p. 141 (July 1937).

† Communicated by the Authors.

with the rigorous series (1), the fundamental idea used here is to split up each of the terms of (1) into a geometrical series, after which the corresponding terms of these geometrical series are combined. This splitting-up process is based on the physical conception of radial waves being reflected several times between the surface and the centre of the sphere. Thereupon each of these new series of radial waves is written in the form of a multiple exponential integral. It next appears that the position of the saddle points of these integrals determines the geometrical points at the surface of the sphere, where a ray joining the point source and

Fig. 12.

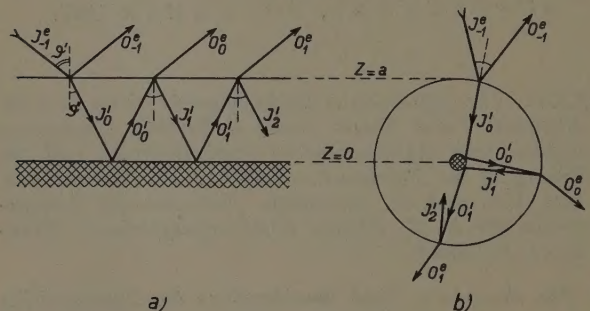

(*a*) infinite slab, (*b*) sphere, showing the different elementary waves.

the observer is refracted and reflected. Thus our saddle point treatment of wave functions appears to be identical with the application of Fermat's principle. The second order approximation of these integrals with the method of stationary phase yields the amplitude of these rays whose geometrical form was given by the above-mentioned saddle points. These rays correspond exactly with the classical geometrical ray treatment of the rainbow which originates from Descartes.

In order to illustrate the fundamental idea of the splitting up of the wave function in successively refracted and reflected waves we treat in this paragraph an analogous simple problem.

Consider the problem with two plane boundaries represented by fig. 12 *a*, where an electrical vertical dipole is situated at $z=b$, $\rho=0$ in the medium 1 with propagation constant k_1. Medium 2, with propagation constant k_2, consists of an infinite slab with *plane* boundaries at $z=a$ and $z=0$. Below $z=0$ we assume a third medium of infinite conductivity ($k_3=\infty$), so that all waves penetrating into the second medium are totally reflected at the boundary surface $z=0$. Later on we shall see that in the spherical analogy (fig. 12 *b*) we again find a total reflexion, but there against the centre of the sphere. This plane problem is easily solved with the well-known integral method of Sommerfeld, and leads, for a primary field $e^{ik_1R}/(ik_1R)$, to a secondary field in the first medium, given by

$$\Pi_{sec}=\frac{1}{ik_1}\cdot\int_0^\infty \frac{\lambda\, d\lambda}{\sqrt{\lambda^2-k_1^2}}\cdot R_\rho(\lambda)\cdot J_0(\lambda\rho)\cdot e^{-\sqrt{\lambda^2-k_1^2}(z+b-2a)}, \quad . \ . \ . \quad (60)$$

where

$$R_\rho=\frac{\frac{\sqrt{\lambda^2-k_1^2}}{k_1^2}-\frac{\sqrt{\lambda^2-k_2^2}}{k_2^2}\cdot Tgh(\sqrt{\lambda^2-k_2^2}a)}{\frac{\sqrt{\lambda^2-k_1^2}}{k_1^2}+\frac{\sqrt{\lambda^2-k_2^2}}{k_2^2}\cdot Tgh(\sqrt{\lambda^2-k_2^2}a)}, \quad (61)$$

and ρ is the horizontal distance from point source to receiver.

If, with Sommerfeld and Weyl, (60) is considered as the superposition of plane waves, λ has the meaning of $k_1 \sin \vartheta'$, where ϑ' is the angle a particular plane wave makes with the vertical. The fundamental idea of this paragraph is to write (61) as the geometrical series

$$R_\rho=R(\lambda)+\sum_{K=0}^{\infty}\{1+R(\lambda)\}\cdot R(\lambda)^K\{1-R(\lambda)\}\cdot e^{-2(K+1)a\sqrt{\lambda^2-k_2^2}}, \quad (62)$$

so that, when inserted into (60), the secondary field in the first medium becomes the sum

$$\Pi_{sec}=O_{-1}^e+O_0^e+O_1^e+O_2^e+O_3^e+\ldots, \quad . \ . \quad (63)$$

where all the O^e_K mean outgoing waves in the first medium, represented by *

$$\left\{\begin{aligned} O^e_{-1} &= \frac{1}{ik_1}\cdot\int_0^\alpha \frac{\lambda\, d\lambda}{\sqrt{\lambda^2-k_1^2}}\cdot R(\lambda)\cdot J_0(\lambda\rho)\cdot e^{-\sqrt{\lambda^2-k_1^2}(z+b-2a)}. \\ &\qquad\qquad\qquad\qquad\qquad\qquad\qquad\qquad\qquad\qquad \text{. . .} \quad (64\,a) \\ O^e_K &= \frac{1}{ik_1}\cdot\int_0^\infty \frac{\lambda\, d\lambda}{\sqrt{\lambda^2-k_1^2}}\cdot\{1+R(\lambda)\}\cdot R(\lambda)^K\cdot\{1-R(\lambda)\} \\ &\quad \cdot J_0(\lambda\rho)\cdot e^{-\sqrt{\lambda^2-k_1^2}(z+b-2a)-2(K+1)a\sqrt{\lambda^2-k_2^2}}, \quad (K\geqq 0), \quad (64\,b) \end{aligned}\right.$$

and where R (λ) has the usual form

$$R(\lambda) = \frac{k_2^2\sqrt{\lambda^2-k_1^2}-k_1^2\sqrt{\lambda^2-k_2^2}}{k_2^2\sqrt{\lambda^2-k_1^2}+k_1^2\sqrt{\lambda^2-k_2^2}}, \quad \text{. . .} \quad (65)$$

meaning physically the Fresnel reflexion coefficient for the waves incident at an angle ϑ', *cf.* (21). The physical meaning of (64 *b*) becomes at once clear if in the integral we put

$$\lambda = k_1 \sin\vartheta' = k_2 \sin\vartheta'',$$

so that we obtain

$$O^e_K = \int_0^{\pi/2-i\infty} \sin\vartheta'\, d\vartheta'\cdot\{1+R(\lambda)\}\cdot R(\lambda)^K\cdot\{1-R(\lambda)\} \cdot J_0(\lambda\rho)\cdot e^{ik_1\cos\vartheta'(z+b-2a)+2ik_2(K+1)a\cos\vartheta''}. \quad (66)$$

The form of (66) is easily interpreted as an outgoing wave in the first medium (see fig. 12 *a*), originating from the primary incident wave I^e_{-1} in the first medium, which first is refracted as the ingoing wave I^i_0 in the second medium, this being afterwards totally reflected at $z=0$, thus becoming O^i_0; this outgoing wave, when reaching $z=a$, is split up in the refracted wave O^e_0 in the first medium and the reflected ingoing wave I^i_1 in the second medium. This process is repeated till finally we obtain O^e_K as the outgoing wave in the first medium, resulting from waves in the second medium which have been reflected up and down in the second medium with K reflexions at $z=a$ and K+1 at $z=0$. It will be clear that the total secondary field Π_{sec}, in accordance with (63), is obtained by superposing all the outgoing waves characterized by K$=-1, 0, +1, +2 \ldots$ etc. in the

* For the symmetry of the notation we give the incident and first reflected wave the suffix -1.

first medium. The notations are chosen such that O and I relate resp. to the outgoing and ingoing waves, whereas the index e or i denotes the first or second medium.

The above physical consideration now makes the form of (66) quite obvious, because the integrand contains the factors

$$\{1+R(\lambda)\}.R(\lambda)^K.\{1-R(\lambda)\}$$

and $$e^{2ik_2(K+1)a\cos\vartheta''},$$

the first of which represents the attenuation $1+R(\lambda)$ at the first refraction, the attenuations $R(\lambda)^K$ due to the K reflexions at $z=a$, and the attenuation $1-R(\lambda)$ at the final refraction into the first medium.

The second factor represents the phase retardation and, for complex k_2, the attenuation due to the fact that the wave has travelled $K+1$ times up and down in the second medium, the form of this factor being quite similar to that obtained in the derivation of the phase retardation in Bragg's well-known formula of crystal reflexion.

10. *The "Spherical Reflexion Coefficients."*

In the last paragraph when we split up the secondary field into an infinity of components we were naturally lead to introduce the ordinary Fresnel reflexion coefficient which belongs to the reflexion of a plane wave against a plane boundary. Before considering in more detail the analogous splitting up of the waves in our spherical problem we shall have to investigate first the extension of the simple Fresnel reflexion coefficient for the reflexion of an incident spherical wave

$$\zeta_n^{(2}(k_1r).P_n(\cos\vartheta)$$

against the concentric sphere $r=a$ separating the first medium (k_1) from the second medium (k_2).

We can write the reflected wave in the first medium as

$$R_{11}.\zeta_n^{(2)}(k_1a).\frac{\zeta_n^{(1)}(k_1r)}{\zeta_n^{(1)}(k_1a)}.P_n(\cos\vartheta), \quad . \quad . \quad (67a)$$

and the refracted wave in the second medium as

$$R_{12}.\zeta_n^{(2)}(k_1a).\frac{\zeta_n^{(2)}(k_2r)}{\zeta_n^{(2)}(k_2a)}.P_n(\cos\vartheta). \quad . \quad . \quad (67b)$$

These forms have been chosen such that, *e. g.*, R_{11} means the ratio of the amplitudes of the reflected and incident waves at $r=a$, and similarly for R_{12}.

The boundary conditions, $\frac{\partial}{\partial r}(r\Pi)$ and $k^2\Pi$ continuous at $r=a$, now fully determine the "*spherical reflexion and refraction coefficients*" R_{11} and R_{12}, which in our case, where we assume the electric field to be in the plane of incidence (electrical dipole), become

$$R_{11}=\frac{-\left[\frac{1}{x}\frac{d}{dx}\log\{x\zeta_n^{(2)}(x)\}\right]_{x=k_1a}+\left[\frac{1}{x}\frac{d}{dx}\log\{x\zeta_n^{(2)}(x)\}\right]_{x=k_2a}}{\left[\frac{1}{x}\frac{d}{dx}\log\{x\zeta_n^{(1)}(x)\}\right]_{x=k_1a}-\left[\frac{1}{x}\frac{d}{dx}\log\{x\zeta_n^{(2)}(x)\}\right]_{x=k_2a}}, \quad . \quad . \quad . \quad (68a)$$

$$R_{12}=\frac{k_1^2}{k_2^2}(1+R_{11}). \quad . \quad . \quad . \quad . \quad . \quad . \quad . \quad . \quad . \quad (68b)$$

It is of interest to contrast the more physical factor R_{11}, which contains ζ functions only, with the formally used R_n of (2), which contains both ζ and ψ functions.

11. *The Splitting-up of the Secondary Field into an Infinity of Spherical Waves originating after* 1, 2, 3 . . . *Reflexions at the Centre and the Surface of the Sphere.*

After having derived the ideas of the spherical reflexion and refraction coefficients we are now able to interpret the spherical case as an analogue of the plane problem of § 9. To this end we follow again the waves on their courses. According to (3 *b*) the primary field for $r<b$ contains the standing waves $\psi_n(k_1r)P_n(\cos\vartheta)$. As

$$\psi_n(k_1r)=\tfrac{1}{2}\zeta_n^{(1)}(k_1r)+\tfrac{1}{2}\zeta_n^{(2)}(k_1r),$$

we can consider the primary field as containing both outgoing $\zeta^{(1)}$ and ingoing $\zeta^{(2)}$ waves. The outgoing part will be presently left aside. The ingoing part is given by

$$I_{-1}^e=\tfrac{1}{2}\sum_{n=0}^{\infty}(2n+1).\zeta_n^{(1)}(k_1b).\zeta_n^{(2)}(k_1r).P_n(\cos\vartheta).$$

As explained in § 10 each of the components, say $\zeta_n^{(2)}(k_1r)P_n(\cos\vartheta)$, is first at $r=a$ split up into a reflected

wave in the first medium and a refracted wave in the second medium, with the reflexion and refraction coefficients R_{11} and R_{12} resp., thus, after summation over n, giving rise to the waves O^e_{-1} in the first medium and I^i_0 in the second (see fig. 12 *b*). Each of the components of the latter, say

$$\tfrac{1}{2}(2n+1).R_{12}.\zeta_n^{(1)}(k_1 b)\zeta_n^{(2)}(k_1 a).\frac{\zeta_n^{(2)}(k_2 r)}{\zeta_n^{(2)}(k_2 a)}.P_n(\cos\vartheta),$$

would, however, cause a singularity at $r=0$, due to the factor $\zeta_n^{(2)}(k_2 r)$, which can only be compensated by an outgoing wave

$$\tfrac{1}{2}(2n+1).R_{12}.\zeta_n^{(1)}(k_1 b)\zeta_n^{(2)}(k_1 a).\frac{\zeta_n^{(1)}(k_2 r)}{\zeta_n^{(2)}(k_2 a)}.P_n(\cos\vartheta),$$

having the same amplitude. This fact can be interpreted as a total reflexion of the ingoing wave I^i_0 against an infinitely small sphere at the centre. This is, moreover, confirmed by the fact that the limit for $a=0$ of the spherical reflexion coefficient (68 *a*) becomes unity independently of the values of k_1 and k_2. Hence it can be said that the incident wave in the sphere is totally reflected against its centre analogous to the reflexion against the plane $z=0$ of the plane problem of § 9.

The summation over n of these totally reflected waves results in the outgoing wave O^i_0, but still being in the second medium. Following this wave further, it will arrive at the inside of the boundary $r=a$, where it will be divided into an ingoing reflected wave I^i_1 in the second medium (see fig. 12 *b*) and an outgoing refracted wave O^e_0 in the first medium, where it has to be noted that now this reflexion and refraction occur with the factors R_{22} and R_{21}, derivable from R_{11} and R_{12} by interchanging k_1 and k_2. This process repeats itself indefinitely in a fully analogous way as described in the plane problem of § 9 (compare fig. 12 *a* and fig. 12 *b*); therefore we have chosen the notations for the different waves quite the same as in § 9.

We thus obtain instead of (63) and (64) the following final formulæ:

for the total field in the first medium

$$\Pi_{\text{tot}} = I^e_{-1}+O^e_{-1}+O_0{}^e+O_1{}^e+O_2{}^e+O_3{}^e+\ldots\ (r>a), \quad (69\,a)$$

and similarly for the total field in the second medium

$$\Pi_{\text{tot}} = \mathrm{I}_0{}^i + \mathrm{O}_0{}^i + \mathrm{I}_1{}^i + \mathrm{O}_1{}^i + \mathrm{I}_2{}^i + \mathrm{O}_2{}^i + \mathrm{I}_3{}^i + \mathrm{O}_3{}^i + \ldots (r<a), \quad \ldots \quad (69\,b)$$

where

$$\mathrm{I}^e_{-1} = \begin{cases} \frac{1}{2}\sum_{n=0}^{\infty}(2n+1)\zeta_n^{(2)}(k_1 b)\zeta_n^{(1)}(k_1 r)\mathrm{P}_n(\cos\vartheta), & (r>b), \\ \qquad \ldots \quad (70\,a) \\ \frac{1}{2}\sum_{n=0}^{\infty}(2n+1)\zeta_n^{(1)}(k_1 b)\zeta_n^{(2)}(k_1 r)\mathrm{P}_n(\cos\vartheta), & (r<b), \\ \qquad \ldots \quad (70\,b) \end{cases}$$

$$\mathrm{O}^e_{-1} = \tfrac{1}{2}\sum_{u=0}^{\infty}(2n+1)\mathrm{R}_{11}\zeta_n^{(1}(k_1 b)\zeta_n^{(2)}(k_1 a)\cdot\frac{\zeta_n^{(1)}(k_1 r)}{\zeta_n^{(1)}(k_1 a)}\cdot\mathrm{P}_n(\cos\vartheta), \quad \ldots \quad (70\,c)$$

$$\mathrm{O}^e_{\mathrm{K}} = \tfrac{1}{2}\sum_{n=0}^{\infty}(2n+1)\mathrm{R}_{12}\mathrm{R}^{\mathrm{K}}_{22}\mathrm{R}_{21}\cdot\zeta_n^{(1)}(k_1 b)\zeta_n^{(2)}(k_1 a) \cdot\left\{\frac{\zeta_n^{(1)}(k_2 a)}{\zeta_n^{(2)}(k_2 a)}\right\}^{\mathrm{K}+1}\cdot\frac{\zeta_n^{(1)}(k_1 r)}{\zeta_n^{(1)}(k_1 a)}\cdot\mathrm{P}_n(\cos\vartheta), \quad (\mathrm{K}\geqq 0), \quad (70\,d)$$

$$\mathrm{I}^i_{\mathrm{K}} = \tfrac{1}{2}\sum_{n=0}^{\infty}(2n+1)\mathrm{R}_{12}\mathrm{R}^{\mathrm{K}}_{22}\cdot\zeta_n^{(1)}(k_1 b)\zeta_n^{(2)}(k_1 a) \cdot\left\{\frac{\zeta_n^{(1)}(k_2 a)}{\zeta_n^{(2)}(k_2 a)}\right\}^{\mathrm{K}}\cdot\frac{\zeta_n^{(2)}(k_2 r)}{\zeta_n^{(2)}(k_2 a)}\cdot\mathrm{P}_n(\cos\vartheta), \quad (\mathrm{K}\geqq 0), \quad (70\,e)$$

$$\mathrm{O}^i_{\mathrm{K}} = \tfrac{1}{2}\sum_{n=0}^{\infty}(2n+1)\mathrm{R}_{12}\mathrm{R}^{\mathrm{K}}_{22}\cdot\zeta_n^{(1)}(k_1 b)\zeta_n^{(2)}(k_1 a) \cdot\left\{\frac{\zeta_n^{(1)}(k_2 a)}{\zeta_n^{(2)}(k_2 a)}\right\}^{\mathrm{K}}\cdot\frac{\zeta_n^{(1)}(k_2 r)}{\zeta_n^{(2)}(k_2 a)}\cdot\mathrm{P}_n(\cos\vartheta), \quad (\mathrm{K}\geqq 0). \quad (70\,f)$$

In deriving these formulæ we started, according to (70 *b*), with the ingoing part only of the primary field. It can, however, easily be shown that, in order to satisfy the boundary conditions, the other, outgoing, part of the primary field must be accompanied by a secondary field which just cancels it, so that our solution (70) gives the total field, satisfying the boundary conditions and having as only singularity the point source at Q.

It may be finally remarked that the physical arguments used in this section are equivalent to the development of the denominator of the general R_n of (2) into a geometrical

series, just as in the plane case of § 9. Thus we get instead of (62) for R_n:

$$R_n = -\tfrac{1}{2}\frac{\zeta_n^{(1)}(k_1a)}{\psi_n(k_1a)} + \tfrac{1}{2}\frac{\zeta_n^{(2)}(k_1a)}{\psi_n(k_1a)} \cdot R_{11} + \tfrac{1}{2}\frac{\zeta_n^{(2)}(k_1a)}{\psi_n(k_1a)} \cdot \sum_{K=0}^{\infty} (1+R_{11})R_{22}^K(1+R_{22}) \cdot \left\{\frac{\zeta_n^{(1)}(k_2a)}{\zeta_n^{(2)}(k_2a)}\right\}^{K+1}. \quad (71)$$

As in § 9, we here again encounter the two factors

$$(1+R_{11})R_{22}^K(1+R_{22}) = R_{12}R_{22}^K R_{21},$$

representing the attenuations caused by the first refraction, the K reflexions, and the last refraction, while the factor

$$\left\{\frac{\zeta_n^{(1)}(k_2a)}{\zeta_n^{(2)}(k_2a)}\right\}^{K+1}$$

represents the phase retardation and attenuation as a result of the waves having travelled K+1 times to and fro between the centre and the surface of the sphere.

It is of importance to note that the factors

$$\zeta_n^{(1)}(k_2a)/\zeta_n^{(2)}(k_2a)$$

tend towards zero for both $k_2 \to \infty$ and $a \to \infty$, proving the fact that (*a*) for a totally reflecting sphere of finite size and (*b*) for a finitely conducting sphere but of infinite radius, and therefore tending to a plane, no reflected waves from the inside will be present. Limiting ourselves to the latter case ($a \to \infty$) we note that, even with the slightest absorption, [$Jm(k_2a) \to 0$], only I^e_{-1} and O^e_{-1} are left as components outside the sphere. The part O^e_{-1}, treated after the method of § 5, leads to the same result as obtained there, viz., the classical expression for the plane case in the form of the λ integral for Π_{sec}.

12. *Reduction of the Subsidiary Waves* O^e_K *to a Sum of Residues.*

In § 3 formula (7) it was shown, following Watson, that Π_{tot} could be transformed into the sum of a closed contour integral and an open line integral along the imaginary axis. This inhomogeneous character of the result was due to the fact that the integrand was not an even function of $n-\frac{1}{2}$. However, the splitting up of Π_{tot} into an infinity of subsidiary waves O'_K (as affected

in § 11) enables us to write each of these waves as a closed contour integral only, encircling poles of the order $K+2$, so that the total field thus becomes rigorously a sum of residues, without any additional open line integral.

This transformation is based on the following consideration. As each of the subsidiary waves O_K^e (as given by (70 *d*)) is represented by a sum over n, n being integral, and as we want to transform the sum into an integral with integrand, which, apart from the factor $2n+1$, is even in $n-\frac{1}{2}$, we are at liberty to continue the functions of n for non-integral values of this variable in different ways before we transform the sum into an integral. Incidentally the result thus obtained expresses each of the subsidiary waves O_K^e itself again as an infinite sum of elementary waves $O_{K,m}^e$, where m denotes the number of times each of these waves has travelled round the sphere (compare § 3, equation (9)).

In order to effect this plan we first notice the identity

$$\{\zeta_n^{(1)}(k_2a)\}^{K+1}.P_n(\cos\vartheta) = \{\zeta_n^{(2)}(k_2ae^{-i\pi})\}^{K+1} .P_n\{\cos(\vartheta-K\pi-\pi)\},$$

with which, *e. g.*, (70 *d*) can be written

$$O_K^e = \sum_{n=0}^{\infty}(2n+1).g(n).P_n\{\cos(\vartheta-K\pi-\pi)\}, \quad (72)$$

with

$$g(n) = \tfrac{1}{2}R_{12}R_{22}^K R_{21}.\zeta_n^{(1)}(k_1b)\zeta_n^{(2)}(k_1a) \left\{\frac{\zeta_n^{(2)}(k_2ae^{-i\pi})}{\zeta_n^{(2)}(k_2a)}\right\}^{K+1} \cdot\frac{\zeta_n^{(1)}(k_1r)}{\zeta_n^{(1)}(k_1a)}.$$

As a consequence of the relation

$$\overset{(1)}{\zeta}{}^{(2)}_{-n-1/2}(z) = e^{\pm in\pi}.\overset{(1)}{\zeta}{}^{(2)}_{n-1/2}(z)$$

it follows that $g(n-\frac{1}{2})$ is built up of factors each even in n. This is also true for the "spherical reflexion coefficients" such as R_{12}, whereas the formerly used coefficient R (equation (2)) is *not* an even function of n.

The fact that $g(n-\frac{1}{2})$ is even in n enables us, following the method of § 3, to transform the sum (72) first to the integral

$$O_K^e = \frac{1}{i}\int_{-\infty+i\epsilon}^{\infty+i\epsilon}\frac{n\,dn}{\cos(n\pi)}.g(n-\tfrac{1}{2}).P_{n-1/2}\{\cos(\vartheta-K\pi-2\pi)\}. \quad . \quad . \quad . \quad (73)$$

As, further, along the whole path of integration $Jm(n)>0$, we may develop the factor $\{\cos(n\pi)\}^{-1}$ as

$$\frac{1}{\cos(n\pi)} = 2\sum_{m=0}^{\infty}(-1)^m . e^{in\pi(2m+1)},$$

so that (73) becomes

$$O^e_K = \sum_{m=0}^{\infty} O^e_{K,m}, \quad . \quad . \quad . \quad . \quad . \quad (74)$$

where

$$O^e_{K,m} = \frac{(-1)^m}{i}\int_{-\infty+i\varepsilon}^{\infty+i\varepsilon} n\,dn\, e^{in\pi(2m+1)} . R_{12}R^K_{22}R_{21} \cdot \zeta^{(1)}_{n-1/2}(k_1b)\zeta^{(2)}_{n-1/2}(k_1a) . \left\{\frac{\zeta^{(2)}_{n-1/2}(k_2ae^{-i\pi})}{\zeta^{(2)}_{n-1/2}(k_2a)}\right\}^{K+1} \cdot \frac{\zeta^{(1)}_{n-1/2}(k_1r)}{\zeta^{(1)}_{n-1/2}(k_1a)} . P_{n-1/2}\{\cos(\vartheta - K\pi)\}. \quad . \quad . \quad (75)$$

This integral (75) can be closed by a half-circle of infinite radius above the real axis, so that its value can be represented by the sum of residues of poles n_s of the order K+2. These poles are the zeros of $M_{n-\frac{1}{2}}=0$, where

$$M_n = \left[\frac{1}{x}\cdot\frac{d}{dx}\log\{x\zeta^{(1)}_n(x)\}\right]_{x=k_1a} - \left[\frac{1}{y}\cdot\frac{d}{dy}\log\{y\zeta^{(2)}_n(y)\}\right]_{y=k_2a}, \quad (76)$$

which occurs in (68 *b*) and is only slightly different from the expression N_n defined by (6). Next making use of the asymptotic formula (12), each of the residues is seen to have as exponential part the factor

$$e^{in_s(\vartheta+2m\pi)},$$

showing, finally, that each of the terms $O^e_{K,m}$ represents an elementary wave which has been *reflected* K *times*, *refracted* 2 *times*, *and diffracted m times* (having encircled the sphere *m* times) before arriving at the receiver.

In considering the theory of the rainbow the most important elementary waves are $O^0_{1,0}$ and $O^0_{2,0}$, whereas in the *radio case* the elementary waves $I^e_{1,0}$ and $O^e_{-1,0}$ form the essential part. A further analysis shows that the

sum $I^e_{-1,0} + O^e_{-1,0}$ can also be transformed to a sum of residues of poles of order unity, yielding

$$I^e_{-1,0} + O^e_{-1,0} = \frac{4\pi i}{(k_1 a)^3} \cdot \sum_{s=0}^{\infty} \frac{n_s \cdot e^{i n_s \pi}}{\left(\frac{\partial M_{n-1/2}}{\partial n}\right)_{n=n_s}}$$

$$\cdot \frac{\zeta^{(1)}_{n_s-1/2}(k_1 b)\zeta^{(1)}_{n_s-1/2}(k_1 r)}{\{\zeta^{(1)}_{n_s-1/2}(k_1 a)\}^2} \cdot P_{n_s-1/2}\{\cos(\pi - \vartheta)\}, \quad (77,$$

and it is on this expression that we will later on base our numerical calculations in the radio case (see § 17).

13. *Transformation of the Elementary Wave* $O^e_{K,m}$ *into a* $(2K+8)$*-dimensional Exponential Integral, the Saddle Point of which determining a* K*-times internally reflected Goemetrical Optical Ray.*

In this paragraph we will develop a totally different aspect of our problem, leaving for the present the residue method. Here we will transform the general elementary wave $O^e_{K,m}$ into a more dimensional exponential integral. It will be seen that the position of its saddle point determines at once the only geometrical optical ray connecting the transmitter and receiver, which has been reflected internally K times. Moreover, a further development of the exponent round the saddle point provides us with an expression for the amplitudes of this ray. Performing this transformation for all values of K we thus succeed in writing the complete solution of our problem as the sum of an infinite number of geometrical optical rays.

In order to affect this transformation of (75) we first note that the denominator only contains $\zeta^{(1)}$ and $\zeta^{(2)}$ functions, each of which possesses an exponential character which we can annul by multiplying the nominator and denominator each by

$$\zeta^{(2)}_{n-1/2}(k_1 a) \cdot \{\zeta^{(1)}_{n-1/2}(k_2 a)\}^{K+1},$$

resulting in a denominator which only contains factors of the form $\zeta^{(1)}_{n-1/2}(x) \cdot \zeta^{(2)}_{n-1/2}(x)$, where the exponential character has disappeared. As the same was already true as regards the factors R_{12} R^K_{22} R_{21}, we are now prepared to transform each of the factors remaining

in the nominator into an exponential integral by the aid of the fundamental expressions

$$\zeta^{(1)}_{n-1/2}(z) = \frac{1}{\sqrt{2\pi z}} \cdot \int_{-\eta+i\infty}^{\eta-i\infty} e^{iz\cos\tau + in(\tau-\pi/2)}\, d\tau, \quad (78\,a)$$

$$\zeta^{(2)}_{n-1/2}(z) = -\frac{1}{\sqrt{2\pi z}} \cdot \int_{\pi-\eta+i\infty}^{\eta-\pi-i\infty} e^{-iz\cos\tau - in(\tau-\pi/2)}\, d\tau, \quad (78\,b)$$

where $-\arg z < \eta < \pi - \arg z$.
Writing finally

$$P_{n-1/2}\{\cos(\vartheta - K\pi)\} = \frac{1}{2\pi} \cdot \int_{-\pi}^{\pi} e^{(n-1/2)\log\{\cos(\vartheta-K\pi)+i\sin(\vartheta-K\pi)\cos\phi\}}\, d\phi,$$

we obtain, instead of (75),

$$O^{e}_{K,m} = \frac{(-1)^m}{8\pi^2 i k_1^2 a \sqrt{br}(2\pi i k_2 a)^{K+1}} \cdot \int_{-\infty}^{\infty} dn\, A(n) \cdot \int_{-\pi}^{\pi} d\phi \int d\tau_1 \ldots d\tau_{2K+6} \cdot e^{f^{e}_{K,m}}, \quad (79)$$

where the non-exponential factor $A(n)$ is given by

$$A(n) = \frac{n \cdot R_{12} R_{22}^{K} R_{21}}{\zeta^{(1)}_{n-1/2}(k_1 a)\zeta^{(2)}_{n-1/2}(k_1 a) \cdot \{\zeta^{(1)}_{n-1/2}(k_2 a)\zeta^{(2)}_{n-1/2}(k_2 a)\}^{K+1}},$$

while the exponential factor exp. $(f^{e}_{K,m})$ has as exponent

$$\begin{aligned} f^{e}_{K,m} = {} & ik_1 b\cos\tau_1 - ik_1 a\cos\tau_2 + ik_2 a \sum_{V=3}^{2K+4} \cos\tau_V \\ & - ik_1 a\cos\tau_{2K+5} + ik_1 r\cos\tau_{2K+6} \\ & + in\left\{\tau_1 - \tau_2 + \sum_{V=3}^{2K+4} \tau_V - \tau_{2K+5} + \tau_{2K+6} + (2m+1)\pi\right\} \\ & + (n-\tfrac{1}{2})\log\{\cos(\vartheta - K\pi) + i\sin(\vartheta - K\pi)\cos\phi\}. \end{aligned} \quad (80)$$

Further, the paths of integration of τ_1, $\tau_3 \ldots \tau_{2K+4}$, τ_{2K+6} are as in (78 *a*), while those of τ_2 and τ_{2K+5} are as in (78 *b*).

The physical character of (79) becomes at once apparent if we consider the position of the multi-dimensional saddle point of exp. $(f^{e}_{K,m})$, which is given by

$$\frac{\partial f}{\partial \tau_1} = \frac{\partial f}{\partial \tau_2} = \ldots = \frac{\partial f}{\partial \tau_{2K+6}} = \frac{\partial f}{\partial n} = \frac{\partial f}{\partial \phi} = 0,$$

the solutions of which are

$$\begin{cases} n=k_1 b \sin\tau_1=k_1 a \sin\tau_2=k_2 a \sin\tau_3=\ldots=k_2 a \sin\tau_{2K+} \\ \qquad\qquad =k_1 a \sin\tau_{2K+5}=k_1 r \sin\tau_{2K+6}, \quad (81\,a) \\ (\tau_2-\tau_1)+\sum_{A=3}^{2K+4}(\tfrac{1}{2}\pi-\tau_\nu)+(\tau_{2K+5}-\tau_{2K+6})=\vartheta+2m\pi, \\ \qquad\qquad \ldots \quad (81\,b) \\ \phi=0. \quad \ldots \quad (81\,c) \end{cases}$$

If we now identify the variables τ *with the angles as shown in the schematic fig.* 13, *which we consider to lie in the plane* $\phi=0$, *the expressions* (81) *determine exactly the geometrical-optical broken ray, which first leaves the transmitter at* Q, *is thereupon refracted at* A_1, *and next internally reflected at* $A_2, \ldots A_{K+1}$, *and which finally leaves the sphere as the refracted ray* $A_{K+2}P$. That this is the case follows immediately from the fact that (81 *a*) represents nothing but Snellius's laws for each reflexion and refraction, and (81 *b*) expresses that the total angular deviation of the ray as measured at the centre O is the sum of the angles $(\tau_2-\tau_1)$, $(\frac{1}{2}\pi-\tau_2)$, etc.

Having thus determined by the position of the saddle points the geometrical optical rays, the intensity of these rays follows from an approximate evaluation of the integrals (79), but before we proceed we first insert a short consideration on the physical meaning of the first, second, third, and fourth order approximations of integrals of the type of (79).

14. *The Physical Meaning of Approximations of Different Order of Saddle Point Integrals.*

A complex exponential integral,

$$\int e^{f(z)}\,dz, \quad \ldots \quad (82)$$

can often be approximated, as already considered, by first finding the position of the saddle point z_0, determined by $f'(z_0)=0$. The path of integration may then often be chosen in one of two ways, determined by

(*a*) $\mathrm{Im}\{f(z)\}=\mathrm{Im}\{f(z_0)\}$, (steepest descend, Debye, Watson);

(*b*) $\mathrm{Re}\{f(z)\}=\mathrm{Re}\{f(z_0)\}$, (stationary phase, Kelvin).

In both cases the main contribution to the integral is furnished by the immediate neighbourhood of the saddle point z_0. In case (a) this follows from the fact

Fig. 13.

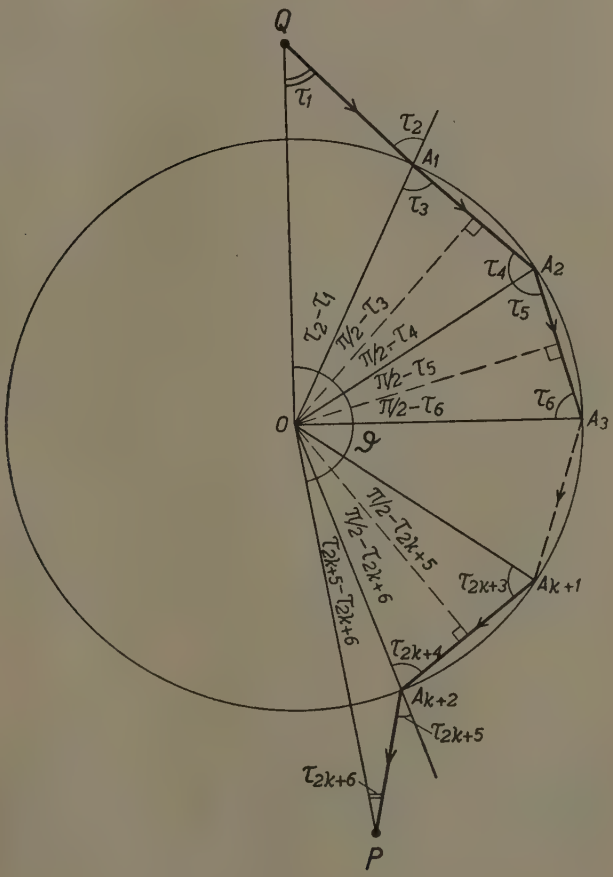

The geometrical optical ray joining Q and P.

that the *modulus* of the integrand most rapidly decreases as we leave z_0, while in case (b) the phase changes more and more rapidly as we leave z_0, causing a cancellation

of the contribution to the integral by the parts of the path far away from z_0 *.

Developing further in (82) $f(z)$ as

$$\int e^{f(z)}\,dz = \int dz\; e^{f(z_0)+\frac{(z-z_0)^2}{2!}f''(z_0)+\frac{(z-z_0)^3}{3!}f'''(z_0)+\frac{(z-z_0)^4}{4!}f^{IV}(z_0)\ldots},$$

we may get a first, second, third, and fourth approximation to the integral by retaining of the exponential series one, two, three or four terms resp. only.

Integrals of the type (82) often occur in diffraction problems. When they correspond to two-dimensional or three-dimensional space, the latter with axial symmetry, $f(z)$ depends not only upon the complex variable z but also on two spatial coordinates x and y. In this case the *first* approximation diverges for all values of x and y when, as in our problem, the limits of integration extend towards infinity. However, this first approximation converges when the limits are finite, and is then usually called the Fraunhofer approximation.

The *second* approximation to (82) leads to *Fresnel integrals*, whose physical interpretation is beautifully illustrated by the well-known *Cornu-spirals*. However, this second approximation may also diverge, viz., in the case when $f''(z_0)=0$. This equation, considered as a function of x and y, determines a curve—the caustic, the envelope of the rays —where therefore this approximation tends to infinity, as will further be shown in the next paragraph.

Considering next the *third* approximation, which leads to Airy's integrals, having the form

$$\int e^{-iz^3+i\alpha z}\,dz,$$

we observe that they may diverge if simultaneously we have $f''(z_0)=f'''(z_0)=0$, being two equations in x and y, and therefore determining isolated points in space only. These points are the cusps of the caustic, *i. e.*, the foci.

Finally, the *fourth* approximation would only diverge if simultaneously we have $f''(z_0)=f'''(z_0)=f^{IV}(z_0)=0$, which in physical problems would lead to three equations in the two variables x and y, which in general are contradictory.

* For a further treatment of these questions we refer to the important paper by L. Brillouin, *Ann. Ec. Norm.* (2) xxxiii., Jan. 1916. See also Van der Corput, 'Compositio mathematica,' i. pp. 15–38 (1934) and iii. pp. 328–372 (1936); J. Bijl, Dissertation, Groningen, 1937.

The multi-dimensional integrals (79) occurring in our problem are a more-dimensional extension of the integral of the type (82). Also in this case we can consider the first, second, third . . . approximations as defined above, and they also diverge in a smaller region of the space coordinates the higher the order of approximation. Therefore a higher order approximation is necessary the nearer the caustic we wish to investigate the field. Especially in the case of the rainbow, for which at infinity the minimum of deviation coincides with the caustic, and as appreciable light is only to be found near this minimum we are forced to consider the third approximation (see § 16). Also in the radio case, between the transmitter and its horizon—at which latter point we reach the caustic—our second approximation remains finite only to diverge at the horizon itself.

In the next paragraphs we shall consider in more detail the evaluation of the second and third approximations for the integrals of the form (79). We saw already that they represent rays, and our next task therefore is to find their intensities.

15. *The Second-Order Approximation to the Intensities of the Rays.*

Our integrals of the form (79) being of a multi-dimensional type, we first give a short *résumé* of their second-order approximation. We therefore consider

$$\mathrm{I}=\int_{-\infty}^{\infty}\int_{-\infty}^{\infty}\cdots\int_{-\infty}^{\infty} e^{f(z_1,\,z_2,\,\ldots\,z_n)}\,dz_1,\,dz_2\ldots dz_n, \quad (83)$$

the saddle point $(z_1{}^0, z_2{}^0, \ldots z_n{}^0)$ of which is determined by

$$\frac{\partial f}{\partial z_1}=\frac{\partial f}{\partial z_2}=\ldots=\frac{\partial f}{\partial z_n}=0.$$

Now the second approximation of (83) is obtained with the aid of the more-dimensional Taylor development of $f(z_1, z_2 \ldots z_n)$ round the saddle point, stopping at the second-order terms, leading to

$$\mathrm{I}\sim\mathrm{I}_2=e^{f(z_1{}^0,\,z_2{}^0,\,\ldots\,z_n{}^0)}\int_{-\infty}^{\infty}\int_{-\infty}^{\infty}\cdots\int_{-\infty}^{\infty}$$

$$\times e^{\frac{1}{2}(z_1-z_1{}^0)^2\left(\frac{\partial^2 f}{\partial z_1{}^2}\right)_0+(z_1-z_1{}^0)(z_2-z_2{}^0)\cdot\left(\frac{\partial^2 f}{\partial z_1\partial z_2}\right)_0+\cdots}\,dz_1\,dz_2\ldots dz_n. \quad (84)$$

Further, the exponent of (84) may be transformed to "normal coordinates" with the aid of the linear transformation

$$z_i - z_i^0 = \sum_{k=1}^{n} p_{ik} u_k,$$

so that the exponent becomes $\sum_{k=1}^{n} a_k u_k^2$, and the multiple integral (84) reduces to the product of n complete error integrals. The result is

$$I_2 = \frac{(i\sqrt{\pi})^n \cdot |p_{ik}|}{\sqrt{a_1 a_2 \ldots a_n}} \cdot e^{f(z_1^0, z_2^0, \ldots z_n^0)}, \quad . \quad . \quad (85)$$

where $|p_{ik}|$ means the determinant of the coefficients p_{ik}. Moreover, according to a well-known theorem of linear transformations we have

$$\sqrt{a_1 a_2 \ldots a_n} = |p_{ik}| \cdot \sqrt{\frac{\Delta}{2^n}},$$

where Δ is Hesse's determinant of order n of $f(z)$, taken at the saddle point, and which is defined by

$$\Delta = \left| \frac{\partial^2 f}{\partial z_i \partial z_k} \right|_0 .$$

Hence (85) leads to the final result

$$I_2 = \frac{(i\sqrt{2\pi})^n}{\sqrt{\Delta}} \cdot e^{f(z_1^0, z_2^0, \ldots z_n^0)}, \quad . \quad . \quad . \quad (86)$$

where, as we shall see further on, the first factor gives the amplitude and the last the phase in our ray problem.

We are now ready to apply (86) to (79), in order to find the second approximation of (79). We therefore identify $f(z_1, z_2 \ldots z_n)$ of (86) with $f^e_{K,m}$ as given by (80), and this for the values of the z's in the saddle point which are known from (81). Referring to fig. 13 we can express the result as

$$(f^e_{K,m})_0 = i\{k_1 . \overline{QA_1} + k_2(\overline{A_1A_2} + \ldots + \overline{A_{K+1}A_{K+2}}) + k_1 . \overline{A_{K+2}P}\} = iS_K, \text{ say}, \quad (87)$$

where S_K is the "*eiconal*" * belonging to the ray which has been reflected internally K times, and which expresses the phase of the ray. In order to find its amplitude we must evaluate Δ, and a further consideration shows that Δ is most elegantly expressed with the aid of

$$\frac{\partial \vartheta}{\partial n} = -\frac{1}{k_1 b \cos \tau_1} + \frac{1}{k_1 a \cos \tau_2} - \sum_{\nu=3}^{2K+4} \frac{1}{k_2 a \cos \tau_\nu} + \frac{1}{k_1 a \cos \tau_{2K+5}} - \frac{1}{k_1 r \cos \tau_{2K+6}}, \quad (88)$$

as

$$\Delta = (-1)^K . k_1 b . k_1 a . (k_2 a)^{2(K+1)} . k_1 a . k_1 r . (n - \tfrac{1}{2}) \sin \vartheta e^{-i\vartheta} . \cos \tau_1 \cos \tau_2 \ldots \cos \tau_{2K+6} . \frac{\partial \vartheta}{\partial n}.$$

The geometrical meaning of $\frac{\partial \vartheta}{\partial n}$ is obtained if, by keeping the transmitter Q (fig. 13) fixed, we imagine the receiver P to move a little distance along its circle round O. Thereby ϑ and n vary with a differential quotient $\frac{\partial \vartheta}{\partial n}$. It is further of interest to note here that the physical geometrical meaning of the variable n, which originally appeared as a separation constant in the harmonic series (1) from which our whole investigation started, according to (81) is nothing but 2π times the length of the orthogonal from the centre O on all cords of the broken ray (expressed in wave-lengths), and which is even true for those parts of the ray which lie outside the sphere.

Returning to (79) $A(n)$ has now to be taken at the saddle point, and further introducing in $A(n)$ approximations of the type

$$\zeta^{(1)}_{ka \sin \tau} \cdot \zeta^{(2)}_{ka \sin \tau} \sim \frac{1}{(ka)^2 \cos \tau}, \quad . \quad . \quad . \quad (89)$$

and limiting ourselves to $m = 0$, we find for $O'_{K,0}$ the final result (second-order approximation)

$$O'_{K,0} \sim \frac{i^K . R_{12} R_{22}^K R_{21}}{k_1 b . k_1 r \sqrt{\sin \vartheta . \frac{\partial \vartheta}{\partial n}}} \cdot \frac{\sqrt{k_1 a \sin \tau_2}}{\sqrt{\cos \tau_1 . \cos \tau_{K+6}}} . e^{iS_K}. \quad (90)$$

* See also Ch. Manneback, 'Recueil des travaux de l'Assemblée Générale de l'Union Radio Scientifique Internationale, tenue à Londres en Sept. 1934': Bruxelles, 1935.

This formula, which represents the ray of order K, confirms the considerations given in § 14 in so far as it becomes infinite where $\frac{\partial \vartheta}{\partial n}=0$, *i. e.*, on the caustic.

With a view to the radio application, where the ray of order -1, which is the ray which has been reflected only once externally and which has to be computed separately, we give here its approximate expression in the form

$$O^{e}_{-1,0} \sim \frac{\sqrt{k_1 a \sin \tau_2}\,.\,R_{11}\,.\,e^{iS-\frac{1}{4}}}{ik_1 b\,.\,k_1 r \sqrt{\sin \vartheta\,.\,\frac{\partial \vartheta}{\partial n}\,.\cos \tau_1\,.\cos \tau_4}}$$

$$=\alpha_{11}\,.\,R_{11}\,.\,\frac{e^{ik_1(R_1+R_2)}}{ik_1(R_1+R_2)}, \quad . \quad (91)$$

where

$$\alpha_{11}=\frac{(R_1+R_2)\sqrt{k_1 a \sin \tau_2}}{k_1 br \sqrt{\sin \vartheta\,.\,\frac{\partial \vartheta}{\partial n}\,.\cos \tau_1 \cos \tau_4}},$$

which, after a slight transformation, becomes

$$\alpha_{11}=\frac{a(R_1+R_2)\sqrt{\sin \tau_2\,.\cos \tau_2}}{\sqrt{br \sin \vartheta}(R_1 r \cos \tau_4+R_2 b \cos \tau_1)}. \quad . \quad (92)$$

Summarizing, we refer to fig. 14 for the meaning of the variables τ and R.

Formula (91) tells us the interesting physical fact that the reflected ray is *not* given by the simple product of the primary ray and the reflexion coefficient R_{11}, but that a factor α_{11}, which we call the " divergence factor," also enters. This is physically obvious, because the reflexion in our case occurs against a curved surface, so that the divergence of two nearby primary rays, contrary to what happens for a reflexion against a plane boundary, is increased, and therefore the amplitude of the secondary ray is diminished, due to the increased divergence (astigmatism). This is confirmed in the two special cases (*a*) $r=a$ (receiver on the sphere), where this extra divergence obviously disappears, and we therefore obtain $\alpha_{11}=1$, and (*b*) $a\to\infty$ (reflexion against plane), where, again, $\alpha_{11}=1$.

Applying, finally, our second approximation to $I^e_{-1,0}$ (of (70)), we find

$$I^e_{-1,0} \sim \Pi_{pr} = \frac{e^{ik_1 R}}{ik_1 R},$$

Fig. 14.

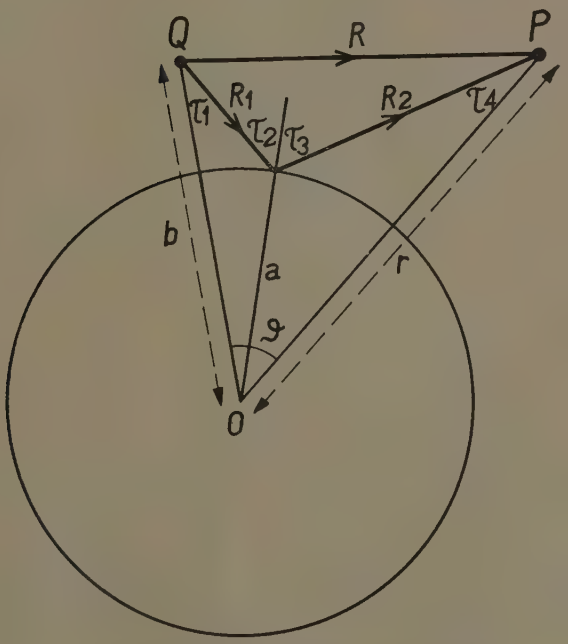

The direct ray together with the once externally reflected ray.

so that in the radio case the second approximation to the total field becomes

$$\Pi_{tot} \sim I^e_{-1,0} + O^e_{-1,0} \sim \frac{e^{ik_1 R}}{ik_1 R}\{1 + \alpha_{11} R_{11} e^{ik_1(R_1+R_2-R)}\}. \quad (93)$$

This extended reflexion formula differs from one occasionally found in the technical literature, where the divergence factor α_{11} is taken as unity, and instead of our spherical reflexion coefficient R_{11} the ordinary plane reflexion

coefficient is used. However, the numerical difference is small in most radio applications.

16. *The Third-Order Approximation to the Intensities of the Rays.*

Having in the previous paragraph considered the second approximation of the elementary waves $O^{e}_{K,0}$ as given by (79), we shall now investigate the third approximation of these waves. As pointed out already in § 14, the third approximation is the fundamental one in the theory of the rainbow, because here light is practically only present near the minimum of deviation, which coincides with the caustic at infinity.

Developing the exponent (80) round the saddle point up to the third-order terms, it is found that the variables τ occur separated, so that the multiple integration over all the τ's can be affected first, thus leading, with $\tau_V - \tau_V{}^0 = u$, to a product of integrals of the type

$$\int_{w_1}^{w_2} e^{-i\alpha u^3 \mp i\beta u^2 - i\gamma u} du = \frac{\pi}{3\sqrt{\alpha}} \cdot e^{\pm i\frac{\pi}{6} - \frac{2}{27} i \frac{\beta^3}{\alpha^2} \pm \frac{i\beta\gamma}{3\alpha}}$$

$$\cdot H^{(1)}_{1/3}\left\{\frac{2\left(\frac{\beta^2}{3\alpha} - \gamma\right)^{3/2}}{3^{3/2}\sqrt{\alpha}}\right\} \sim \sqrt{\frac{\pi}{\beta}} \cdot e^{\mp i\frac{\pi}{4} \pm \frac{i}{4}\frac{\gamma^2}{\beta} \pm \frac{i}{8}\frac{\alpha\gamma^3}{\beta^3}}, \quad (94)$$

where the paths of integration are as given in fig. 15, W_1 belonging to the functions $\zeta^{(1)}$ and W_2 to the functions $\zeta^{(2)}$.

The last approximation of (94) can be obtained in two different ways : (*a*) as the first term of the asymptotic series of the Hankel function, and (*b*) by applying (86) to the integral of (94). In both cases it is assumed that

$$\beta^3 >> \alpha^2,$$

$$\beta^2 >> \alpha\gamma,$$

which in the case of (79) comes to

$$ka \cdot \frac{\cos^3\tau}{\sin^2\tau} >> 1,$$

$$ka \cdot \frac{\cos^2\tau}{\sin\tau} >> n - n_0.$$

Having thus affected all the τ integrations we are left with the integrals over ϕ and n. The integral over ϕ

appears to be a nearly complete Fresnel integral, which can be approximated by unity. The remaining integral over n contains an exponent which can be developed again up to the third-order terms in $n-n_0$, thus leading to an integral of the form (*cf.* fig. 15) :

$$\int_{W3} e^{-i(n-n_0)^3+i\delta(n-n_0)}\,d(n-n_0)=\frac{\pi}{3}\sqrt{\delta}e^{i\pi/6}\cdot \mathrm{H}^{(1)}_{1/3}\left(\frac{2\delta^{3/2}}{3^{3/2}}\cdot e^{-i\pi}\right),$$

Fig. 15.

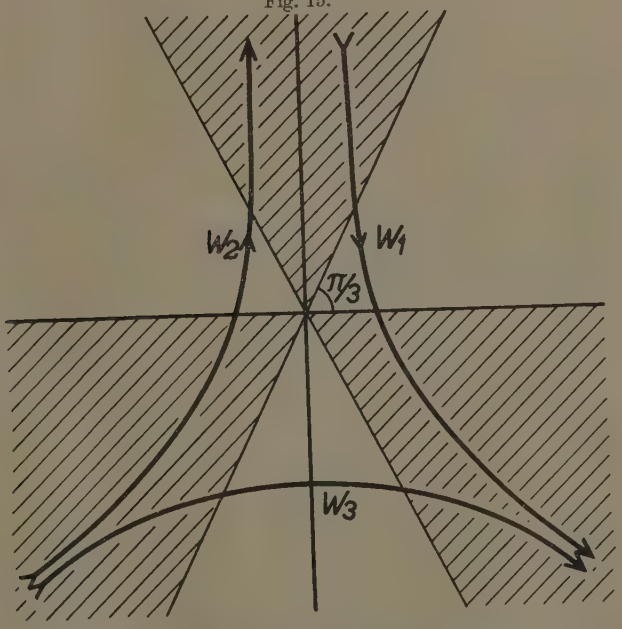

Path of integration of third-order integrals.

giving as final result

$$\mathrm{O}'_{\mathrm{K},0}\sim\frac{(-1)^{\mathrm{K}+1}e^{\frac{5}{12}i\pi+i\mathrm{S}_{\mathrm{K}}}\sqrt{\pi a\sin\tau_2}}{k_1^{3/2}br\sqrt{6\sin\vartheta\cdot\cos\tau_2\cdot\cos\tau_{2\mathrm{K}+6}}}\cdot \mathrm{R}_{12}\mathrm{R}^{\mathrm{K}}_{22}\mathrm{R}_{21}$$
$$\cdot\frac{\partial\vartheta}{\partial n}\Big/\frac{\partial^2\vartheta}{\partial n^2}\cdot e^{-\frac{1}{3}\left(\frac{\partial\vartheta}{\partial n}\right)^3/\left(\frac{\partial^2\vartheta}{\partial n^2}\right)^2}\cdot \mathrm{H}^{(1)}_{1/3}\left(\frac{\left(\frac{\partial\vartheta}{\partial n}\right)^3}{3\left(\frac{\partial^2\vartheta}{\partial n^2}\right)^2}\right), \qquad (95)$$

where in the result analogous to (88) we have, apart from $\frac{\partial \vartheta}{\partial n}$, also introduced $\frac{\partial^2 \vartheta}{\partial n^2}$, the latter being given by the geometrical relation

$$\frac{\partial^2 \vartheta}{\partial n^2} = -\frac{\sin \tau_1}{k_1^2 b^2 \cos^3 \tau_1} + \frac{\sin \tau_2}{k_1^2 a^2 \cos^3 \tau_2} - \sum_{\nu=3}^{2K+4} \frac{\sin \tau_\nu}{k_2^2 a^2 \cos^3 \tau_\nu} + \frac{\sin \tau_{2K+5}}{k_1^2 a^2 \cos^3 \tau_{2K+5}} - \frac{\sin \tau_{2K+6}}{k_1^2 r^2 \cos^3 \tau_{2K+6}}; \quad (96)$$

(95) therefore constitutes our third approximation to the elementary waves represented by (79).

The factor $H_{1/3}^{(1)}$ contains in the argument the factor $\left(\frac{\partial \vartheta}{\partial n}\right)^3$, which is zero on the caustic and has different signs on its sides, and this nicely demonstrates a well-known general property of waves near caustics, viz., that their amplitude falls off exponentially at one side of the caustic and in an oscillatory manner at the other side, this fact being demonstrated by the exponential behaviour of $H_{1/3}^{(1)}(x)$ for $x>0$ and the oscillator character of the same function for $x<0$. This behaviour is due to the fact that at the convex side of the caustic, where $\frac{\partial \vartheta}{\partial n}<0$, each point is in general reached by two different rays causing an interference pattern.

It is also possible, as a further analysis shows, to give the geometrical meaning of the argument of $H_{1/3}$ in (95). In fig. 16 the caustic is represented by the full-drawn curve C, while the wave-front W, cutting the caustic C in the cusp W_0 orthogonally, is shown dotted *. Further, there are represented two rays, W_1P and W_2P, touching the caustic at K_1 and K_2 resp., and which rays arrive at P with a path difference $\triangle = \overline{W_1P} - \overline{W_2P}$. Due to the caustic being the evolute of the wave-front W, this expression may be replaced by

$$\Delta = \overline{K_1P} + \overline{PK_2} - \text{arc } K_1K_2,$$

* See also R. Wood, ' Physical Optics,' p. 148 (New York, 1919).

and a somewhat elaborate transformation, moreover, shows that

$$-\frac{2}{3}\frac{\left(\frac{\partial\vartheta}{\partial n}\right)^3}{\left(\frac{\partial^2\vartheta}{\partial n^2}\right)^2}\sim k_1\Delta,$$

Fig. 16.

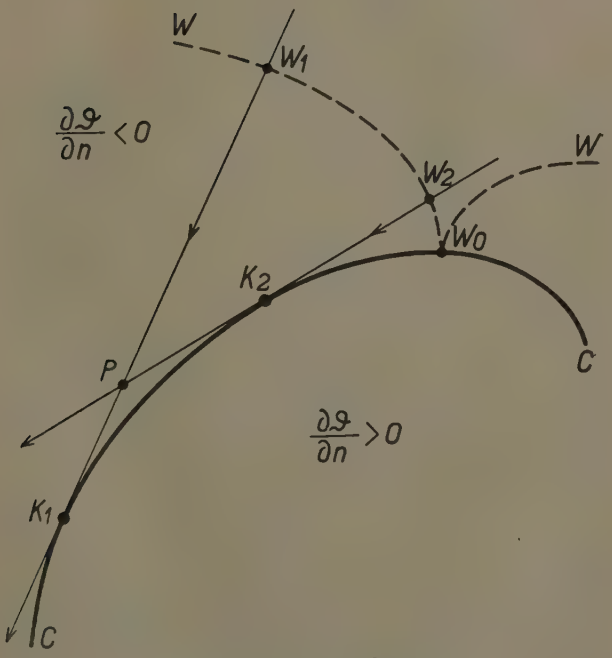

Caustic with wave-front.

so that the argument of $H_{1/3}$ in (95) simply becomes $\frac{1}{2}.e^{-i\pi}.k_1\triangle$. The asymptotic expression of $H_{1/3}$ then yields two terms, representing the two rays with a phase difference $k_1\Delta$. We will return to these third-order approximations in § 18.

17. *Numerical Results for the Radio Case.*

Summarizing, we have now available for numerical interpretation for the radio case the following expressions :—

(*a*) Watson's expression, which is a special case of (15), viz. for $b=a$, and therefore only refers to the case where both transmitter and receiver are situated on the ground, and which is based on the residue method.

(*b*) The expression (15), which is also based on the residue method, but here either the transmitter or the receiver is situated above the ground *.

(*c*) The expression (77), covering all cases, and which was derived with the residue method after the total field was broken up into elementary waves and after it was shown that in the radio case waves reflected against the centre of the sphere were negligible. Thus the denominator $\frac{\partial M}{\partial n}$ of (77) differs from Watson's $\frac{\partial N}{\partial n}$ of (15) as a consequence of the fact that the direct radiation and the only once externally reflected radiation were maintained.

(*d*) The reflexion formula (93), which was derived after the total field was broken up into elementary waves, the direct radiation and the only once externally reflected radiation being maintained, the derivation being obtained with the aid of the saddle point method, yielding (1) the spherical reflexion coefficient R_{11}, and (2) the divergence factor α_{11}.

As to the ranges of applicability of the different expressions, these are most clearly described when we consider first the field far beyond the horizon of the transmitter. There formula (77) can be used, and its first term already gives a very good approximation. When we approach the horizon from beyond the number of terms of (77) to be considered rapidly increases, although at the horizon no more than six to ten terms are necessary in practice. Going further towards the transmitter, as we have passed the horizon, the number of terms of (77) to be retained rapidly increases still further, and in our examples we have gone up to eighteen terms.

* After the present investigation was finished a paper appeared by Wwedensky, ' Technical Physics of U.S.S.R.', iii. p. 915 (1936), giving a formula analogous to our expression (15).

This shows the practical applicability of our general expression (77), which, however, is formally valid everywhere even when the receiver approaches the transmitter indefinitely.

We have further found it convenient in applying (77) to limit ourselves to two limiting cases (which have already been considered before), viz.,

(1) *Total reflexion* : $\sigma=\infty$ (see § 7 *b*),

(2) *Maximum absorption* :

$$|\delta| = \left| \frac{i}{x^{1/3}} \cdot \frac{k_2^2/k_1^2}{\sqrt{k_2^2/k_1^2-1}} \right| << 1$$

(see § 8),

for in these cases the values of τ_s and τ_s' can easily be calculated (see (40 *a*) and (55)).

It is thus seen that, while approaching the transmitter, the number of necessary terms of (77) soon becomes unwieldy. Mostly there is still left a transition region, dotted in the figures to be given later on, but then we soon approach shorter distances from the transmitter, where we can apply the reflexion formula (93). The values of the field in the transition region can, however, mostly be properly estimated by interpolation.

Already in Part I. of this paper we gave some numerical results also for either the transmitter or the receiver above the ground, these cases being equivalent according to the principle of reciprocity (see fig. 8). The effect in (77) of raising the height is expressed by the factors

$$f_s = \left\{ \frac{\zeta_n^{(1)}(k_1 b)}{\zeta_n^{(1)}(k_1 a)} \right\}_{n=x+x^{1/3}\tau_s},$$

present in each term of the series. If both transmitter and receiver are raised above the ground two of these factors are present, the second one with b replaced by r. In order to discuss the numerical effect of these factors f_s the ζ functions can be replaced by the approximation (17), yielding (after a slight simplification based on $x^{1/3}\vartheta_0^5 << 1$, where $\vartheta_0 = \cos^{-1} b/a$) :

$$f_s \sim \sqrt{1-\frac{\chi_0^2}{2\tau_s}} \cdot \frac{H_{1/3}^{(1)}\left\{\frac{\chi_0^3}{3}\left(1-\frac{2\tau_s}{\chi_0^3}\right)^{3/2}\right\}}{H_{1/3}^{(1)}\left\{\frac{(-2\tau_s)^{3/2}}{3}\right\}}, \quad . \quad (97)$$

and a similar expression when τ_s is replaced by τ_s'. Here we have introduced the new variable $\chi = x^{1/3}\,\vartheta = (ka)^{1/3}$; the special value of χ for a point at the horizon is designated by $\chi_0 = x^{1/3}\vartheta_0$ if either the transmitter or the receiver is above the ground. If both are raised above the ground (see fig. 17) the transmitter as well as the receiver each has its own horizon, for which the χ's are denoted by $\chi_1 = x^{1/3}\vartheta_1$ and $\chi_2 = x^{1/3}\vartheta_2$.

Fig. 17.

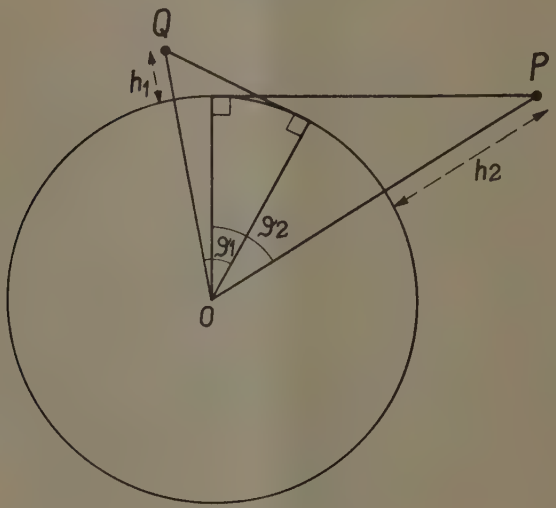

Definitions of ϑ_1 and ϑ_2.

Returning to (97) a very important physical property is expressed by these factors, viz., the increase of the field with the height. This increase appears to be a function of (*a*) the numerical constants τ_s depending upon the electrical constants of the ground and the wave-length and (*b*) the geometrical variable χ_0. Now it appears that the argument of the Hankel function in the nominator of (97) is of the order $1/3\,\chi_0^3$, and the numerical behaviour of this Hankel function is totally different in the two cases $1/3\,\chi_0^3 < 1$ and $1/3\,\chi_0^3 > 1$, corresponding

resp. to $h<56\lambda^{2/3}$ and $h>56\lambda^{2/3}$, where $h=b-a$ and λ are both measured in metres *.

When $h<<56\lambda^{2/3}$ the Hankel functions in (97) may be approximated by the first terms of their power series development, leading to

$$f_s\sim\frac{1+0{\cdot}459e^{2\cdot3i\pi}(\chi_0{}^2-2\tau_s)-0{\cdot}0417(\chi_0{}^2-2\tau_s)^3\ldots}{1+0{\cdot}459e^{2\cdot3i\pi}(-2\tau_s)-0{\cdot}0417(\chi_0{}^2-2\tau_s)^3\ldots}. \quad (98)$$

When, on the other hand, $h>>56\lambda^{2/3}$, we approximate the Hankel function in the nominator by the first term of the asymptotic development, while the Hankel function in the denominator must first be written as

$$H^{(1)}_{1/3}(z)=\frac{e^{-i\pi/6}}{\sin\pi/3}\cdot\{J_{1/3}(ze^{i\pi})+J_{-1/3}(ze^{i\pi})\},$$

and then the first term of the asymptotic development of both $J_{1/3}$ and $J_{-1/3}$ can be taken. This leads to the following final formulæ, valid therefore for $\chi_0{}^3>>3$, $\chi_1{}^3>>3$, $\chi_2{}^3>>3$:

Values of τ:

(1) $\sigma=\infty$: $\quad\tau_s\sim\frac{1}{2}\{3\pi(s+\frac{1}{4})\}^{2/3}\cdot e^{i\pi/3}$,

(2) $|\delta|<<1$: $\quad\tau_s'\sim\frac{1}{2}\{3\pi(s+\frac{3}{4})\}^{2/3}\cdot e^{i\pi/3}-\delta$,

$$\left(\text{for } s<<\frac{1}{30\delta^3}\right).$$

Values of height-gain factors:

$$\left.\begin{aligned}&(1)\ \sigma=\infty:\\&f_s\sim\frac{(-1)^s(-2\tau_s)^{1/4}}{2\sqrt{\chi_0}}\cdot e^{i\frac{\chi_0{}^3}{3}\left(1-\frac{2\tau_s}{\chi_0{}^2}\right)^{3/2}+i\frac{\pi}{4}},\\&(2)\ |\delta|<<1:\\&f_s\sim-\frac{12}{5}\frac{(-1)^s(-2\tau_s')^{7/4}}{\sqrt{\chi_0}}\cdot\frac{e^{i\frac{\chi_0{}^3}{3}\left(1-\frac{2\tau_s'}{\chi_0{}^2}\right)^{3/2}+i\frac{\pi}{4}}}{\left\{1-\frac{96}{5}\delta\tau_s'^2\right\}}.\end{aligned}\right\} \quad (99)$$

* In an investigation of the same problem by Mr. T. L. Eckersley who recently kindly communicated to us his results (not yet published) obtained with his "phase integral method," the effect of raising the transmitter is called the "height gain"; he also finds a critical height given as $h=50\lambda^{2/3}$, which corresponds well with our $h=56\lambda^{2/3}$, as found above.

Attenuation factors for $b=r=a$:

$$\left.\begin{aligned} &(1)\ \sigma=\infty: \quad \frac{\Pi_{\text{tot}}}{\Pi_{\text{pr}}}\sim\sqrt{2\pi i\chi}\cdot\sum\frac{e^{i\tau_s\chi}}{\tau_s},\\ &(2)\ |\delta|<<1: \quad \frac{\Pi_{\text{tot}}}{\Pi_{\text{pr}}}\sim-2\delta^2\cdot\sqrt{2\pi i\chi}\cdot\sum e^{i\tau_s'\chi}. \end{aligned}\right\} \quad . \quad . \quad (100)$$

Attenuation factors for $b\neq a$, $r=a$;

$$\left.\begin{aligned} &(1)\ \sigma=\infty:\\ &\frac{\Pi_{\text{tot}}}{\Pi_{\text{pr}}}\sim\sqrt{-\frac{2\pi\chi}{\chi_0}}\cdot\sum\frac{(-1)^{s+1}}{(-2\tau_s)^{3/4}}\cdot e^{i\tau_s\chi+i\frac{\chi_0^3}{3}\left(1-\frac{2\tau_s}{\chi_0^2}\right)^{3/2}},\\ &(2)\ |\delta|<<1:\\ &\frac{\Pi_{\text{tot}}}{\Pi_{\text{pr}}}\sim\frac{24}{5}\delta^2\cdot\sqrt{-\frac{2\pi\chi}{\chi_0}}\cdot\sum(-1)^s(-2\tau_s')^{7/4}\\ &\qquad\cdot\frac{e^{i\tau_s'\chi+\frac{i\chi_0^3}{3}\left(1-\frac{2\tau_s'}{\chi_0^2}\right)^{3/2}}}{\left\{1-\frac{96}{5}\delta\,\tau_s'^2\right\}}. \end{aligned}\right\} \quad . \quad (101)$$

Attenuation factors for $b\neq a$, $a=r$:

$$\left.\begin{aligned} &(1)\ \sigma=\infty:\\ &\frac{\Pi_{\text{tot}}}{\Pi_{\text{pr}}}\sim\sqrt{\frac{\pi\chi}{2i\chi_1\chi_2}}\\ &\qquad\cdot\sum\frac{e^{i\tau_s\chi+\frac{i\chi_1^3}{3}\left(1-\frac{2\tau_s}{\chi_1^2}\right)^{3/2}+\frac{i\chi_2^3}{3}\left(-\frac{2\tau_s}{\chi_2^2}\right)^{3/2}}}{\sqrt{-2\tau_s}},\\ &(2)\ |\delta|<<1:\\ &\frac{\Pi_{\text{tot}}}{\Pi_{\text{pr}}}\sim\frac{576}{25}\delta^2\cdot\sqrt{\frac{\pi\chi}{2i\chi_1\chi_2}}\\ &\qquad\cdot\sum\frac{(-2\tau_s')^{7/2}\cdot e^{i\tau_s'\chi+\frac{i\chi_1^3}{3}\left(1-\frac{2\tau_s'}{\chi_1^2}\right)^{3/2}+i\frac{\chi_2^3}{3}\left(1-\frac{2\tau_s'}{\chi_2^2}\right)^{3/2}}}{\left\{1-\frac{96}{5}\delta\tau'^2_2\right\}^2}. \end{aligned}\right\} \quad . \quad (102)$$

Figs. 18–20 were calculated with the aid of the above formulæ, where occasionally a still higher approximation for f_s than given above was made use of. These figures refer to

Fig. 18, $\sigma=\infty$, $h_1=100$ m., $h_2=0$,
Fig. 19, $\sigma=10^{-13}$, $\epsilon=4$, $h_1=100$ m., $h_2=0$,
Fig. 20, $\sigma=10^{-13}$, $\epsilon=4$, $h_1=h_2=100$ m.,

Fig. 18.

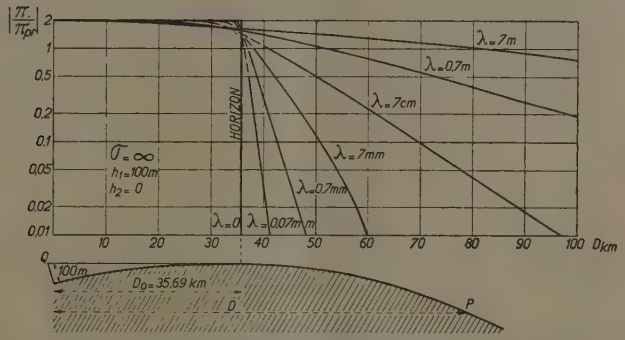

Influence of the wave-length on the field directly on the surface of the earth for a transmitter at a height of 100 m. ($\sigma = \infty$).

Fig. 19.

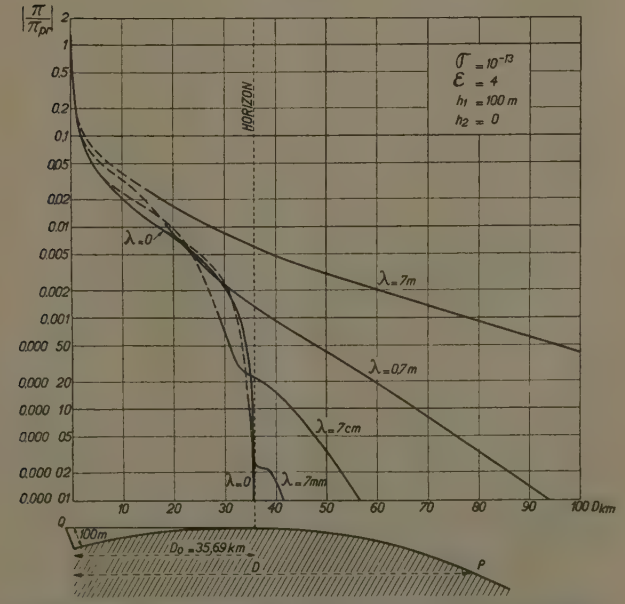

Influence of the wave-length on the field directly on the surface of the earth for a transmitter at a height of 100 m. ($\epsilon = 4$; $\sigma = 10^{-13}$).

and they represent $|\Pi_{tot}|$ divided by the modulus of the primary field $e^{ik_1R}/(ik_1R)$, and therefore represent the attenuation factors with which the undisturbed radiation must be multiplied due to the presence of the earth.

Fig. 18 (for $\sigma=\infty$) clearly shows that waves longer than about $\lambda=10$ cm. do not present a pronounced effect at the horizon, while shorter waves rapidly fall

Fig. 20.

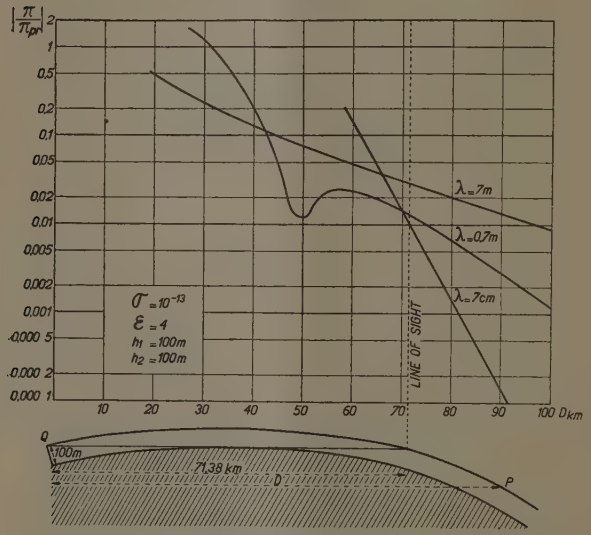

Influence of the wave-length on the field for both transmitter and receiver at a height of 100 m. ($\epsilon=4$; $\sigma=10^{-13}$).

off behind the horizon, tending to a discontinuous drop to zero for waves $\lambda\to 0$.

Fig. 19 (with absorption) shows a similar behaviour of the waves, apart then from the absorption which is already present for all wave-lengths considered. The case of the limiting wave-length $\lambda\to 0$ is here fully determined by ϵ only, the conduction current becoming negligible in comparison with the displacement current.

Fig. 20 (with absorption) again shows a similar behaviour

of the waves ; only the wave $\lambda=70$ cm. has a pronounced minimum before the line of sight. The interference maxima and minima, which undoubtedly are present, fall outside the part of the curves so far calculated.

Herewith we conclude our investigation of the radio problem, and in the next paragraph we consider in further detail the application of our formulæ to the theory of the rainbow.

18. *Theory of the Rainbow.*

While in the radio case it was sufficient to consider the direct wave together with the wave which was once externally reflected only, because of the big absorption of all the other waves entering the earth, in considering the rainbow the conditions are just reversed, because the rainbow is observed near the minimum of deviation of rays which have been once ($K=1$; primary bow) and twice ($K=2$; secondary bow) reflected inside the raindrops.

But as our theory has been developed generally, we are ready to apply it in the present case. It only needs two extensions : (*a*) the source (here the sun) will be considered at infinite distance, and (*b*) the receiver (the observer) also at a very great distance. Moreover, if in the radio case we consider a vertical electric dipole at an infinite height above the earth, due to the radiation characteristic of this dipole being zero in its own axis, no energy would reach the earth at all. We now have therefore, following Debye*, to replace the electric dipole of the radio case by a combination of a contribution of an electric and a magnetic character, the sum of which represents a plane polarized wave.

Whereas in the classical theory of the rainbow the usual procedure was first to find the wave-front after K internal reflexions, then approximating this wave-front round its inflexion point and summing the different contributions from there with the aid of a Kirchhoff integral, leading in its turn to Airy's theory (the so-called Rainbow-integral), we will here follow a totally different way, and develop the result starting from our rigorous

* P. Debye, " Der Lichtdruck auf Kugeln von beliebigem Material " (Inaugural Dissertation, München, 1908); *Ann. d. Phys.* xxx. p. 57 (1909).

solution of the wave equation, which was split up in the subsidiary waves O'_K of (70 *d*). The third-order approximation of the multi-dimensional saddle point integral of O'_K, as considered in § 16, then leads to an extension of Airy's classical results. It is just this extension which here enables us to determine in a rigorous way (*a*) the absolute intensity of the rainbow, (*b*) the losses at the reflexions and refractions, and (*c*) the state of polarization. Whereas these points had formally to be introduced *ad hoc* in a more or less arbitrary way *, they are quite naturally present in our theory, due to the fact that it was derived from a rigorous wave solution.

In order to be able to compare later on our results with the classical ones we shall now recall some formulæ of the older theory, which gives us the opportunity to compare the notations used here with the classical ones.

Referring to fig. 21, let the sun be situated at the infinite point Q, corresponding to $\vartheta=0$, and the observer at the infinite point P at an angular distance ϑ from Q. A typical ray belonging to the primary bow ($K=1$) is represented by $QA_1A_2A_3P$, this ray having a total deviation $D=\pi-\vartheta$. As before, we will designate the rays by the value of the parameter n, see (81 *a*), which is given by

$$n=k_1a\sin\tau_2=k_2a\sin\tau_3=\ldots=k_2a\sin\tau_{2K+4}=k_1a\sin\tau_{2K+5}.$$

Expressed in the variable n, the deviation $D(n)$ then becomes

$$D(n)=2\sin^{-1}\left(\frac{n}{k_1a}\right)-2(K+1).\sin^{-1}\left(\frac{n}{k_2a}\right)+K\pi, \quad (103)$$

and the minimum of deviation, round which the light energy is concentrated, is given by

$$\frac{dD(n)}{dn}=0.$$

Further, for this ray, suffering the minimum of deviation, it is easily found that the corresponding τ_2 becomes $\tau_{2\,\min}$ determined by

$$\sin\tau_{2\,\min}=\sqrt{\frac{(K+1)^2-k_2^2/k_1^2}{K(K+2)}}, \quad . \quad . \quad (104)$$

* See, *e. g.*, W. Möbius, *Ann. d. Phys.* xxxiii. p. 1493 (1910), and xl. p. 736 (1913).

from which it follows that the ray of lowest order corresponds to K=1 (causing the primary bow), because for water in the optical range we have $k_2^2/k_1^2=1{\cdot}78$. The secondary bow corresponds with K=2.

Referring further to fig. 21, the classical theory considers the wave-front W determined by

$$k_1 . \overline{RA_1}+k_2(\overline{A_1A_2}+\ldots+\overline{A_{K+1}A_{K+2}})+k_1 . \overline{A_{K+2}P}=k_1 a,$$

and the ray of minimum deviation cuts this wave-front at its inflexion point O′. It was further usual to introduce new rectangular coordinates ξ and η with O′ as centre.

Fig. 21.

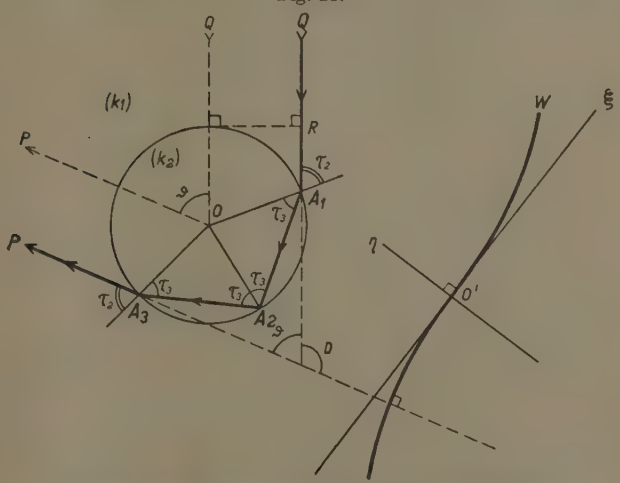

The geometrical-optical ray QP in the primary rainbow, together with a wave-front W.

Expressed in these coordinates the first approximation for this wave-front round its inflexion point was given as

$$\eta=\frac{h}{3a^2}\cdot\xi^3,$$

with

$$h=\frac{K^2(K+2)^2}{(K+1)^2}\cdot\frac{\sqrt{(K+1)^2-k_2^2/k_1^2}}{(k_2^2/k_1^2-1)^{3/2}}, \quad . \quad (105)$$

and it was the interference of the waves originating from this wave-front round O′ which lead to the classical theory.

In the present electromagnetic theory of the rainbow we have to start with a plane polarized wave as primary field, *i. e.*

$$E_x = -ik_1 . e^{-ik_1 z} ; \quad H_y = \frac{k_1^2 c}{i\mu_1 \omega} . e^{-ik_1 z} ; \quad E_y = E_z = H_x = H_z = 0. \qquad . \quad . \quad . \quad (106)$$

This plane wave is polarized in the y direction, but we shall later on have to take the mean square values over all directions of polarizations at right angles to the z-axis in order to account for the unpolarized light from the sun. The two parts of the Hertzian vector, introduced by Debye, necessary to describe this field are

$$\Pi_{\text{tot}} = \Pi_{\text{tot, el}} + \Pi_{\text{tot, magn}},$$

and the components E and H of the electromagnetic field are derived from this wave potential as

$$\left.\begin{aligned} E &= \text{curl curl } (r\Pi_{\text{el}}) + \frac{i\mu\omega}{c} . \text{ curl } (r\Pi_{\text{magn}}), \\ H &= \frac{ck^2}{i\mu\omega} . \text{ curl } (r\Pi_{\text{el}}) + \text{curl curl } (r\Pi_{\text{magn}}). \end{aligned}\right\} . \quad (107)$$

The proper primary field (106) is then obtained from (107) by taking $\Pi_{\text{pr}} = \Pi_{\text{pr, el}} + \Pi_{\text{pr, magn}}$, where

$$\left.\begin{aligned} \Pi_{\text{pr, el}} &= \frac{\cos\phi}{ik_1 r \sin\vartheta} \\ &\quad . \{e^{-ik_1 r\cos\vartheta} - \cos(k_1 r) + i\sin(k_1 r)\cos\vartheta\}, \\ \Pi_{\text{pr, magn}} &= \frac{ic}{\mu_1\omega} . \frac{\sin\phi}{r\sin\vartheta} \\ &\quad . \{e^{-ik_1 r\cos\vartheta} - \cos(k_1 r) + i\sin(k_1 r)\cos\vartheta\}. \end{aligned}\right\} . \quad (108)$$

Through this artifice the Hertzian vector has a radial component only given by $r\Pi_{\text{tot}}$.

In order again to fulfil the boundary conditions we want instead of (108) the equivalent harmonic series

$$\left.\begin{aligned} \Pi_{\text{pr, el}} &= -\cos\phi \\ &\quad . \sum_{n=1}^{\infty} (2n+1) i^{-n} \psi_n(k_1 r) . P_n^{\ 1}(\cos\vartheta), \\ \Pi_{\text{pr, magn}} &= -\sin\phi \\ &\quad . \sum_{n=1}^{\infty} (2n+1) i^{-n} \psi_n(k_1 r) . P_n^{-1}(\cos\vartheta). \end{aligned}\right\} . \quad (109)$$

As is also well known in the plane problem the boundary conditions are different for Π_{el} and Π_{magn}. So far in this paper we have used the electric boundary conditions only, whereas now we have to fulfil the two separate conditions

$$\frac{\partial}{\partial r}(r\Pi_{\text{tot, el}}) \text{ and } k^2\Pi_{\text{tot, el}} \text{ continuous at } r=a,$$

$$\frac{\partial}{\partial r}(r\Pi_{\text{tot, magn}}) \text{ en } \Pi_{\text{tot, magn}} \text{ continuous at } r=a.$$

Extending the results of § 10, where we derived the spherical reflexion coefficients R_{11} and R_{12}, which we shall further call $R_{11,\text{el}}$ and $R_{12,\text{el}}$, we shall have to introduce as well $R_{11,\text{magn}}$ and $R_{12,\text{magn}}$, which are at once derived from the magnetic boundary conditions, and which are found to be

$$R_{11,\text{magn}} = \frac{-\left[x\frac{d}{dx}\log\{x\zeta_n^{(2)}(x)\}\right]_{x=k_1a} + \left[x\frac{d}{dx}\log\{x\zeta_n^{(2)}(x)\}\right]_{x=k_2a}}{\left[x\frac{d}{dx}\log\{x\zeta_n^{(1)}(x)\}\right]_{x=k_1a} - \left[x\frac{d}{dx}\log\{x\zeta_n^{(2)}(x)\}\right]_{x=k_2a}},$$

$$R_{12,\text{magn}} = 1 + R_{11,\text{magn}}.$$

All the results obtained heretofore for the electric dipole may at once be applied in slightly extended form for the present rainbow case. The essential differences are :

1. Here we have $\Pi_{\text{el}}+\Pi_{\text{magn}}$ instead of Π_{el} only.
2. Both the source Q and the observer P are at infinite distance from the centre of the sphere (raindrop).
3. The occurrence of $\left.\begin{matrix}\cos\phi\\ \sin\phi\end{matrix}\right\}.P_n^{-1}(\cos\vartheta)$ instead of $P_n^0(\cos\vartheta)$.

Now the rainbows of different order K are rigorously given by the subsidiary waves O_K^e. Thus we find instead of (70 *d*) the series

$$(O_K^e)_{\text{el}} = -\tfrac{1}{2}\cos\phi \cdot \sum_{n=1}^{\infty}(2n+1)i^{-n}.(R_{12}R_{22}^K R_{21})_{\text{el}} \cdot \left\{\frac{\zeta_n^{(1)}(k_2a)}{\zeta_n^{(2)}(k_2a)}\right\}^{K+1} \cdot \frac{\zeta_n^{(2)}(k_1a)}{\zeta_n^{(1)}(k_1a)} \cdot \zeta_n^{(1)}(k_1r).P_n^{-1}(\cos\vartheta),$$

and an analogous series for the magnetic contribution.

As, moreover, the actual bows are concentrated near

the minimum of deviation (*i. e.*, the caustic), we have, as explained in § 16, for numerical evaluation to use at least the third-order approximation for the elementary waves $O^{e}_{K,0}$, for which the electric part is easily found to be

$$(O^{e}_{K,0})_{el} \sim \frac{e^{iS_K}}{ik_1 r} \cdot \sqrt{\frac{\pi}{6k_1 a \,.\, \sin\tau_2 \,.\, \sin\vartheta}} \cdot (R_{12} R^{K}_{22} R_{21})_{el} \,.\, \cos\phi \cdot \frac{dD}{dn} \Big/ \frac{d^2D}{dn^2} \cdot e^{\frac{i}{3}\left(\frac{dD}{dn}\right)^3 / \left(\frac{d^2D}{dn^2}\right)^2} \cdot H^{(1)}_{1/3}\left\{ \frac{\left(\frac{dD}{dn}\right)^3}{3\left(\frac{d^2D}{dn^2}\right)^2} \cdot e^{-i\pi} \right\}, \quad (110)$$

which is the equivalent of (95) and where the derivatives of $D(n)$ are at once found from its definition (103). The expression for the corresponding magnetic part is again quite analogous.

In order, further, to obtain the actual field components from the wave potential (110) we apply (107), bearing in mind that only S_K has to be differentiated, because $ka >> 1$. Now the physiological intensity of the observed light is usually considered as given by the E vector * and can therefore be represented by $I = \overline{E^2}$, where the dash over the E^2 means the value averaged over all polarization directions ϕ. Now $E_r = 0$, and we are left with E_ϑ, corresponding to the component at right angles ($\perp$) to the arc of the rainbow, and E^ϕ, which corresponds to the component along the arc ($\parallel$) of the bow. Calling further I_0 the intensity of the E_0 vector of the incident light, we are interested in

$$\frac{I_\parallel}{I_0} = \frac{\overline{E_\phi^2}}{\overline{E_0^2}} \left(= \frac{\overline{H_\vartheta^2}}{\overline{H_0^2}} \right),$$

$$\frac{I_\perp}{I_0} = \frac{\overline{E_\vartheta^2}}{\overline{E_0^2}} \left(= \frac{\overline{H_\phi^2}}{\overline{H_0^2}} \right).$$

We thus obtain from (110):

(a) *the absolute intensity*

$$\frac{I_\parallel}{I_0} \sim \frac{\pi}{12} \cdot \frac{(R_{12} R^{K}_{22} R_{21})_{el}^2}{k_1 a \,.\, (k_1 r)^2 \,.\, \sin\tau_2 \sin^3 D} \cdot \left(\frac{dD}{dn} \Big/ \frac{d^2D}{dn^2} \right)^2 \cdot \left[H^{(1)}_{1/3}\left\{ \frac{\left(\frac{dD}{dn}\right)^3}{3\left(\frac{d^2D}{dn^2}\right)^2} \cdot e^{-i\pi} \right\} \right]^2, \quad (111)$$

* M. Born, 'Optik' (Berlin, 1933), p. 24.

(b) *the degree of polarisation*

$$\frac{I_{\parallel}}{I_{\perp}} \sim \frac{c^2 k_1^2}{\mu_1^2 \omega^2} \cdot \left\{ \frac{(R_{12} R_{22}^K R_{21})_{el}}{(R_{12} R_{22}^K R_{21})_{magn}} \right\}^2 \quad . \quad . \quad . \quad (112)$$

In order to facilitate a comparison of our result (111) with the classical Airy theory all we have to do is to replace $H_{1/3}$ by its equivalent Airy integral, and to approximate its argument by its development near $D = D_{min}$. The coefficient h of (105) then appears to be

$$h = \tfrac{1}{2} k_1^2 a^2 \cdot \left(\frac{d^2 D}{dn^2} \right)_{min},$$

and (111) can be written

$$\frac{I_{\parallel}}{I_0} \sim \frac{1}{\pi^2} \cdot \sqrt[3]{\frac{g}{128} \cdot \frac{a\lambda^5}{h^2 r^6}} \cdot \frac{(R_{12} R_{22}^K R_{21})_{el}^2}{\sin \tau_2 . \sin^3 D}$$

$$\cdot \left[\int_0^{\infty} \cos \left\{ \frac{\pi}{2} u^3 - \frac{\pi}{2} \cdot \sqrt[3]{\frac{48 a^2}{h\lambda^2}} (D - D_{min}) . u \right\} du \right]^2,$$

which may be compared, *e.g.*, with expression (27) as given in Handb. d. Phys. xx. (Berlin, 1928), p. 78.

Finally, as to the polarization which is given by (111), this may numerically be evaluated by remembering that $ka >> 1$, which allows us to replace the spherical reflexion coefficients R_{kl} by their plane Fresnel equivalents, and taking further $\epsilon_1 = \mu_1 = 1$ and $\sigma_1 = 0$, we can simplify (112) to

$$\frac{I_{\parallel}}{I_{\perp}} \approx \frac{\cos^{2K}(\tau_2 + \tau_3)}{\cos^{2K+4}(\tau_2 - \tau_3)}, \quad . \quad . \quad . \quad . \quad (113)$$

which well-known expression can thus be derived directly from a rigorous wave solution.

For the primary bow ($K = 1$) formula (113) has the value 25, showing that the E vector is greatest in the direction along the arc of the rainbow, which, according to customary practice, is expressed as the rainbow being mainly polarized at right angles to the arc. The corresponding degree of polarization of the secondary bow is about 10.

An observation with "polaroid" spectacles of a rainbow visible in Eindhoven 16. 4. 1937 at 16.30 qualitatively confirmed the above derived state of polarization. That part of the rainbow became invisible for which the tangent was parallel to the line joining the two glasses. The

spectacles are constructed in such a way that with normal use the reflexion of natural light against a horizontal surface shows maximum extinction *.

Eindhoven.
21st May, 1937.

LXXVII. *The Change of Surface Tension with Time.* *By* W. N. Bond, *M.A., D.Sc., F.Inst.P., Lecturer in Physics, and* H. O. Puls, *B.Sc., Senior Wantage Scholar, University of Reading* †.

Summary.

EXPERIMENTS by the authors and others show that the surface tension of pure liquids has reached its steady value in less than 0·005 sec. Hence it is concluded that the newly introduced surface phase attains equilibrium very quickly (in less than 0·005 sec. and quite probably in 10^{-9} sec.).

In the case of solutions, the surface layer ultimately contains an excess (or deficit) of solute. S. R. Milner suggested that there is delay in attaining equilibrium, due to the time required for solute to diffuse into (or out from) the surface layer. In this paper the consequences of Milner's hypothesis are developed mathematically and the results are tested experimentally. The surface tensions of aqueous solutions of sodium chloride, potassium carbonate, soap, thymol, *p*-toluidine and of butyl, amyl, *n*-hexyl, and *n*-heptyl alcohols are measured by the moving liquid-sheet method, that of soap solution being also measured by Rayleigh's oscillating-jet method. According to theory and experiments, the surface tension of solutions is initially equal to that of the solvent; and the time required for the surface tension to pass half-way towards its final value may be less than 0·0002 second or more than 1 minute, according to the substance

* Mr. C. R. Burrows, of the Bell Telephone Laboratories, kindly drew our attention to a draftsman's error in fig. 8 of part I. where the lower curve (labelled $h=0$), which refers to a plane surface, should be replaced by the lowest drawn curve of fig. 11, which refers to a spherical surface.

† Communicated by the Authors.

concerned. Exceptional cases, where the transition occurs much more slowly than had been predicted, may give evidence of association of the molecules of the solute.

Introduction.

The surface tension of a freshly formed liquid surface may change with time owing to the occurrence of chemical action at the surface, in the liquid, or in the surrounding material. But even when there is no chemical action, time may be required for the surface tension to attain a steady value. The formation of the new surface constitutes the introduction of a new phase into the system—the surface phase ; and equilibrium between this phase and the other phases is not reached immediately. This paper is concerned with the change of surface tension that occurs whilst equilibrium is being reached.

Pure Liquids.

In the case of pure liquids (not solutions) it seems probable that the time required for the establishment of the surface phase is very small ; for it is only necessary for the atoms near the surface to become adjusted to the new boundary conditions. Consequently we should expect the surface tension to attain its final value very quickly indeed. In the main this conclusion is supported by experiment. Thus Rayleigh [1], Pederson [2], and Bohr [3] (using Rayleigh's oscillating-jet method) found that a water-air surface which had been in existence about 1/200th second had a surface tension sensibly equal to the static value. Pederson [2] also found that the surface tension for aniline-air and toluene-air had attained their final values in less than 1/200th second. Again, Satterly and Strachan [4] found the surface tension of a water-air surface about 1/40th second old by measuring stationary waves on a vertical jet, and obtained a value in close accord with the static value. In our previous experiments on moving liquid sheets we found that the surface tensions of water-air (Bond [5]) and mercury-air (Puls [6]) had reached their static values in less than 1/100th second.

Various workers, however, have found values of the surface tension of freshly formed liquid surfaces that do not agree with the static values. Thus Hiss [7] and

Schmidt and Steyer [8] let an air-jet blow on the liquid meniscus until a very short time before the observation was made. According to them the surface tension of water decreases from 103·6 dynes/cm. (very shortly after the surface is formed) to 73·7 dynes/cm. at 0·005 second after the formation of the surface. It is desirable that these experiments should be confirmed by some other method before accepting the results as conclusive. Buchwald and König [9], using their water-bell method, obtained a value for water-air of 79·4 ± 0·8 dynes/cm. (at 12° C.), 1/200th second after the formation of the surface. They also obtained, for other pure liquids, dynamical values that were considerably in excess of the static values. Their results not only disagree with the results of Rayleigh, Pederson, Bohr, Bond, and Puls, but also do not agree in magnitude with those of Hiss, and Schmidt and Steyer. Finally, we may notice that Satterly and Strachan [4] found that a mercury-air surface 1/20 second old had a surface tension from 15 to 21 per cent. higher if the mercury had been recently distilled than if it had previously been allowed to stand exposed to the air for a few weeks.

We consider that the experimental evidence indicates that the surface tension of pure liquids (not solutions) attains its final value in less than 0·005 second. It is quite probable that the surface phase is established and the static value of the surface tension reached in less than 10^{-9} second.

Solutions: Theory.

In general, if the surface tension of a solution decreases with increase in the concentration, then there is ultimately an excess of solute at the free surface (and *vice versa*). The amount of excess at the surface has been deduced by Willard Gibbs [10], and his theory has been verified experimentally [11]. The excess per unit area, q, can usually be calculated [12] by using the following form of Gibbs's equation:

$$\bar{q} = -\frac{c}{RT} \cdot \frac{d\gamma}{dc}, \quad \ldots \ldots \quad (1)$$

where $\bar{\gamma}$ is the static value of the surface tension, c the amount of solute per unit volume in the bulk of the solution, T the absolute temperature, and R the gas

constant. (The values of q, c, and R may be expressed in gram-molecule or in molecular units.)

If a fresh surface is formed on the solution, the excess of solute at the surface will originally be zero, but will gradually approach its final value, q. There will be a corresponding change in the surface tension. It has been suggested by Milner [13] that the delay in attaining equilibrium is chiefly dependent on the time required for the solute to reach the surface by diffusion from the interior of the liquid. We may estimate approximately the time required for the surface tension to pass half-way to its equilibrium value. The depth of solution that would have to be completely denuded of solute in order to form the surface layer is equal to q/c; and the half-way time will be of the order of magnitude

$$\tau = \frac{(q/c)^2}{D} \quad . \quad . \quad . \quad . \quad . \quad . \quad . \quad (2)$$

where D is the coefficient of diffusion. For quite dilute solutions we obtain (from equations (1) and (2))

$$\tau = \frac{(-d\gamma/dc)^2_{c\to 0}}{DR^2T^2}, \quad . \quad . \quad . \quad . \quad . \quad (3)$$

where $(d\gamma/dc)_{c\to 0}$ denotes the limiting value of $(d\bar{\gamma}/dc)$ for indefinitely dilute solutions. These equations can also be used in cases in which there is a *raising* of the surface tension.

Next let us investigate in more detail the variation of surface tension with time. For certain aqueous solutions it was found by Milner [13] and Szyszkowski [14] that the surface tension was given by

$$\gamma_0 - \bar{\gamma} = B\gamma_0 \log_e (1 + c/A), \quad . \quad . \quad . \quad . \quad (4)$$

where A and B are constants and γ_0 is the surface tension of water.

From equations (1) and (4) we may deduce that

$$c\left(\frac{q_\infty - q}{q}\right) = \frac{A}{q}\, q, \quad . \quad . \quad . \quad . \quad . \quad (5)$$

where the maximum possible value of q, when $c \to \infty$, is $q_\infty = \frac{B\gamma_0}{RT}$. Now the number of molecules of solute

that cross any plane of unit area inside the solution per second is proportional to $\bar{c}$; and $\frac{\bar{\bar{q}}-\bar{q}}{\bar{\bar{q}}}$ is the fraction of the effective area of the free surface of the liquid that is as yet unoccupied by molecules of the solute. Hence the left-hand side of equation (5) is probably proportional to the number of solute molecules entering unit area of the free surface-layer per second. Equation (5) represents the equilibrium condition when the rate of reception of molecules equals the rate of emission. Thus we conclude that the rate of emission of solute molecules into the liquid from unit area of the surface layer is proportional to $A\bar{q}/\bar{\bar{q}}$, and is, therefore, proportional to the surface concentration, $\bar{q}$.

At time t, during the formation of the surface layer, let the surface concentration be q; let the concentration in the liquid be c; and let the concentration inside the liquid, but close to the surface layer, be c_0. Then we may assume that the net rate of arrival of solute at the surface is given by

$$\frac{dq}{dt} = ac_0\left(\frac{\bar{\bar{q}}-\bar{q}}{\bar{\bar{q}}}\right) - bq, \quad . \quad . \quad . \quad . \quad . \quad (6)$$

where a and b are constants and

$$\frac{a}{b} = \frac{\bar{\bar{q}}}{A} = \frac{B\gamma_0}{ART} = \frac{1}{RT}(-d\bar{\gamma}/d\bar{c})_{\bar{c}\to 0} = \sqrt{D}\tau.$$

At a distance x inside the liquid we have the usual diffusion equation

$$\frac{dc}{dt} = D\left(\frac{d^2c}{dx^2}\right) \quad . \quad . \quad . \quad . \quad . \quad . \quad . \quad (7)$$

We also have

$$\frac{dq}{dt} = D\left(\frac{dc}{dx}\right)_{x\to 0} \quad . \quad . \quad . \quad . \quad . \quad . \quad (8)$$

At $t=0$ we have $q=0$, and $c=\bar{c}$ for all values of x. We shall assume that the solutions are dilute, so that $\frac{\bar{q}}{\bar{\bar{q}}}$ is sufficiently small for us to replace equation 6 by the simpler equation.

$$\frac{dq}{dt} = ac_0 - bq. \quad . \quad . \quad . \quad . \quad . \quad (6\,a)$$

The thickness of the surface layer will usually be very much less than the distance $\bar{q}/\bar{c}$ of equation (2). Under these circumstances a and b tend to infinity, but their ratio is still equal to $\sqrt{D\tau}$. The solution of equations (7), (8), and (6 a) then gives

$$\frac{q-\bar{q}}{\bar{q}} = e^{-\frac{2}{\sqrt{\pi}}\sqrt{\frac{t}{\tau}}}, \quad . \quad . \quad . \quad . \quad . \quad (9)$$

where τ is defined by equation (3).

For dilute solutions $\gamma_0-\bar{\gamma}$ is nearly proportional to $\bar{c}$, and we find further, by equation (1), that c is then proportional to q. Thus the lowering of the surface tension is nearly proportional to the excess surface concentration. We shall assume that this is also true at any instant during the establishment of the surface layer. Thus the lowering of the surface tension at time t after the formation of the surface (namely, $\gamma_0-\gamma$) is related to the final lowering ($\gamma_0-\bar{\gamma}$) by the equation

$$\frac{(\gamma_0-\bar{\gamma})-(\gamma_0-\gamma)}{\gamma_0-\bar{\gamma}} = e^{-\frac{2}{\sqrt{\pi}}\sqrt{\frac{t}{\tau}}} \quad . \quad . \quad . \quad . \quad (10)$$

where τ is defined by equation (3). Equation (10) assumes that the delay is entirely due to the time taken for diffusion; and this equation is only strictly true for weak solutions for which $d\gamma/d\bar{c}$ is sensibly constant. (We have succeeded in developing the theory for stronger solutions, but the equations are more complicated, and have not helped in the interpreting of the experimental results.)

In order to calculate τ from equation (3) we must know the slope of the (concentration-surface tension) curve at zero concentration. For some of the solutions subsequently used, where the formula of Szyszkowski [4] applies fairly well, the slope was calculated from the values of the constants A, B, and γ_0; for the other solutions the slope was obtained from the graph. This value of τ will be termed the "predicted value" ($\tau_{\text{pr.}}$).

In the dynamical experiments, described below, the value of the surface tension γ at time t was measured. Knowing the ultimate value, $\bar{\gamma}$, and the value for the solvent, γ_0, the value of $(\gamma_0-\gamma)/(\gamma_0-\bar{\gamma})$ at time t was calculated. Then equation (10), or the corresponding

graph (fig. 1) enabled the values of t/τ, and hence of τ, to be deduced. This value of τ will be termed the "observed value" ($\tau_{obs.}$).

Fig. 1.

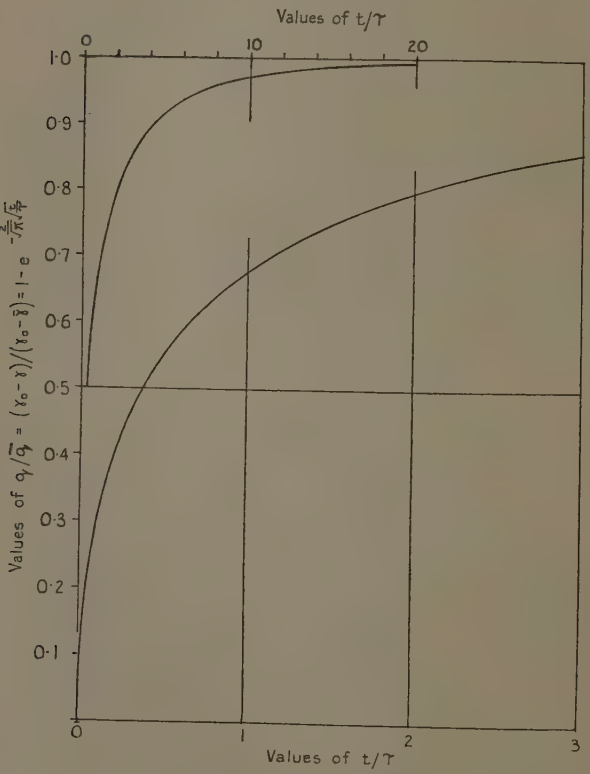

Theory of the Moving Liquid-sheet Method of Measurement.

The theory of the moving liquid-sheet method of measuring the surface tension [5], [6] may be extended

to the case where the surface tension is changing with time. The essential equation becomes

$$Q\rho[v \sin\theta] = 4\pi[\gamma x \sin\theta].$$

From this we find that the surface tension is measured at the instant the liquid reaches the outer edge of the liquid disk ; the age of the surface at that place is $R/v = 2\pi r^2 R/Q$, the notation being as in our previous papers. The diffusion theory given above will, however, require modifying in two ways. In the first place the area of free surface between specified molecules of the solvent is proportional to the age of the surface, so that accumulation of solute per unit area of surface is delayed. Secondly, the thickness of the liquid sheet is inversely proportional to the age of the surface, so that concentration gradients of the solute are being increased, and the rate of diffusion is enhanced. During the early stages of growth of the surface layer on stationary fluid we have $c_0 = 0$ and $q = 2q\sqrt{t/\pi\tau}$. For the expanding and thinning film equations (7) and (8) are replaced by

$$\left(\frac{\partial c}{\partial t}\right)_{x t=\text{const.}} = D\left(\frac{\partial^2 c}{\partial x^2}\right)_{t=\text{const.}},$$

$$\frac{q}{t} + \frac{dq}{dt} = D\left(\frac{dc}{dx}\right)_{x\to 0},$$

and (for the initial stages) equation (6 *a*) is replaced by $c_0 = 0$. Hence we obtain $q = 2\bar{q}\sqrt{t/3\pi\tau}$ for the early stages of growth.

Thus, when the surface tension of a solution is measured by the moving liquid-sheet method, the effective age of the surface is equal to about a third of the time required for a particle of liquid to pass from the centre to the edge of the liquid disk. (The thickness of the liquid sheet should be appreciably larger than $2\bar{q}/\bar{c}$, in order that there shall be enough solute present in the sheet to form the surface layers on its two faces.)

Solutions : Experimental.

Dupré [15] and Rayleigh [16] found that freshly formed surfaces of aqueous solutions of soap had initially almost the same surface tension as water. This is in agreement

with equation (10), according to which the surface tension of a new surface of soap solution is initially equal to that of water, and takes about 1/5th sec. to pass half-way to its final static value.

Pederson [2], on the other hand, found that the surface tension of an aqueous solution of ammonia attained its static value in less than 1/200th second. This is again in agreement with equation (10), according to which the predicted value of τ is about 10^{-9} sec.

In order to make measurements of the surface tension of fresh surfaces of aqueous solutions, the apparatus used by one of us (H. O. Puls) [6] for mercury was completely overhauled. The steel pump was replaced by a small brass motor-car water-circulating pump of the centrifugal type. To prevent contamination of the solutions this pump was nickel-plated throughout. The sump was a nickel-plated trough, and the constant-level reservoir a bakelite dish ; the nozzles and connecting tubes were of glass. The joints between tubes, pump, sump, and reservoir were sealed with picien, which was found to be unaffected by the cleaning agent used (chromic acid) and by the liquids used in the experiments. The lower nozzle was kept fixed and was surrounded by a glass funnel to collect the falling liquid. The upper nozzle was held in the adjustable clamps, previously described. Each nozzle was connected directly to the reservoir by a glass tube, the tube to the upper nozzle being sufficiently flexible to enable slight adjustment of the nozzle. The entrance to each tube was obstructed by a fairly tightly fitting glass rod ; by raising or lowering these rods the rate of flow from the reservoir into the two tubes could be accurately controlled. The rate of flow was measured by collecting the liquid that had flowed through the nozzles during a measured time and weighing it ; the rate of flow was found to be remarkably constant.

It was found necessary to introduce a device for steadying the liquid disk, similar to that used in the experiments (Bond) [5] on water. A glass ring, slightly smaller than the liquid disk, was used for this purpose, and was supported inside the collecting funnel by glass rods.

Having established the validity of the method by our previous experiments on water and mercury, it was not necessary to measure the effective radius of the jets

directly, as it could be obtained more easily by calibrating the apparatus with water. Here, and in all subsequent calculations, the value of the surface tension of water-air has been taken as $73{\cdot}7_8$ dynes/cm. at 15° C., with a temperature coefficient of −0·157 dynes/cm. per ° C. The results of the calibration with water are given below :—

Rate of flow (gm./sec.).	Radius of disk (cm.).	Δ (cm.)	Temp. (°C.).	Jet-diameter ($2r$).
7·693	3·987±0·016	0·36	20·5	$0{\cdot}1425_6$
7·650	3·983±0·016	0·39	21·8	$0{\cdot}1428_1$
7·701	4·007±0·015	0·33	21·1	$0{\cdot}1424_3$

From this the average value of $2r$ is 0·1426 cm.

"*Lux*" *in Water.*

It was decided to make the first experiments with a soap solution. Large quantities were thought to be needed, so "Lux" was chosen, as it seems to be one of the simpler and purer soaps that is readily obtainable. For comparison purposes, and in order to get some idea of the strength of solutions that it would be advisable to use, static measurements of the surface tension of various solutions were first made. In this and later experiments the surface tension was measured by the ordinary capillary rise method. Though doubts have sometimes been thrown on the accuracy of this method, we found it quite accurate for comparison purposes, results agreeing well with those obtained by other workers. The capillary tubes were thoroughly cleaned with chromic acid and then washed in water, subsequently being left to soak in water for a long time in order to remove all the acid. The tubes had a diameter of about 0·067 cm. The tubes were standardized with water, and the depth of the tube in the liquid was adjusted so that the meniscus was always formed at the same part of the tube. For water the capillary rise (corrected for the height of the meniscus) at 16·9° C. was 4·445±0·005 cm. Density determinations were made by comparison with water, using an ordinary specific gravity bottle.

Some of the results for the static value of the surface tension of "Lux" solution/air are :—

Concentration (gm./ litre).	Surface tension (dynes/cm.).	Temperature ($^{\circ}$ C.).
50·0	29·7	18·4
10·0	25·2	19·0
2·5	25·2	16·9
1·0	30·7	16·9
0·5	32·7	17·3
0·3	42·6	16·8
0·1	71·4	16·4

Two litres of "Lux" solution of strength 10 gm./litre were made up and circulated in the apparatus. The results obtained with this and another solution are given below :—

Concentration (gm./litre).	Time to edge of liquid disk (sec.).	Surface tension (dynes/cm.).	Temperature ($^{\circ}$ C.).
10·0	0·0101	57·4	20·7
	0·0100	57·0	19·7
	0·0106	56·6	21·5
	0·0102	57·6	19·8
2·5	0·0089	66·3	19·8
	0·0094	63·7	20·7

In the case of these solutions the surface tension has fallen 33 per cent. and 17 per cent. (respectively) of the way from the value of water to the final static value (25·0 dynes/cm.) in about 1/100 sec. As was explained above, the conditions are equivalent to a stationary liquid surface of a third of the age, namely, 0·003 sec. Hence we can deduce, using equation (10) or fig. 1, that the "observed values" of the characteristic time ($\tau_{obs.}$) are 0·028 and 0·13 second respectively.

Equation (3), together with the static values of the surface tension of dilute solutions, enables the "predicted value," $\tau_{pr.}$, to be deduced; the result obtained is 0·18 second.

The time τ is that required for the surface tension of a new stationary surface of solution to pass 68 per cent. of its way from the water value to the static value. For the two "Lux" solutions this had a predicted value of 0·18 second, and observed values of 0·028 and 0·13 second. The agreement is satisfactory, for it should be remembered that the solutions are rather concentrated, and do not obey equation (4) accurately. These and later results are shown collectively in the table on p. 884.

In order to investigate in more detail the change of surface tension with time, some experiments were carried out by Lord Rayleigh's oscillating-jet method. The nozzle used was similar in construction to those employed in the main experiments, but had an orifice (of mean radius 0·082 cm.) that was not quite circular. The nozzle was mounted so as to squirt a jet of liquid horizontally. It was fed from a constant-level reservoir, and the rate of flow was measured by collecting liquid during a measured time and weighing it. The jet was illuminated from the side from which it was viewed, thus showing up the first six to ten nodes easily; after that point the jet began to spread out and break into drops. The distance between the nodes was measured by means of a metre scale placed immediately behind the jet. Calibration tests with water gave remarkably good results, despite the fact that all experiments were done without taking any elaborate precautions to ensure accuracy.

The surface tension is calculated from the formula given by Bohr [3]:—

$$\gamma = \frac{4M^2}{\lambda^2 \rho a n \left\{ n^2 - 1 + \left(\frac{2\pi a}{\lambda} \right)^2 \right\} \left\{ 1 + \frac{2(\pi a)^2}{(n^2+1)\lambda^2} \right\}},$$

where

M = mass per second;

λ = distance between successive nodes (the "wave-length");

ρ = density of liquid;

a = mean radius of nozzle;

n = a constant integer, depending on the mode of vibration of the jet ($n=3$ in the present instance).

Aqueous solution of	Concentration (gm. mol./litre).	Surface tension (in dynes/cm.).		Per cent. of way to static value.	Characteristic time, τ (in seconds).	
		Static.	When effective age of surface is 0·003 sec.		Predicted.	Observed.
Ammonia (Reference (2))	1·2	71·25	71·7	100 ?	10^{-9}	$<0·005$
	3·1	68·00	69·0	100 ?	10^{-9}	$<0·005$
	6·5	64·70	66·1	100 ?	10^{-9}	$<0·005$
NaCl.....	4·95	82·0	$81·3\pm0·6$	92 ± 7	5×10^{-10}	$<0·000,5$
K_2CO_3.....	2·65	82·5	$82·2\pm0·6$	97 ± 7	5×10^{-10}	$<0·000,3$
"Lux"	10	25·0	57·1	33	0·18	0·028
	2·5	25·0	65·0	17	0·18	0·13
	1·75–5·0	25·0	(See fig. 2.)		0·18	0·14
Thymol	0·0033	56·6	68·5	28	0·011	0·033
p-toluidine	0·028	60·9	64·1	70	0·000,2	0·025
Butyl alcohol	0·183	$47·5\pm0·2$	$47·8\pm0·5$	$100\pm1·5$	2×10^{-5}	$<0·000,2$
	0·156	$50·0\pm0·1$	$49·7\pm0·5$			
Amyl alcohol	0·184	33·6	35·4	96	0·000,17	0·000,6
	0·091	48·7	49·8	95·3	0·000,17	0·000,5
n-hexyl alcohol.....	0·0189	47·2	$51·0\pm0·4$	84·8	0·001	0·001,1
	0·0170	48·6	$51·4\pm0·4$	89	0·001	0·000,9
			$51·7\pm0·2$	87·5	0·001	0·001,1
n-heptyl alcohol	0·00598	44·3	$60·7\pm0·6$	45·1	0·017	0·011
	0·00520	46·0	$61·0\pm0·6$	46·2	0·017	0·011
Decylic acid (Reference [19]) ...	0·000064	55·9	(Various data.)		28	103

The term $\frac{2(\pi a)^2}{(n^2+1)\lambda^2}$ was negligible in the present experiments.

When soap solutions were used it became apparent that the further the liquid had moved from the nozzle, or, in other words, the older the surface, the longer became the distance between the nodes. From this it is obvious that the older the surface the lower the surface tension. The actual " wave-lengths " were measured, and hence

Fig. 2.

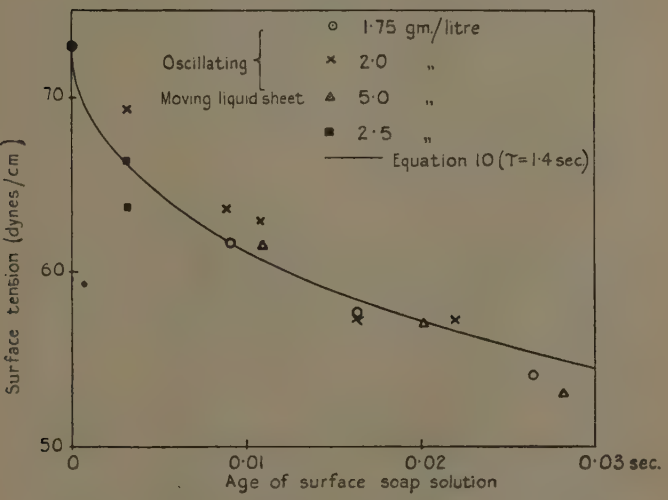

the surface tension at various points along the jet could be calculated. The results of these measurements are shown in fig. 2. The results previously obtained by the liquid disk method for a solution of comparable concentration are also plotted in the diagram.

A curve (fig. 2) of the form given by equation (10) has been fitted to the observations by selecting a suitable value of τ. The value of $\tau_{obs.}$ thus obtained is 0·14 second. This agrees satisfactorily with the previous estimates.

For the subsequent investigations substances of various types were chosen, in order to test the method and theory under as diverse conditions as possible. It is necessary

to choose solutions that have a static surface tension differing considerably from that of water, in order that it shall be possible to measure this difference with reasonable precision. Strong electrolytes as a general rule raise the surface tension above that of water. As representative substances sodium chloride and potassium carbonate were chosen. Both are very soluble, so that a considerable raising of the surface tension is obtainable.

For studying the properties of solutions that have a lower surface tension than that of water thymol and *p*-toluidine were chosen as representative of the cyclic compounds. For the aliphatic compounds a series of homologous alcohols was found very suitable, especially as the gradual change in properties with increase in the length of the chain could be observed. For the latter substances the curve relating static surface tension and concentration can be fitted by the empirical equation (4) given by Szyszkowski.

Sodium Chloride in Water.

The static values of the surface tension of solutions of sodium chloride as given by other workers (International Critical Tables) were confirmed by capillary tube measurements.

In order to get as large a change as possible in the surface tension very concentrated solutions were used. The results obtained were :—

Concentration (gm. mol./litre) of solution.	Static value of surface tension (dynes/cm.).	Time to edge of liquid disk (sec.).	Surface tension (dynes/cm.).	Temperature (° C.).
4·95	82·0	0·00905	80·1	22·2
		0·00838	82·4	19·0

The mean of the dynamical determinations is 81·3 $\pm$0·6 dynes/cm. at 20° C. The ultimate rise in the surface tension, from the water value, is 82·0—73·0=9·0 dynes/cm. Of this rise (92$\pm$7) per cent. has already occurred after an effective time, 0·0029 second.

Hence from equation (10), or fig. 1, we find that $\tau_{obs.}=0{\cdot}000{,}5_5$ $\pm 0{\cdot}000{,}5$ second. Thus τ is probably not greater than about 1/2000 sec.

From equation (3) it is found that $\tau_{pr.} = 5 \times 10^{-10}$ second.

Potassium Carbonate in Water.

A solution of concentration 2·65 gm. mol./litre was used. The static surface tension was found to be 82·5 dynes/cm. at 15° C. (the International Critical Tables give 82·0 dynes/cm.). The dynamical surface tension was 82·2 dynes/cm. at 15° C. at an effective time 0·003 sec. after the formation of the surface. The dynamical and statical values of the surface tension do not differ by a significant amount, and it can be concluded that $\tau_{obs.}$ is not greater than 0·000.3 sec. The value deduced from equation (3) is $\tau_{pr.} = 5 \times 10^{-10}$ sec. The experimental results support the theoretical prediction that, in the cases of sodium chloride and potassium carbonate solutions, the surface tension reaches its static value very quickly indeed. Further experiments were not made with potassium carbonate solution, as the capillary rise experiments gave evidence that the solution was slowly dissolving the glass of the capillary tube.

Thymol in Water.

Thymol was used for the next experiments, as it produces a considerable reduction in the surface tension of water, even though it is not very soluble. The results obtained are given below :—

Concentration (gm. mol./litre) of solution.	Static value of surface tension (dynes/cm.).	Time to edge of liquid disk (sec.).	Surface tension (dynes/cm.).	Temperature (° C.).
0·0033	56·6 at 17° C.	0·0089	67·4	18·7
		0·0089	69·8	20·2
		0·0091	69·1	18·9
		0·0090	67·5	18·9

The average result for the dynamical surface tension is 68·5 dynes/cm. at 19·2° C. The surface tension has gone 28 per cent. of the way to its static value in an effective time 0·003 sec. Hence from fig. 1 we find $\tau_{obs.} = 0{\cdot}033$ sec.

From equation (3), using the (surface tension, concentration) data given in the International Critical Tables, we find that $\tau_{pr.} = 0{\cdot}011$ sec.

The predicted and observed values of τ are of the same order of magnitude, though the agreement is not very close. The experiments suggest that the attainment of equilibrium may be rather slower than indicated by the theory.

p-Toluidine in Water.

The following values of the surface tension of *p*-toluidine solutions were obtained by the capillary tube method :—

Concentration (gm./litre).	Static surface tension at 16° C. (dynes/cm.).
0	$73{\cdot}6_3$
0·3	$73{\cdot}0_1$
0·6	$72{\cdot}6_9$
0·9	$71{\cdot}9_9$
2·1	$65{\cdot}6_6$
3·0	$60{\cdot}9_0$

These values do not agree with those given by Edwards [17], but the curve is of the same strange shape. The graph is not rectilinear, nor does it follow Szyszkowski's logarithmic law equation (4). Hence it is not to be expected that *p*-toluidine will conform to the general theory which we have given.

The following dynamical measurements were made :—

Concentration (gm. mol./litre).	Time to edge of liquid disk (sec.).	Surface tension (dynes/cm.).	Temperature (° C.).
0·028	0·0094	$65{\cdot}2_3$	20·0
	0·0095	$62{\cdot}9_7$	
	0·0093	$63{\cdot}4_8$	
	0·0094	$64{\cdot}3_1$	
	0·0093	$64{\cdot}2_4$	

At an effective time 0·0031 sec. after the formation of the surface the surface tension has gone 70 per cent. of the way to its final value. This corresponds to $\tau_{obs.} = 0{\cdot}025$ sec. On the other hand, from the surface tension/concentration graph we obtain $\tau_{pr.} = 0{\cdot}000{,}2$ sec.

The solute appears to accumulate at the surface at only about a thousandth of the predicted rate. As was suggested above, this may be related to the peculiar type of (surface tension/concentration) curve that is found for *p*-toluidine.

Butyl Alcohol in Water.

Among the substances for which the (surface tension/concentration) curve can be expressed by Szyszkowski's formula (equation (4)) are the aqueous solutions of aliphatic alcohols. Calculation from the (surface tension, concentration) data available showed that the characteristic time, $\tau_{pr.}$, for methyl, ethyl, and propyl alcohols would be so small as to be unmeasurable by the method here employed. Butyl alcohol also showed a very small value of $\tau_{pr.}$, but an attempt was made to see if any difference between the static and dynamic values of the surface tension could be detected for this substance. The results are given below :—

Constants in Szyszkowski's formula :

$$A = 0{\cdot}23,$$

$$A = 0{\cdot}052 \text{ gm. mol./litre.}$$

Calculated characteristic time :

$$\tau_{pr.} = 2{\cdot}2 \times 10^{-5} \text{ sec.}$$

Concentration (gm. mol./litre) of solution	Static value of surface tension (dynes/cm.).	Time to edge of liquid disk (sec.).	Surface tension (dynes/cm.).	Temperature (° C.).
0·183	47·5±0·2	0·01	47·8±0·5	18
0·156	50·0±0·1 at 17° C.	0·01	49·7±0·5	17

Hence we find that $\tau_{obs.} < 0{\cdot}0002$ second.

Amyl Alcohol in Water.

For amyl alcohol the following results were obtained :—

Constants in Szyszkowski's formula :

$$B = 0{\cdot}22,$$

$$A = 0{\cdot}018 \text{ gm. mol./litre.}$$

Calculated characteristic time :

$$\tau_{pr.} = 0{\cdot}000{,}17 \text{ sec.}$$

Concentration (gm. mol./litre) of solution.	Static value of surface tension (dynes/cm.).	Time to edge of liquid disk (sec.).	Surface tension (dynes/cm.).	Temperature (° C.).
0·184	33·6 at 17·5° C.	0·015	35·3	18·9
		0·016	35·5	17·5
0·091	48·7 at 16° C.	$0{\cdot}012_2$	49·1	17·9
		$0{\cdot}012_2$	49·9	17·1
		$0{\cdot}011_8$	50·0	15·3
		$0{\cdot}010_2$	50·4	16·4

For these two solutions the surface tension has gone 96 per cent. and 95·3 per cent. of the way to the static value in effective times of 0·005 and 0·0038 second (respectively). Hence we obtain two estimates of the characteristic time, $\tau_{obs.}$, namely, 0·000,6 and 0·000,5 second.

n-Hexyl Alcohol in Water.

No data were available for the static values of the surface tension of aqueous solutions of this alcohol, so the following measurements were made by the capillary tube method :—

Concentration (gm. mol./litre).	Static surface tension (dynes/cm., at 17 C.).
0·0500	31·9 $\pm$0·2
0·0250	$42{\cdot}8_7 \pm 0{\cdot}0_4$
0·0100	$54{\cdot}9_0 \pm 0{\cdot}0_6$
0·0050	$62{\cdot}3_3 \pm 0{\cdot}0_6$

From these results the constants in equation (4) are found to be

$$B = 0{\cdot}259, \quad A = 0{\cdot}0063_3 \text{ gm. mol./litre.}$$

Hence it is deduced that

$$\tau_{pr.} = 0{\cdot}001 \text{ sec.}$$

The results of the dynamical measurements are given below :—

Concentration (gm. mol./litre) of solution.	Static value of surface tension (dynes /cm.).	Time to edge of liquid disk (sec.).	Surface tension (dynes/cm.).	Temperature (° C.).
0·0189	47·2 at 19·4° C.	0·0098	51·0±0·4	20
0·0170	48·6 at 17·8° C.	0·0101	51·4±0·4	17
		0·0110	51·7±0·2	18

In these instances the surface tension has gone 84·8 per cent. of the way to the static value in an effective time of 0·0033 sec., 89 per cent. in 0·0034 sec., and 87·5 per cent. in 0·0037 sec., giving these observed values of the characteristic time, namely,

$$\tau_{obs.} = 0{\cdot}001,1_7 \text{ sec.}, \quad 0{\cdot}000,8_7 \text{ sec.}, \quad \text{and } 0{\cdot}001,0_9 \text{ sec.}$$

respectively. The mean of the three,

$$\tau_{obs.} = 0{\cdot}001,0_4 \pm 0{\cdot}000,0_6 \text{ second,}$$

is in very good agreement with the predicted value.

n-Heptyl Alcohol in Water.

No data were available for the (surface tension/concentration) curve, so measurements were made by the capillary tube method. A check was also obtained by making one determination with a stalagmometer, using the method and corrections given by Harkins and Brown [18]. The results were as follows :—

Concentration (gm. mol./litre).	Static surface tension (dynes/cm. at 13° C.).
0·00171	60·0
0·00310	52·7
0·00342	50·2
0·00620	44·8
0·00660	42·3
0·00696	43·0 (stalagmometer).

Hence the constants in equation (4) are found to be

$$B = 0{\cdot}31_0 \text{ and } A = 0{\cdot}0021 \text{ gm. mol./litre.}$$

From the data and equation (3) we find $\tau_{pr} = 0{\cdot}017$ second. The results of the experiments were as follows :—

Concentration (gm. mol./litre) of solution.	Static value of surface tension (dynes/cm.).	Time to edge of liquid disk (sec.).	Surface tension (dynes/cm.).	Temperature (° C.).
0·00598..	44·3 at 12·6° C.	0·0089	60·7±0·6	12·3
0·00520..	46·0 at 15·0° C.	0·0099	61·0±0·6	15·5

The surface tension has passed 45·1 per cent. and 46·2 per cent. of its way towards the final value in effective times of 0·0030 and 0·0033 second, giving a characteristic time, $\tau_{obs.} = 0{\cdot}011$ second in each case. This is the only instance (except for the concentrated solution of "Lux") in which the surface tension decreases appreciably more rapidly than had been predicted by the theory.

Decylic Acid in Water.

The results of Harkins and King's [19] work on the change of surface tension of a 0·000,064 gm. mol./litre solution of decylic acid in water were examined in the light of the above theory.

The constants of Szyszkowski's equation are $A = 0{\cdot}000{,}05$ gm. mol./litre and $B = 0{\cdot}3$, so that $\tau_{pr.} = 28$ seconds (approximately).

Calculation from the (surface tension/time) curve give the results :—

Time (seconds).	Surface tension (dynes/cm.).	Per cent. of way to static value.	t/τ.	$\tau_{obs.}$ (seconds).
0	72·8	0	—	—
30	65·7	42	0·23	130
60	62·0	63·9	0·82	73
300	58·2	86·5	3·12	96
480	57·6	90	4·2	114
1800	56·0	99·5	—	—
	55·9 *	100	—	—

* Extrapolated.

The average of the observed values of the characteristic time is $\tau_{obs.} = 103$ seconds. The predicted and observed values are of the same order of magnitude, though not in close numerical agreement.

Other Aqueous Solutions.

Experiments on the change with time of the surface tension of aqueous solutions of cetyl pyridinium bromide have been made by N. K. Adam [20] and R. C. Brown [21]. The curves differ appreciably from the form given by equation (10) (see fig. 3). Moreover, the mean of the values of $\tau_{obs.}$ deducible from the measurements is much

Fig. 3.

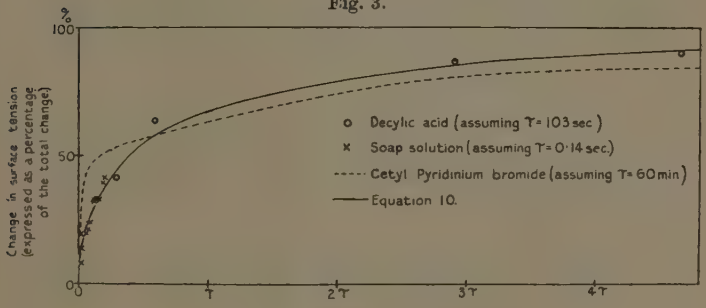

greater than our estimate of $\tau_{pr.}$ In estimating $\tau_{pr.}$, however, we have been obliged to use the value of $\left(\frac{\gamma_0 - \bar{\gamma}}{\bar{c}}\right)^2$ in place of $(d\bar{\gamma}/d\bar{c})^2_{c \to 0}$ in equation (3), as no data were available for the latter. Now, according to Adam [20], the ultimate surface tensions of the various solutions he used were nearly the same as one another. Hence we can conclude that the $(\bar{\gamma}, \bar{c})$ curve falls rapidly near the origin and later flattens out. The slope near the origin will be greater than our estimate. Consequently the time value of $\tau_{pr.}$, which is proportional to the square of the slope, will be greater than our estimate.

Measurements on the change with time of the surface tension of an aqueous solution of " Benzopurpurin 6 B " have been made by K. S. Gururaja Doss [22]. Again

we find that $\tau_{obs.}$ is much greater than $\tau_{pr.}$, but in this case also we have not the data necessary to estimate $\tau_{pr.}$ properly.

The Shape of the (γ, t) *Curves.*

Our data for soap solutions and Harkins and King's [19] data for decylic acid solutions give curves that agree in shape with the curve given by equation (10). This agreement is illustrated in fig. 3. The diagram also indicates the way in which the curve for cetyl pyridinium bromide differs in shape from our theoretical curve. The data for "Benzopurpurin 6 B" given by K. S. Gururaja Doss [22] do not include an estimate of the ultimate value of the surface tension, so we are unable to compare this curve with our theory. It is noticeable, however, that the curve given for "Benzopurpurin 6 B" does not commence by descending vertically as does our theoretical curve. On the other hand experimental curves (given in the same paper [22]) for the increase in surface concentration with time *do* indicate a rapid initial rise.

Conclusions.

The chief results of the investigations may be summarized as follows :—

1. The surface tension of a pure liquid (not a solution) attains its final value in a very short time (in 0·005 second, and quite probably in 10^{-9} second).

2. New surfaces of aqueous solutions have a surface tension equal to that of water.

3. For the solutions the surface phase (the ultimate concentration of which is given by Gibbs's equation) is gradually formed. Initially the rate of change of surface tension (and of surface concentration) is sensibly infinite.

4. The subsequent decrease in the rate of change of surface tension is chiefly due to the time required for solute to arrive at the boundary by diffusion from inside the liquid (Milner's hypothesis).

5. The characteristic time (during which the first 68 per cent. of the change takes place) is given (at any rate approximately) by equation (3).

6. The fraction of the transition that has occurred after any specified time is given (at any rate approximately) by equation (10).

7. Exceptional cases, in which the transition occurs at a slower rate than had been predicted, may give evidence of association of the molecules of the solute.

8. The observations on rather concentrated solutions are in fair accord with the theory developed for weak solutions. An attempt to extend the theory to the case when the solutions are concentrated did not help in explaining the experimental results.

Acknowledgments.

We have pleasure in thanking Prof. J. A. Crowther, in whose laboratories this work has been carried out, for his continued interest in the work.

To Dr. Paul White we are indebted for much help, particularly in regard to the solution of differential equations. Our thanks are also due to Mr. J. S. Burgess, the laboratory steward, who has been of assistance in the construction of apparatus.

References.

(1) Rayleigh, Proc. Roy. Soc. xxix. p. 71 (1897).
(2) P. O. Pederson, Phil. Trans. A, ccvii. p. 341 (1907).
(3) N. Bohr, Phil. Trans. A, ccix. p. 281 (1909).
(4) J. Satterly and J. C. Strachan, Roy. Soc. Can. Trans. xxix. p. 105 (1935).
(5) W. N. Bond, Proc. Phys. Soc. xlvii. p. 549 (1935).
(6) H. O. Puls, Phil. Mag. (7) xxii. p. 970 (1936).
(7) R. Hiss, Diss., Heidelberg, 1913.
(8) F. Schmidt and H. Steyer, *Ann. d. Phys.* lxxix. p. 442 (1926).
(9) E. Buchwald and H. König, *Ann. d. Phys.* (5) xxvi p. 659 (1936).
(10) W. Gibbs, Collected Papers, i. p. 233 (1913).
(11) J. W. MacBain and R. C. Swain, Proc. Roy. Soc. cliv. p. 608 (1936).
(12) I. Langmuir, Amer. Chem. Soc. J. xxxix., ii. p. 1848 (1917).
(13) S. R. Milner, Phil. Mag. (6) xiii. p. 102 (1907).
(14) Szyszkowski, *Z. phys. Chem.* lxiv. p. 385 (1908).
(15) A. Dupré, ' Théorie Méchanique de la Chaleur,' Paris (1869).
(16) Rayleigh, Proc. Roy. Soc. xlvii. p. 281 (1890).
(17) J. Edwards, Chem. Soc. cxxvii. p. 744 (1925).
(18) W. D. Harkins and F. E. Brown, Amer. Chem. Soc. J. xli. p. 499 (1919).

(19) W. D. Harkins and King, Kansas State Agr. Coll., Tech. Bull. No. 9.
(20) N. K. Adam, Trans. Farad. Soc. xxxi. p. 204 (1935).
(21) R. C. Brown, Proc. Phys. Soc. xlviii. p. 312 (1936).
(22) K. S. Gururaja Doss, Proc. Ind. Acad. Sci. iv. p. 97 (1936).

Department of Physics,
The University of Reading.
June 17th. 1937.

Obituary Notice.

While this paper was passing through the press the early death of Dr. W. N. Bond has been reported to us. We greatly sympathise with his relatives and friends on their bereavement and purpose to deal with the matter further in a later issue.—A. W. P.

LXXVIII. *On Bessel Product Functions.*

By Prof. Pierre Humbert *.

In a very interesting paper which appeared in Phil. Mag. p. 310 (1936), Dr. Costello has introduced four new functions defined by the following equations:

$$\mathrm{X}_n^b(x)=\mathrm{ber}_n^2(x)+\mathrm{bei}_n^2(x),$$
$$\mathrm{V}_n^b(x)=\mathrm{ber}_n'^2(x)+\mathrm{bei}_n'^2(x),$$
$$\mathrm{Z}_n^b(x)=\mathrm{ber}_n(x)\mathrm{ber}_n''(x)+\mathrm{bei}_n(x)\mathrm{bei}_n''(x),$$
$$\mathrm{W}_n^b(x)=\mathrm{ber}_n(x)\mathrm{bei}_n'(x)-\mathrm{bei}_n(x)\mathrm{ber}_n'(x),$$

which he named "Bessel product functions." I propose to make here two remarks concerning (*a*) the hypergeometric nature of these functions, and (*b*) their operational representation.

(*a*) The expansions in infinite series of the four above functions, as given by Dr. Costello, suggest at once that they can be expressed through hypergeometric functions. For instance, we have

$$\mathrm{X}_n^b(x)=\sum_0^\infty \frac{\left(\frac{x}{2}\right)^{2n+4r}}{r!\,(n+r)!\,(n+2r)!},$$

* Communicated by Prof. E. T. Whittaker.

and a very simple transformation shows that we can write

$$X_n^b(x) = \frac{x^{2n}}{2^{2n} n\,!\; n\,!}\,{}_0F_3\left(n+1,\ \frac{n}{2}+1,\ \frac{n}{2}+\frac{1}{2};\ \frac{x^4}{2^6}\right).$$

Similarly, we have

$$W_n^b(x) = \frac{x^{2n+1}}{2^{2n+1} n\,!\,(n+1)\,!}\,{}_0F_3\left(n+1,\ \frac{n}{2}+1,\ \frac{n}{2}+\frac{3}{2};\ \frac{x^4}{2^6}\right)$$

and so on. From these formulæ we can obtain readily a number of properties for the new functions, such as their differential equations (of the fourth order), and recurrence formulæ.

(*b*) If in the above hypergeometric formula for X we replace $\frac{x}{2^6}$ by x^2, we find

$$X_n^b(2\sqrt{2x}) = \frac{2^n x^n}{n\,!\; n\,!}\,{}_0F_3\left(n+1,\ \frac{n}{2}+1,\ \frac{n}{2}+\frac{1}{2};\ x^2\right).$$

We can now use a well-known formula of Heaviside symbolic calculus, namely,

$$p^{-m}\Gamma(m+1)\,{}_{r+2}F_s\left(\frac{m}{2}+1,\ \frac{m}{2}+\frac{1}{2},\ \alpha, \ldots;\ \gamma, \ldots;\ \frac{4}{p^2}\right) \doteqdot x^m\,{}_rF_s(\alpha, \ldots;\ \gamma, \ldots;\ x^2),$$

and write

$$X_n^b(2\sqrt{2x}) \doteqdot \frac{2^n}{n\,!\; n\,!}\,p^{-n}\Gamma(n+1)\,{}_2F_3\left(\frac{n}{2}+1,\ \frac{n}{2}+\frac{1}{2};\ \frac{n}{2}+1,\ \frac{n}{2}+\frac{1}{2},\ n+1;\ \frac{4}{p^2}\right)$$

or

$$X_n^b(2\sqrt{2x}) \doteqdot \frac{2^n}{n\,!}\,p^{-n}\,{}_0F_1\left(n+1;\ \frac{4}{p^2}\right).$$

This very simple operational formula can be written

$$X_n^b(-2\sqrt{2ix}) \doteqdot (-1)^n 2^n J_n\left(\frac{4}{p}\right),$$

where J_n is the ordinary Bessel function.

Let us write a property of the function X_n, which is certainly unknown, and which is easily obtained through

symbolic calculus; if we consider the Bessel functions of third order *, $J_{m,n}$, we have the symbolic image

$$J_n\left(-2\sqrt{\frac{1}{p}}\right) \doteqdot J_{2n,n}(3\sqrt[3]{x}).$$

But if $f(p) \doteqdot h(x)$, we have

$$f(\sqrt{p}) \doteqdot \frac{1}{\sqrt{\pi x}}\int_0^\infty e^{-\frac{s^2}{4x}} h(s)\,ds.$$

Hence the result

$$J_{2n,n}(3\sqrt[3]{x}) = \frac{(-1)^n}{\sqrt{\pi x}}\int_0^\infty e^{-\frac{s^2}{4x}} X_n^b(-2\sqrt{2is})\,ds.$$

LXXIX. *The Refractive Index of the Alkali Halides at Low Concentrations. By* L. W. Parkin, *M.Sc., University College, Exeter* †.

1. *Introduction.*

THE molecular refractivity R of an aqueous solution is obtained by means of the expression

$$R = \frac{M}{x}\left(\frac{n_s^2-1}{n_s^2+2}\cdot\frac{100}{d_s} - \frac{n_w^2-1}{n_w^2+2}\cdot\frac{100-x}{d_w}\right),$$

where

x = percentage of salt by weight in 100 gm. of solution,
n_s = refractive index of solution,
n_w = refractive index of water,
d_s = density of solution,
d_w = density of solvent,
M = molecular weight of salt.

Measurements of this quantity for solutions of varying concentration furnish valuable information regarding ions in solution. Departures from additivity of this function indicate the existence of mutual action both among the ions themselves and between the ions and water molecules.

* P. Humbert, *Atti Pontif. Accad. Scienze*, anno 83, 1930, and anno 87, 1934.

† Communicated by Prof. F. H. Newman, D.Sc.

Recently a great deal of work has been done in this direction by Fajans, Geffcken *, Brodsky and Scherschewer † and co-workers, but, except in a few isolated cases, values are not available for solutions below a concentration of ·001 normal.

Measurements of the refractivity of dilute solutions entail methods in which the difference δn of the refractive indices and the difference δd of the densities of solution and solvent must be observed with great precision. For example, Kohner ‡ has shown that for concentrations of the order 10^{-1} to 10^{-2} gram molecules per litre the values of δn and δd must be measured with a precision of the order 10^{-6} to 10^{-7}. The measurement of δn to such a high order of accuracy can be made with an interferometer type of apparatus, and does not present such difficulties as are met with in the determination of δd.

Now we may represent the refractivity of a dissolved substance as the sum of two factors, viz. :—

$$\psi(C_v\,\delta n) \quad \text{and} \quad \phi(C_v\,\delta d),$$

where

$$\psi = \frac{1000}{C_v}\left(\frac{n^2-1}{n^2+2} - \frac{n_0^2-1}{n_0^2+2}\right),$$

$$\phi = \frac{n_0^2-1}{n_0^2+2}\left(\frac{M}{d_0} - \frac{1000\,\delta d}{C_v\,d_0}\right),$$

n and n_0 being the refractive indices of a solution and solvent respectively of concentration C_v gram molecules per litre. To first approximation we may take

$$R = \psi + \phi = \text{const.},$$

so that to this degree of accuracy the ψ and ϕ curves are symmetrical with respect to the concentration axis. Since it is very difficult to determine the function ϕ at concentrations below 0·001 normal, whereas by interferometer measurements the determination of ψ presents no great difficulty, it was decided to measure δn for various very dilute electrolytic solutions.

The alkali halides in aqueous solution were chosen, since, containing univalent ions, they probably form the simplest ionic solutions.

* *Zeits. f. Phys. Chem.* xxiii. p. 175 (1933).
† *Ibid.* xxiii. p. 412 (1933).
‡ *Ibid.* i. p. 427 (1928).

2 *Experimental Technique.*

A standard Hilger Rayleigh refractometer was employed to measure the refractive indices, using white light to obtain the fringes. One half of the cell contained distilled water, the other the solution whose refractive index was to be determined.

For the low concentrations used the relative retardation between the two beams of light, caused by the difference in the refractive indices of the solutions and distilled water, was very small, the largest, produced by 0·002 normal cæsium iodide solution, being less than one D line sodium wave-length. Due to this, special precautions had to be taken in the measurement of the fringe shift to reduce all errors to a minimum.

In the first place, to obviate any errors due to slight irregularities in the thickness of the cell, it was firmly fixed in position on the refractometer. Both sides of the cell were thoroughly cleaned and filled with distilled water from a special container, which was filled at the beginning of each set of experiments, and which held sufficient for the one sample from the still to be used as a standard throughout. When the temperatures of both sides of the cell were constant and equal a set of ten drum readings, corresponding to coincidences of both sets of fringes, was taken, the mean value being obtained. Before proceeding to use the samples of solutions of different strengths the solution compartment of the cell was emptied, again cleaned, and refilled with a second sample of distilled water. Another set of readings was taken, giving in all twenty values, the mean of which was taken as the zero position for subsequent measurements. On completing these measurements the distilled water was removed from the solution compartment of the cell and the latter thoroughly washed out with the first of the solutions to be used. It was then filled with a sample of the solution under test, and conditions again allowed to settle. In general half an hour was allowed between filling the cell and taking the first reading. The temperatures being constant and equal a series of readings of the drum was taken for this sample, as in the case with distilled water. This was repeated with a second sample of the same solution, the mean of twenty results being obtained.

Since it was impossible to use all the solutions of different concentrations in one day four or five were chosen,

well spaced over the concentration range. Readings were taken for these solutions in the manner already described, using the various solutions in the order of increasing concentration. The work was repeated with the solutions in the reverse order. This was repeated on successive days, using a different set of concentrations, but always beginning and ending with distilled water in both sides of the cell. This method of procedure was preferred, since any systematic error which might be introduced from day to day would be distributed at various points over the concentration range and not be confined to any part of it. Thus values of the refractive index of at least four samples of solution of each concentration were obtained, and, in addition, the results were checked by repeating the measurements rapidly, using one sample only of each solution. In general all the values so obtained for the various samples of each solution agreed well with each other.

Separate pipettes were used for the distilled water and the solution. Great care was exercised in ensuring that no inaccuracies were introduced on account of small residues of samples of different concentration from the one under test being left in that part of the cell containing the solutions.

The temperature of the cell and solution was maintained constant to within 0·1° C. throughout a set of experiments. Further, it was noted that providing the temperature of the two halves of the cell remained equal a slight variation in the temperature produced no measurable effect on the position of the fringes. This is to be expected, since we are concerned with the difference between the temperature coefficients for the water and the solutions, which, for the very small concentrations used, would be of the second order of smallness. It was thus decided to take readings when the temperature of the two halves of the cell were equal, providing there was no appreciable deviation of this temperature from the average value.

The drum of the refractometer was standardized by means of the D lines of sodium, readings of consecutive coincidences of the two sets of fringes being plotted against the number of the coincidence. The curve was linear, and over the range used seventeen drum divisions are equivalent to a relative retardation of one wave-length of sodium light. In setting the drum to observe coincidence

of the two sets of fringes it was ensured that the drum was always rotated in the same direction.

The refractometer and source of light were adjusted at the beginning of the experiments, and were fixed on a table, so that with the cell in position the paths of the two interfering beams remained constant except for changes in the refractive index of the solution.

In making up the solutions distilled water from one still was prepared in large quantities, and solutions were prepared from the one sample. With all the salts used an accurate decinormal solution was prepared, chemically pure salt being used. It was ensured that the salt was free from moisture by prolonged heating prior to the weighing out of the salt and the preparation of the solution. Since potassium fluoride is very hygroscopic special precautions had to be taken in preparing a standard solution of this salt.

A solution of concentration 0·01 normal was prepared from the accurate 0·1 normal solution, this being used as a substandard. All the other solutions were made from this substandard solution, although 0·001 normal solution, prepared from this standard, was employed for making all the solutions of lower concentration. The measuring flasks and pipettes used were certified by the National Physical Laboratory, and great care was taken in preparing each solution to ensure that the more concentrated solution from which it was diluted was thoroughly mixed. The preparation of more dilute solutions was deferred until this latter solution was homogeneous. This was ensured by periodically shaking the solutions and allowing them to stand for an interval. In general two days were allowed to elapse between preparing and using any solution. Any error in concentration could only be due to an error in the decinormal solution first prepared, and it is probable that the relative concentrations are accurate to a high degree.

The main source of error in the measurements made lies in the matching of the two sets of fringes to a sufficiently accurate degree. The smallest value of δn observed for ·0001 normal LiF solution was $0{\cdot}69\times10^{-6}$. This corresponds to a drum difference of 0·2 or 1/80 of a fringe shift. At these low concentrations great difficulty was experienced in making accurate measurements of the extremely small fringe shift. It was found that in a

series of observations variations in the drum readings were likely to be as large as $\pm 0{\cdot}1$, but in general the values for any series of observations were very constant. When working with higher concentrations this discrepancy has less effect, and the percentage error for these stronger solutions was much smaller.

3. *Experimental Results.*

The refractive indices of the solutions were calculated from the observed mean difference δr between the drum reading corresponding to coincidence of the two sets of fringes with distilled water in one half of the cell and the solution in the other, and that corresponding to coincidence of the two sets of fringes with distilled water in both halves of the cell. The equation employed was

$$\delta n = \frac{\delta r}{t \times 17} \times 5893 \times 10^{-8},$$

where t is the thickness of the cell in cm., which in the instrument used was unity. The refractive index of water for the yellow D lines of sodium 5893 Å.U. is given by *

$$n_t = n_{20} - 10^{-5}[0{\cdot}124(t-20) + {\cdot}1993(t^2-400) - 5{\cdot}10^{-6} \times (t^4-160{,}000)],$$

where $n_{20} = 1{\cdot}333000$, the value of the refractive index of distilled water at a temperature of 20° C. The experiments were carried out at a room-temperature of 18° C., for which temperature n_{18}, obtained from the above expression, is 1·333151.

Since

$$\psi = \frac{1000}{c_v}\left(\frac{n^2-1}{n^2+2} - \frac{{n_0}^2-1}{{n_0}^2+2}\right),$$

if we denote the difference $n-n_0$ by δn, it is evident that we may put

$$\psi = \frac{1000}{C_v}\left[\frac{(n_0+\delta n)^2-1}{(n_0+\delta n)^2+2} - \frac{{n_0}^2-1}{{n_0}^2+2}\right]$$

and expand $\dfrac{(n_0+\delta n)^2-1}{(n_0+\delta n)^2+2}$ by Taylor's Theorem.

* Int. Crit. Tables, vii. p. 13.

Thus we have, putting

$$f(n_0)=\frac{n_0^2-1}{n_0^2+2} \quad \text{and} \quad f(n_0+\delta n)=\frac{(n_0+\delta n)^2-1}{(n_0+\delta n)^2+2},$$

$$f(n_0+\delta n)=f(n_0)+\delta n\frac{df(n_0)}{dn_0}+\frac{\delta n^2}{2}\cdot\frac{d^2f(n_0)}{dn_0^2}+\ldots,$$

and

$$\psi=\frac{1000}{C_v}\left[\delta n\frac{df(n_0)}{dn_0}+\frac{\delta n^2}{2}\frac{d^2f(n_0)}{dn_0^2}+\frac{d^3f(n_0)}{dn_0^3}+\ldots\right]$$

$$=\frac{1000}{C_v}\left[\delta n\frac{6n_0}{(n_0^2+2)^2}-\delta n^2\frac{9n_0^2-6}{(n_0^2+2)^3}+12\delta n^3\frac{n_0^3-2n_0}{(n_0^2+2)^4}+\ldots\right].$$

Substituting for n_0 the value obtained above, 1·333151, we have

$$\psi=\frac{1}{C_v}[560\cdot68\delta n-185\cdot50\,\delta n^2+17\cdot55\,\delta n^3\ldots].$$

The maximum value obtained for δn throughout the experiments was $5\cdot1998\times10^{-5}$. It is obvious then that in this expression for ψ we need only take into account the first term, so that we finally obtain

$$\psi=\frac{1}{C_v}[560\cdot68\,\delta n].$$

From the values of δn obtained for the various solutions ψ was calculated by means of this expression, the results obtained being shown in Tables I. to VII.

TABLE I.

Values of δn and ψ for Cæsium Chloride Solutions.

Concentration of solution (normal).	Difference between zero and drum readings for solution.	Values of $\delta n\times10^6$.	Values of ψ (refractivity function).
·002	7·4	25·6	7·18
·0016	6·5	22·5	7·58
·0013	5·7	19·8	8·31
·001	4·5	15·6	8·75
·0008	3·9	13·5	9·47
·0006	3·0	10·4	9·72
·0005	2·5	8·7	9·72
·0004	2·0	6·9	9·72

TABLE II.

Values of δn and ψ for Lithium Fluoride Solutions.

Concentration of solution (normal).	Difference between zero and drum readings for solution.	Values of $\delta n \times 10^6$.	Values of ψ (refractivity function).
·002	2·8	9·7	2·7
·0016	2·5	8·7	2·8
·0013	2·1	7·3	3·1
·001	1·6	5·5	3·1
·0009	1·5	5·2	3·2
·0008	1·3	4·5	3·2
·0007	1·1	3·8	3·1
·0006	1·0	3·5	3·2
·0005	·8	2·8	3·1
·0004	·7	2·4	3·2
·0003	·5	1·7	3·2
·0002	·3	1·0	3·0

TABLE III.

Values of δn and ψ for Sodium Fluoride Solutions.

Concentration of solution (normal).	Difference between zero and drum reading for solution.	Values of $\delta n \times 10^6$.	Values of ψ (refractivity function).
·002	3·4	11·80	3·30
·0016	3·0	10·4	3·5
·0013	2·5	8·7	3·8
·001	2·0	6·9	3·9
·0009	1·8	6·3	3·9
·0008	1·6	5·6	3·9
·0007	1·4	4·9	3·9
·0006	1·2	4·2	3·9
·0005	1·0	3·5	3·9
·0004	·8	2·8	3·9
·0003	·6	2·1	3·9
·0002	·4	1·4	3·9

TABLE IV.

Values of δn and ψ for Potassium Fluoride Solutions.

Concentration of solution (normal).	Difference between zero and drum reading for solution.	Values of $\delta n \times 10^6$.	Values of ψ (refractivity function).
·002	4·2	14·56	4·08
·0016	3·7	12·82	3·31
·0013	3·0	10·75	4·50
·001	2·4	8·1	4·65
·0009	2·2	7·6	4·7
·0008	1·9	6·6	4·6
·0007	1·7	5·9	4·7
·0006	1·4	4·9	4·6·
·0005	1·2	4·2	4·7
·0004	1·0	3·5	4·8
·0003	·7	2·4	4·6
·0002	·5	1·7	4·8

TABLE V.

Values of δn and ψ for Sodium Iodide Solutions.

Concentration of solution (normal).	Difference between zero and drum reading for solution.	Values of $\delta n \times 10^6$.	Values of ψ (refractivity function).
·002	11·8	40·91	11·47
·0016	10·4	36·05	12·13
·0013	8·6	29·8	12·54
·001	6·5	22·5	12·66
·0009	5·8	20·1	12·52
·0007	4·6	15·9	12·8
·0006	4·0	13·9	12·9
·0004	2·6	9·0	12·7
·0002	1·3	4·5	12·7

TABLE VI.

Values of δn and ψ for Potassium Iodide Solutions.

Concentration of solution (normal).	Difference between zero and drum reading for solution.	Values of $\delta n \times 10^6$.	Values of ψ (refractivity function).
·002	12·4	42·98	12·05
·0016̇	10·8	37·4	12·59
·0013̇	9·0	31·2	13·12
·001	7·0	24·3	13·61
·0009	6·2	21·5	13·39
·0008	5·6	19·4	13·6
·0007	5·0	17·3	13·6
·0006	4·2	14·6	13·6
·0005	3·5	12·1	13·6
·0003	2·1	7·3	13·6
·0002	1·4	4·9	13·6

TABLE VII.

Values of δn and ψ for Caesium Iodide Solutions.

Concentration of solution (normal).	Difference between zero and drum reading for solution.	Values of $\delta n \times 10^6$.	Values of ψ (refractivity function).
·002	15·0	52·0	14·58
·0016̇	12·8	44·4	14·94
·0013̇	10·7	37·1	15·60
·001	8·1	28·1	15·69
·0009	7·3	25·3	15·76
·0008	6·5	22·5	15·8
·0007	5·7	19·6	15·7
·0006	4·9	17·0	15·8
·0005	4·0	13·9	15·6
·0004	3·1	10·8	15·6
·0003	2·3	8·2	16·0
·0002	1·6	5·6	15·6

The difference δn between the refractive index of the solution and that of water was plotted as a function of the square root of the concentration $\sqrt{C_v}$, the results being shown in figs. 1 and 2. The refractivity function ψ was plotted as a function of the reciprocal of the square root of the concentration $\frac{1}{\sqrt{C_v}}$; the curves obtained are shown in figs. 3 and 4.

Fig. 1.

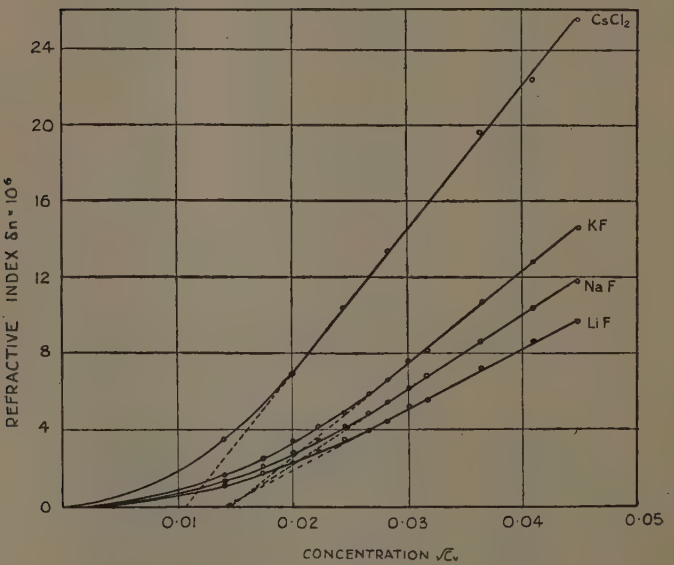

Variation of the refractive index with concentration.

3 *Discussion of Results.*

(a) *Variation of Refractive Index with Concentration.*

An interesting feature in figs. 1 and 2 is the linear relationship between δn and $\sqrt{C_v}$, which extends in all cases from the highest concentrations employed, viz., 0·002 normal down to a concentration which varies with the type of salt in the solution. For the three iodides, CsI, KI, and NaI, the linear relationship ceases at a

concentration approximately 0·0008 normal in the three cases. After this the curve approaches asymptotically the $\sqrt{C_v}$ axis. With the fluorides the linear relationship between δn and $\sqrt{C_v}$ holds from 0·002 normal down to 0·0007 normal, and for weaker solutions the curves approach the $\sqrt{C_v}$ axis asymptotically. Since the refractive index, or, rather, δn, is not a characteristic property of the constituents, such as, for example, is the refractivity, no useful theoretical results follow from these interesting features. It is noteworthy, however, that at any given

Fig. 2.

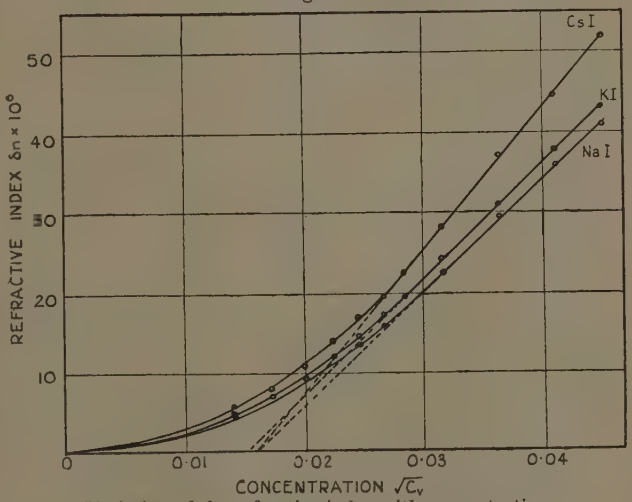

Variation of the refractive index with concentration.

concentration of the different electrolytic solutions there are the same number of ions per c.c., and therefore it appears that for the fluoride solutions some definite change in the ionic forces occurs at 0·0007 normal. This change may be in the degree, or disappearance altogether, of associated ions—*i. e.*, oppositely charged ions in contact—or in the number of water molecules associated with, or attached to, the individual ions. The fact that the departure from linear relationship in the case of the iodide solutions occurs at a higher concentration, viz., 0·0008 normal, may be attributed to the size of the iodide ion.

(b) *The Variation of ψ (Refractivity Function) with Concentration.*

Owing to the extremely small value of δn for the solutions of concentration below about 0·0008 normal a very slight experimental error in δn creates a large error in the value of ψ. For example, an error of 10^{-7} in the

Fig. 3.

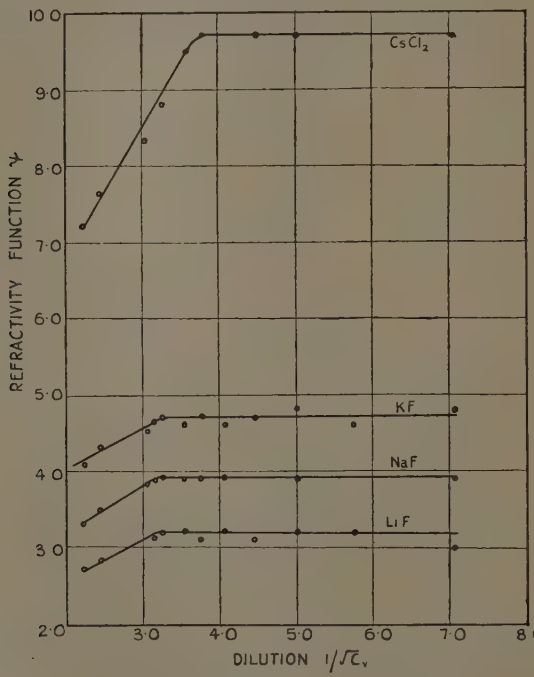

Variation of refractivity with concentration.

determination of δn—which is the limit of accuracy of measurement—at a concentration of 0·0002 normal represents an error of 0·2 in the subsequent value of ψ. Whereas at a concentration of 0·002 normal the limit of accuracy of ψ is 0·02, so it is to be expected that the values of ψ at the lowest concentration will be subject to considerable experimental errors. In general this is born out by the results obtained for ψ, as shown in figs. 3.

and 4. But the course of all these curves at the higher concentrations is linear, ψ increasing with dilution. With the fluorides for concentrations less than 0·0008 normal this linear relationship ceases, and ψ is approximately constant from this concentration to the greatest dilution used in the experiments. In the case of the iodides ψ also becomes constant for concentrations less than 0·0008 normal. Although, as was mentioned above, the experimental errors in the determination of δn for these very dilute solutions give rise to a considerable

Fig. 4.

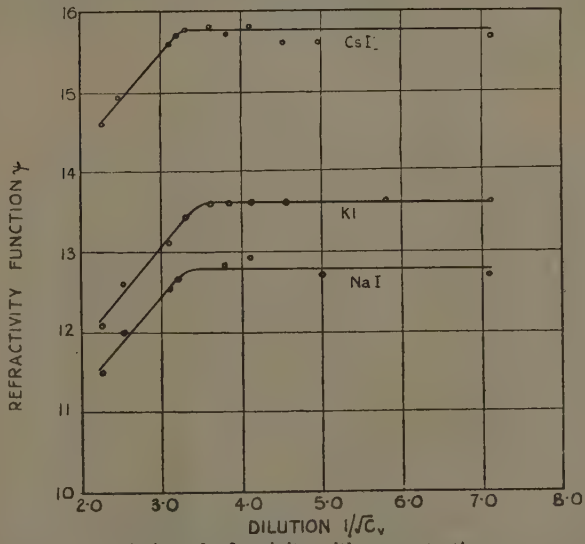

Variation of refractivity with concentration.

percentage error in the values of ψ, there is no doubt from the curves that ψ is constant, while in the cases of NaF and KI this constancy of ψ is most marked.

Another interesting feature is the difference between these constant values of ψ for salts containing either a similar cation or anion, *e. g.*,

$$\psi_{KF}-\psi_{NaF}= 4·7- 3·9=0·8,$$
$$\psi_{KI}-\psi_{NaI}=13·6-12·8=0·8,$$

and the difference, which must be attributed to the difference $\psi_{K^+}-\psi_{Na^+}$, is the same for the two sets of salts. This indicates that ionic deformation of any kind

must be absent, and we have the actual difference in the values of the function ψ for the K^+ and Na^+ ions.

Similarly,

$$\psi_{KI} - \psi_{KF} = 13{\cdot}6 - 4{\cdot}7 = 8{\cdot}9,$$
$$\psi_{NaI} - \psi_{NaF} = 12{\cdot}8 - 3{\cdot}9 = 8{\cdot}9.$$

The differences here are attributed to the difference $\psi_{I^-} - \psi_{F^-}$, and is the same for the two sets of salts. Again, the common difference represents the difference in the value of the function ψ for the I^- and F^- ions, and any deformation due to ionic forces must be absent.

For a strong electrolyte completely dissociated the Debye and Huckel theory requires the ϕ curve to approximate asymptotically to the limiting straight line on increasing dilution :

$$\phi = \phi_0 + a\sqrt{C_v},$$

but the theory has not yet been applied to the variation of ψ with concentration. If the refractivity is to be constant the refractivity function ψ should increase with dilution as found in the present experiments. Actually, recent experiments quoted in the introduction have shown that the refractivity for most strong electrolytes decreases with dilution for very highly diluted solutions, so the variation of ψ with C_v is unlikely to follow the complementary curve for the variation of ϕ with C_v. Actually, with the stronger solutions used in the present experiments ψ is inversely proportional to $\sqrt{C_v}$.

The constancy of ψ for the most dilute solutions is attributed to the absence of any type of deformation of the ions, whether due to the proximity of oppositely charged ions or whether due to ionic forces between the ions and the molecules. In other words, we have at these concentrations independent ionic action, *i. e.*, no associated ions or water molecules associated with ions, and the forces on any one particular ion due to the ionic cloud in the solution must be negligible.

I should like to express my gratitude to Professor F. H. Newman for suggesting this problem to me and for his interest and help during the time that the experiments were performed

I also wish to thank Col. Ransom Pickard, C.B., G.M.G., F.R.G.S., for the gift of the Hilger Rayleigh refractometer, with which this research was carried out, and also the College Council for a research scholarship.

LXXX. *Acoustical Experiments with Telephone Receivers.* —Part II. *By* E. Tyler, *D.Sc., M.Sc., F.Inst.P., A.F.R.Ae.S., Department of Physics, Leicester College of Technology.**

Part II.

IN this series of experiments, measurements of the velocity of sound in air contained in pipes and free space are made, employing a second telephone receiver purely as a detector of sound and in conjunction with a two-valve amplifier (fig. 10) and photronic cell rectifier.

Fig. 10.

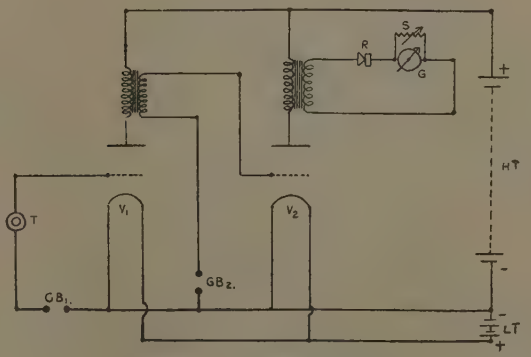

Diagram of detector circuit.

T = Telephone receiver.
V_1 = 4V. DEH ·1 valve.
V_2 = 4 V. DEP ·25 valve.
R = Photronic cell or Westinghouse rectifier.
G = Reflecting galvo.
S = Galvo shunt.

Near the resonant frequency of the receiver diaphragm, it is only necessary to use a simplified circuit comprising the telephone receiver, Westinghouse or Photronic cell rectifier, and reflecting galvanometer.

* Communicated by the Author.

Measurement of the Velocity of Sound in Air contained in Pipes by Dual Telephone Method.

(a) *Pipe Systems Used.*

Three different pipe systems were used, namely :

(1) Sliding pipes with telephone source at one end and receiver telephone at the other (fig. 11).
(2) Resonance tube with side tube leading to second telephone receiver (fig. 12).
(3) Quincke tube with source on one side and receiver connected to outlet tube on remote side (fig. 13).

Fig. 11.

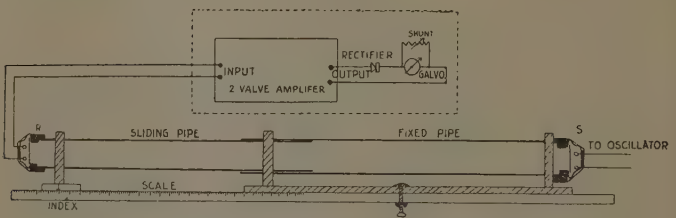

Sliding pipe—Dual telephone arrangement.

R = Telephone receiver.
S = Maintained source.
Same pipes as in Part I. Diameter = 3·80 cm.

Both telephones were freed from direct mechanical vibration transmitted by the source along the walls of the pipe by means of rubber washers placed between the free parts of the tubes and the casings of the telephones.

The methods of operating and controlling the frequency of the source by valve oscillator and neon tube were the same as in the first series of experiments (Part I.), likewise in the determination of the frequency stroboscopically. As a check on the mains frequency, a stroboscopic disk was run at a controlled constant speed by means of a gramophone turn-table, motor driven from the same A.C. supply as that energizing an Osglim lamp acting as the stroboscopic illuminant. The timing of a number of revolutions of the disk with an accurate reading stop-watch over a fairly long period indicated that the mains frequency could be relied upon to $50 \pm \cdot 02$ cycles/sec.

Fig. 12.

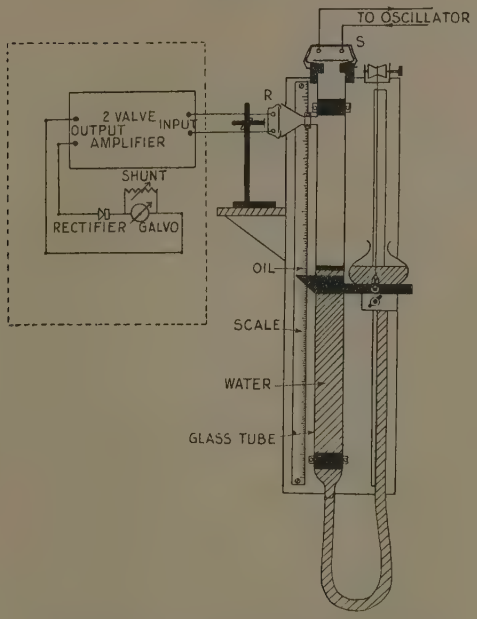

Resonance tube—Dual telephone arrangement.

S = Maintained source.
R = Receiver telephone.

Diameter of glass tube = 2·50 cm.

Fig. 13.

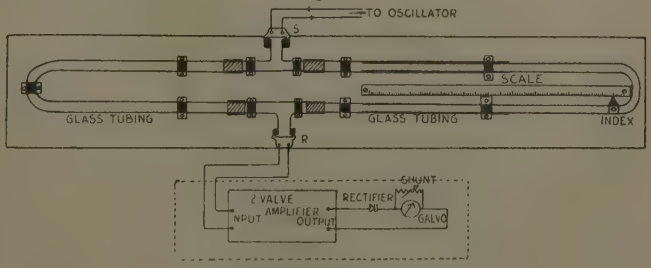

Quincke tube arrangement.

S = Maintained source.
R = Telephone receiver.

Diameter of sliding tube = 1·0 cm.

(b) *Determination of the Wave-length of Sound in Air contained in Pipes.*

It is obvious from the pipe systems employed (figs. 11, 12, & 13) that the aerial conditions affecting the vibrations of the second telephone receiver R are different in each case. Concerning the sliding pipes (fig. 11), when the distance between the source S and receiver R is equal to a number of half wave-lengths of the sound produced by the source, stationary waves are formed within the pipes. Now, the diaphragm of the receiver, since it is free to vibrate, will consequently respond to the pressure variations at that end of the pipe. Thus, as the pipe length is gradually increased, the pressure effects on the diaphragm vary periodically accordingly as we increase the pipe length by successive half wave-lengths. The resulting rectified currents passing through the receiver subsequently produce variations in galvanometer deflexions, and the response curves for increasing pipe lengths exhibit very marked maxima and minima (figs. 14 & 15). The distance between successive maxima (peaks) or minima is a measure of the half wave-length.

With regard to the resonance tube arrangement (fig. 12), the telephone receiver R responds to the resultant effect of the sound waves sent down the tube by the source and those arriving at R after being reflected at the other end of the pipe (*i. e.*, oil surface) *. When the two sets of waves arrive in phase at R, reinforcement takes place with maximum vibration of the diaphragm. If the wave trains arrive at R 180° out of phase, then minimum effect on the diaphragm is produced. Thus, as the length of air column is gradually increased, the effects at R on the diaphragm undergo periodic alternations accordingly as the path difference between the two sets of waves is increased by a wave-length, *i. e.*, as the length of air column is increased by successive half wave-lengths. The galvanometer response curves for varying lengths of air column again exhibit maxima and minima with separation distance between successive peaks equivalent to half wave-length (fig. 16). Maximum vibration of the diaphragm does not necessarily occur at resonance condition within the pipe. The condition for these two

* *Vide* N. W. Robinson, 'School Science Review,' xvii. no. 65 (Oct. 1935).

Fig. 14.

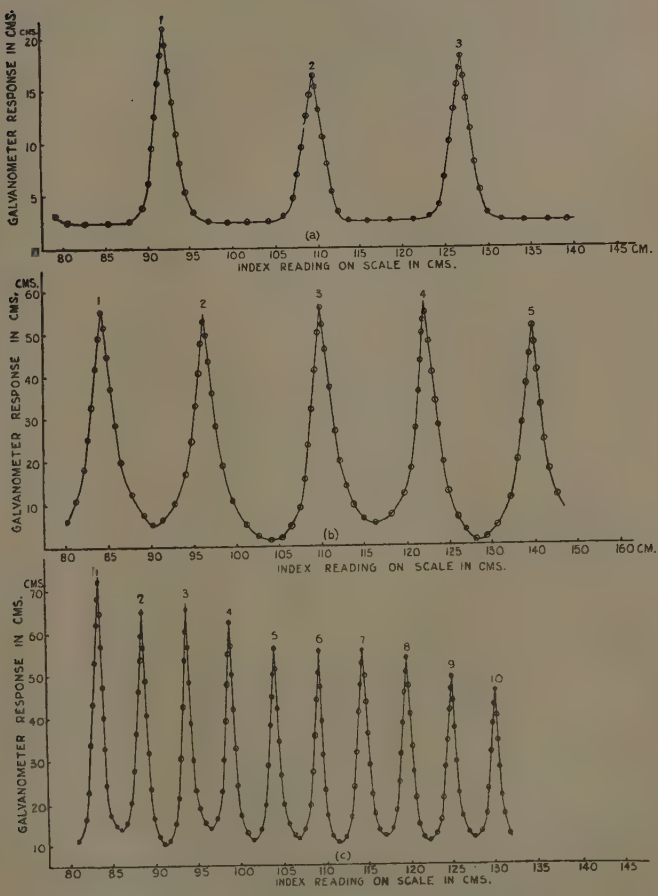

Sliding pipe results in air—Dual telephone method.
Valve oscillator controlled source.

(*a*) Rectifying circuit comprising double crystal, phones, and galvanometer only. N=990. Temp.=18·0° C. (See Table VI.)

(*b*) Two-valve amplifier and photronic cell rectification (fig. 10). N=1330. Temp.=18·5° C. (See Table VI.)

(*c*) Two-valve amplifier and photronic cell rectification. N=3260. Temp.=14·0° C. (See Table VI.)

effects to occur simultaneously depends upon the length of the air column between the source and the receiver, in addition to the length of the air column between the source and the oil surface.

Fig. 15.

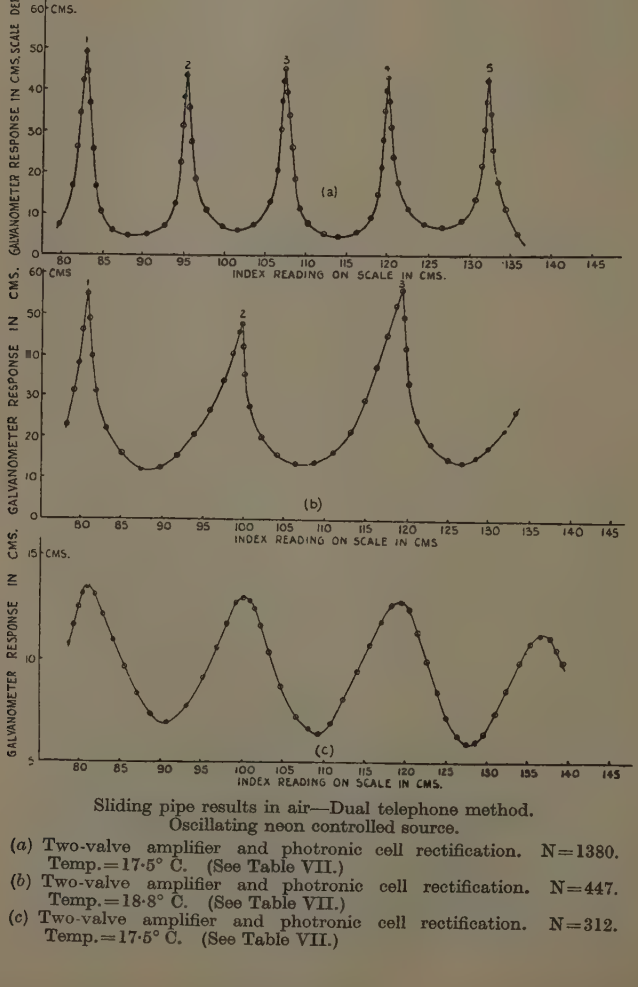

Sliding pipe results in air—Dual telephone method. Oscillating neon controlled source.

(*a*) Two-valve amplifier and photronic cell rectification. N=1380. Temp.=17·5° C. (See Table VII.)

(*b*) Two-valve amplifier and photronic cell rectification. N=447. Temp.=18·8° C. (See Table VII.)

(*c*) Two-valve amplifier and photronic cell rectification. N=312. Temp.=17·5° C. (See Table VII.)

The conditions producing maximum pressure variations at the receiver in the Quincke tube method is controlled by the two sets of waves arriving at R *via* the two branch paths. When the two wave trains arrive at R in phase, the resulting pressure changes reinforce each other, thus producing maximum effect on the diaphragm. Should they arrive at R 180° out of phase, minimum pressure variations are experienced by the diaphragm. Such

Fig. 16.

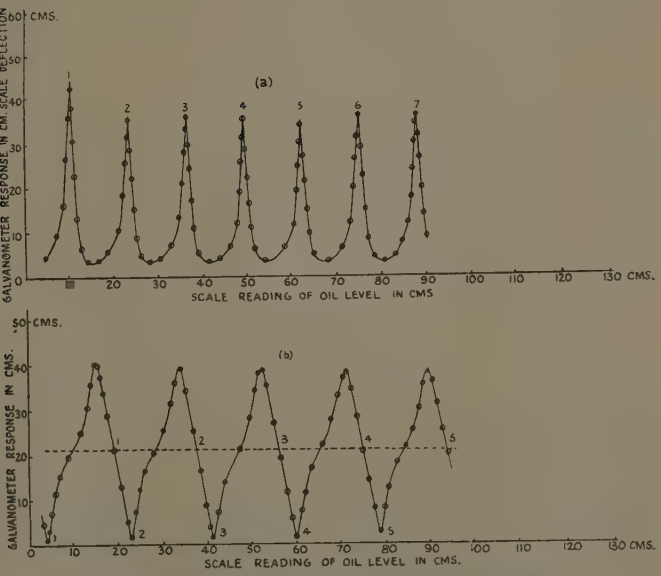

Resonance tube results in air—Dual telephone method.
Valve oscillator controlled source.

(*a*) Two-valve amplifier and photronic cell rectification. N = 1310. Temp. = 15·5° C. (See Table VIII.)
(*b*) Two-valve amplifier and photronic cell rectification. N = 905. Temp. = 14·5° C. (See Table VIII.)

maximum and minimum effects are produced when the path differences equal either a number of whole wave-lengths or odd number of half wave-lengths respectively. As the sliding tube is therefore moved so as to increase this path difference, the galvanometer response undergoes alternations in a like manner, and the response curves

Fig. 17.

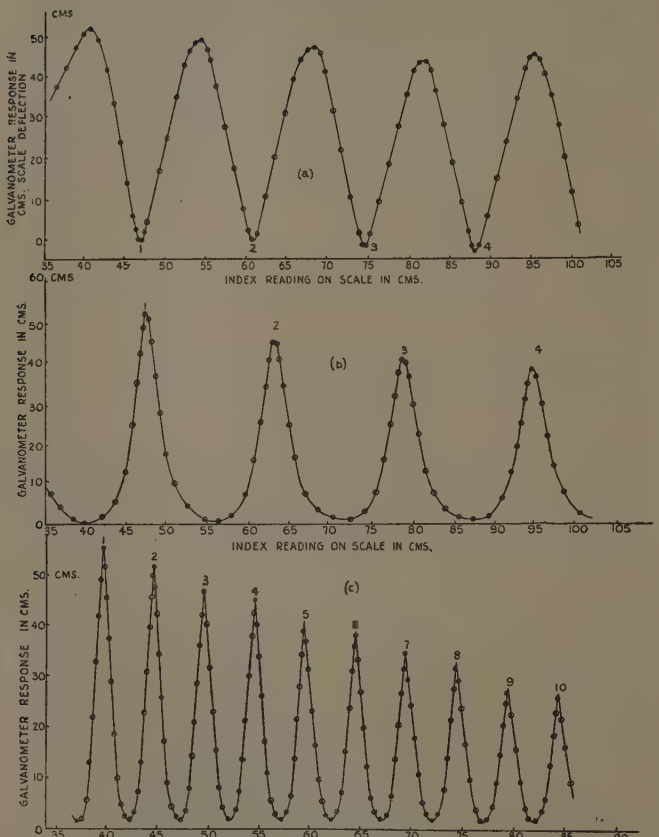

Quincke tube results in air—Dual telephone method.
Valve oscillator controlled source.

(*a*) Two-valve amplifier and photronic cell rectification. N=1237. Temp.=14·7° C. (See Table IX.)

(*b*) Rectifying circuit consisting of Westinghouse rectifier, telephone receiver, and galvanometer only. N=1064. Temp.=14·0° C. (Table IX.)

(*c*) Rectifying circuit consisting of Westinghouse rectifier, telephone receiver, and galvanometer only. N=3410. Temp.=14·0° C. (See Table IX.)

plotted as galvanometer deflexion against the index-mark reading also exhibit marked peaks (fig. 17), the distance between successive maxima being equivalent to one wave-length, since movement of the index mark by half a wave-length means an alteration in path difference of one whole wave-length.

(c) *Specimen Results for Velocity of Sound in Air contained in Pipes, using Dual Telephone Methods.*

Typical results for the sliding pipes are shown in figs. 14 & 15, and Tables VI. & VII. It will be observed the peaks of the response curves are much sharper than those obtained in the earlier experiments in which the reactive effects at the source are measured. When using the oscillating neon controlled source, we must operate it at a sub-multiple frequency of that natural to the receiver diaphragm at the other end of the pipe. Although the galvanometer deflexions are much bigger in comparison with those of the earlier experiments with the oscillating neon arrangement (Part I.), the peaks are not so sharp.

The resonance tube results are shown in figs 16 and Table VIII. Similar characteristics are exhibited as with the sliding pipe results, and excellent agreement is revealed in the computed values of the velocity of sound.

Concerning the Quincke tube results with the valve oscillator controlled source, these are included in fig. 17 and Table IX. In this set, excellent curves with very marked peaks are obtained (fig. 17 *b* & *c*), even when using the simplified rectifying circuit comprising a Westinghouse rectifier, telephone receiver, and reflecting galvanometer. There is a diminution in the galvanometer response as the length of air column in the sliding tube is increased, due to friction and absorption of energy by the walls of the tube. Such an effect is more marked in this series of results owing to the higher frequency and narrower tube employed, but it does not affect in any way the positions of the peaks.

Measurement of the Velocity of Sound in Free Air by a Dual Telephone Stationary Wave Method.

In Part I. a stationary wave method has been described employing a single telephone source in conjunction with

Table VI.

Sliding Pipe Results in Air—Dual Telephone Method.

Valve oscillator controlled source at one end of pipe.
Telephone receiver and amplifier at other end of pipe.

Response curve.	Number of peak.	Readings (cm.).	Wave-length λ (cm.).	Mean λ (cm.).	Temp. ($t°$ C.).	N.	V_t metres per sec.	V_0 metres per sec.
Fig. 14 *a*	1	92·50	(3)–(1)	34·50	18·0	990	341·5	330·9
	2	109·50	=34·50					
	3	127·00						
Fig. 14 *b*	1	84·30	(3)–(1)	35·75	18·5	1330	342·6	331·5
	2	96·50	=25·70					
	3	110·00	(4)–(2)					
	4	122·30	=25·80					
	5	*(135·00)						
			5/2 λ.					
Fig. 14 *c*	1	83·50	(6)–(1)	10·36	14·0	3260	337·8	329·6
	2	88·70	=26·00					
	3	93·90	(7)–(2)					
	4	99·00	=25·80					
	5	104·15	(8)–(3)					
	6	109·50	=25·85					
	7	114·50	(9)–(4)					
	8	119·75	=26·00					
	9	125·00	(10)–(5)					
	10	130·10	=25·95					
			Mean =25·92					

* Too near end of sliding pipe.

Table VII.

Sliding Pipe Results in Air—Dual Telephone Method.

Oscillating neon controlled source at one end of pipe.
Telephone receiver, amplifier, and rectifier at the other end.

Response curve.	Number of peak (max.).	Readings. (cm.).	Wave-length λ (cm.).	Mean λ (cm.).	Temp. ($t°$ C.).	N.	V_l metres per sec.	V_0 metres per sec.
Fig. 15 *a*	1	83·00	(3)–(1)	24·60	17·5	1380	339·0	328·7
	2	95·00	=24·50					
	3	107·50	(4) (2)					
	4	120·00	=24·60					
	5	132·20	(5)–(3)					
			=24·70					
Fig. 15 *b*	1	81·0	(3)–(1)	38·40	18·8	(N/2) *447	343·3	332·1
	2	99·8	=38·40					
	3	119·4						
Fig. 15 *c*	1	82·0	(3)–(1)	37·00	17·5	(N/3) *312	344·7	334·3
	2	100·0	=37·00					
	3	119·0	(4)–(2)					
	4	137·0	=37·00					

* Actual frequencies of source.

Table VIII.

Resonance Tube Results in Air—Dual Telephone Method.

Valve oscillator controlled source.
Two valve amplifier and photo-cell rectifier.

Response curve.	No. of peak or mid-transit point.	Readings (cm.).	Wave-length (cm.).	Mean λ (cm.).	Temp. ($t°$ C.).	N.	V_t metres per sec.	V_0 metres per sec.
			(2λ)					
Fig. 16 *a*	1 (max.)	10·70	(5)–(1)	25·78	15·5	1310	336·9	327·7
	2	23·80	=51·55					
	3	36·70	(6)–(2)					
	4	49·60	=51·60					
	5	62·25	(7)–(3)					
	6	75·40	=51·55					
	7	88·25						
			Mean =51·56					
			(λ)					
Fig. 16 *b*	1 (min.)	4·25	(3)–(1)	37·33	14·5	905	337·8	329·2
	2	23·00	=37·35					
	3	41·60	(4)–(2)					
	4	60·35	=37·35					
	5	78·90	(5)–(3)					
			=37·30					
Fig. 16 *b*	1 (mid-pts.)	19·50	(3)–(1)	37·23	14·5	905	336·8	328·1
	2	38·10	=37·25					
	3	56·75	(4)–(2)					
	4	75·30	=37·20					
	5	94·00	(5)–(3)					
			=37·25					

TABLE IX.

Quincke Tube Results in Air—Dual Telephone Method.

Valve oscillator controlled source.
Diameter of tube = 1 cm.

Response curve.	Number of peak.	Readings (cm.).	Wave-length (cm.).	Mean λ (cm.).	Temp. (t° C.).	N.	V_t metres per sec.	V_0 metres per sec.
			(λ)					
Fig. 17 *a*	1 (min.)	47·00	(3)–(1)	27·25	14·7	1237	337·0	328·3
	2	61·00	= 27·50					
	3	74·50	(4)–(2)					
	4	88·00	= 27·00					
Fig. 17 *b*	1 (max.)	47·60	(3)–(1)	31·70	14·0	1064	337·0	329·1
	2	63·45	= 31·65					
	3	79·25	(4)–(2)					
	4	95·20	= 31·75					
Fig. 17 *c*	1 (max.)	39·70	(5/2 λ)	9·91	14·0	3410	338·5	330·1
	2	44·70	(6)–(1)					
	3	49·60	= 24·75					
	4	54·60	(7)–(2)					
	5	59·50	= 24·75					
	6	64·45	(8)–(3)					
	7	69·45	= 24·80					
	8	74·40	(9)–(4)					
	9	79·45	= 24·80					
	10	84·30	(10)–(5)					
			= 24·80					
			Mean = 24·78					

a plane reflector. If we dispense with the reflector and use a second telephone receiver and valve amplifier instead, successful measurement of the speed of sound in air is possible, provided we enclose both the source and receiver in a chamber of convenient size and having walls with good acoustical absorbing material. This condition is attained by employing a large wooden packing case and lining the inner walls with several thick layers of cotton wool, each layer having an air-space between it and the next, (fig. 18). The source and receiver are mounted facing each other along a horizontal line passing through the centre of the box. Whereas the source is kept fixed, the receiver is attached to a metal

Fig. 18.

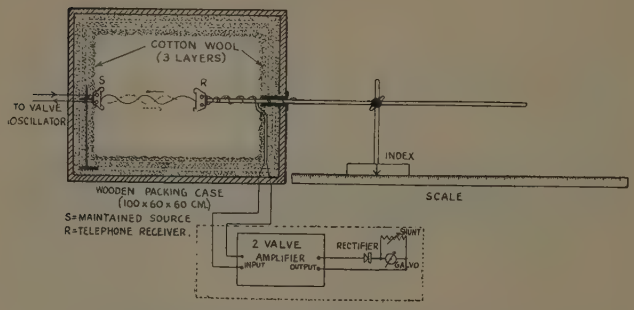

Dual telephone stationary wave method for measuring the velocity of sound in free air.

rod passing through a side hole in the box and fixed to a movable stand. The latter moves over a reference scale on an optical bench and so enables the distance between the source and receiver to be varied at will.

Now, in view of the nature of the surrounding walls, only sound waves sent out direct by the source are received at the receiver. Some of this energy is reflected back and finally reaches the source, but owing to the smallness of the receiver diaphragm in comparison with the large reflector used in the stationary wave method (Part I.), very little energy gets back to the source. The reactive effects at the source are consequently very small and were practically unobservable. The energy received

directly by the receiver telephone is, however, sufficiently large enough for analysis with the two-valve amplifier.

When the distance between the source and the receiver is an exact number of half wave-lengths of the sound waves emitted by the source, stationary waves are formed between the source and receiver, and marked nodal and anti-nodal positions exist in the intervening space. For the receiver diaphragm to occupy a nodal position maximum variation in pressure on the diaphragm must occur, and when at an anti-nodal position, minimum variation in pressure exists. Thus, as the distance between the source and receiver is gradually increased, the resulting vibrations of the receiver diaphragm undergo periodic alternations in amplitude for each successive increase in half wave-length. In a like manner the rectified currents pass through a series of maxima and minima as the distance between the source and receiver is increased, and the corresponding galvanometer deflexions exhibit similar characteristics, the distance between successive maxima or minima being half a wave-length.

Specimen Results for the Velocity of Sound in Free Air, using Dual Telephone Stationary Wave Method.

Typical results for a frequency of 1613 are shown in fig. 19 and Table X. There is again excellent agreement

Fig. 19.

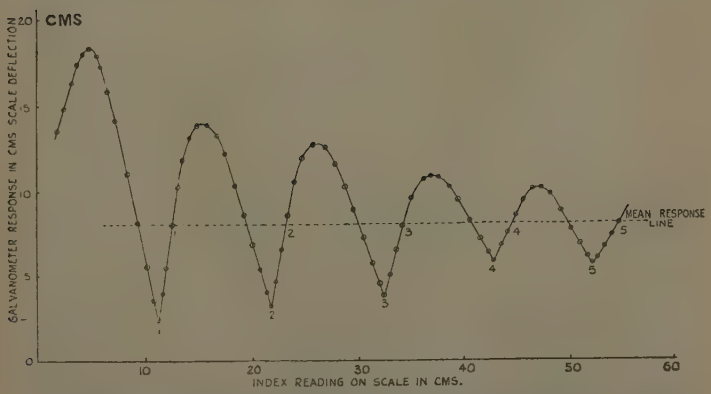

Results in air by dual telephone stationary wave method. Valve oscillator controlled source. Two-valve amplifier, photronic cell rectification. N=1613. Temp.=16·0° C. (See Table X.)

Table X.

Results in Air—Dual Telephone Stationary Wave Method.

Valve oscillator controlled source.

Response curve.	Number of peak or mid-transit point.	Readings (cm.).	Wave-length λ (cm.).	Mean λ (cm.).	Temp. (t° C.).	N.	V_t metres per sec.	V_0 metres per sec.
Fig. 19.....	1 (min.)	11·30	(3)–(1)	21·10	16·0	1613	338·8	329·4
	2	21·90	=21·20					
	3	32·50	(4)–(2)					
	4	42·90	=21·00					
			Mean =21·10					
Fig. 19	1 (mid-pts.)	12·60	(3)–(1)	21·20	16·0	1613	342·0	332·4
	2	23·20	=21·60					
	3	34·20	(4)–(2)					
	4	44·60	=21·40					
	5	54·80	(5)–(3)					
			=20·60					
			Mean =21·20					

with the results obtained by the other methods. The peaks of the response curve are sufficiently sharp to allow of their interpolation. Owing to the symmetry of the curve, it is also possible to interpolate the points of intersection along the mean response line and so compute the half wave-length.

This stationary wave method holds a decided advantage over both the pipe methods and the former interference stationary wave arrangement, since interference effects due to movement of the observer, and reflexion from the surrounding walls are eliminated. The corrections necessary with pipe experiments are also overcome, and the temperature and humidity of the enclosed air can also be readily determined with accuracy. Owing to the smallness of the reactive effects at the source, changes in frequency of the source are less liable, and once the oscillator has settled down to steady conditions, continuous critical control of the frequency is not necessary, the system thus operates at constant frequency and energy output.

Measurement of the Velocity of Sound in Air by a Rotating Reflector—Dual Telephone Method.

Successful demonstration of the optical analogue of Lloyd's interference bands and the law of reflexion of sound waves is possible * by employing a high frequency telephone source of sound, plane reflector, and sensitive flame as a detector. If we replace the sensitive flame by a second telephone, amplifier, and rectifying circuit, means are available for measuring the speed of sound in air, *i. e.*, by a rotating reflector—dual telephone method.

The principle of the method is one of interference and is outlined in fig. 20. Telephones T_1 and T_2 are attached to the ends of similar pipes P_1 and P_2. T_1 is electrically maintained, and T_2 connected to the amplifier and rectifying circuit. Both pipes are mounted horizontally and inclined to each other at a pre-set angle. They are so arranged to have their open ends equidistant from the centre of a vertical plane glass reflector AB when the latter is equally inclined to both pipes. To affect this condition, the glass plate is clamped vertically across the centre of a horizontal turn-table T (50 cm.

* *Loc. cit.* Ref. (Humby) Part I.

diameter) provided with a graduated scale around its edge. A plumb-line hangs from the upper edge of the plate and is so adjusted to be coincident with the centre of the turn-table. Correct alignment of the pipes is then made by sighting through the plate and adjusting until the plumb-line is coincident with the axes of the pipes and the vertical centre lines across each of the open ends of the pipes. By this means we ensure that the axes of the pipes intersect at the centre of the turn-table, and also in the plane of the reflector. Any position of the

Fig. 20.

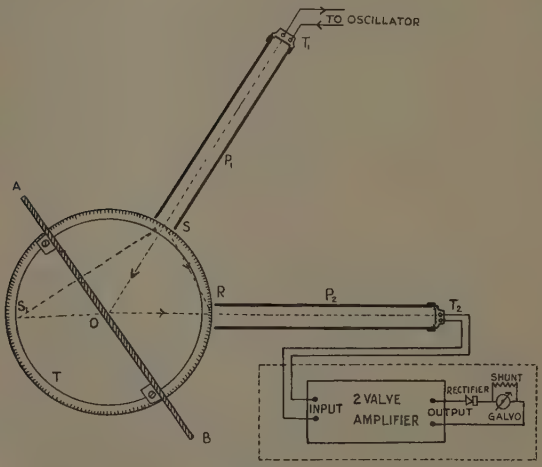

Arrangement for measuring the velocity of sound in air by a rotating reflector—dual telephone method.

P_1P_2=Similar metal pipes. T_1=Telephone source. T_2=Telephone receiver. AB=Vertical glass plate reflector. T=Turn-table with graduated scale on base.

reflector relative to the pipes is then obtained by sighting the plumb-line and the vertical centre line across the end of each pipe for coincidence, and then noting the reading of the lower end of the plumb-line on the circular scale. Since the plate is thin, we may neglect refraction effects. Now in view of certain experiments performed by West *,

* W. West, Journ. I.E.E. lxvii. p. 1117 (1929); *vide* also Andrade and Parker, Proc. Roy. Soc. A, clix. (April 15, 1937).

we may regard the maintained source with resonating tube as equivalent to a point source of sound situated at the plane of the opening of the pipe. Likewise the receiver and second pipe, this we can regard as an equivalent receiver placed in the plane of the opening of the second pipe.

Referring now to fig. 20 and applying the method of images for reflexion at a plane barrier, sound-waves arrive at R by direct propagation along SR and also by reflexion along SO and OR, *i. e.*, as though they came from S_1 the image of S. When the path difference between

Fig. 21.

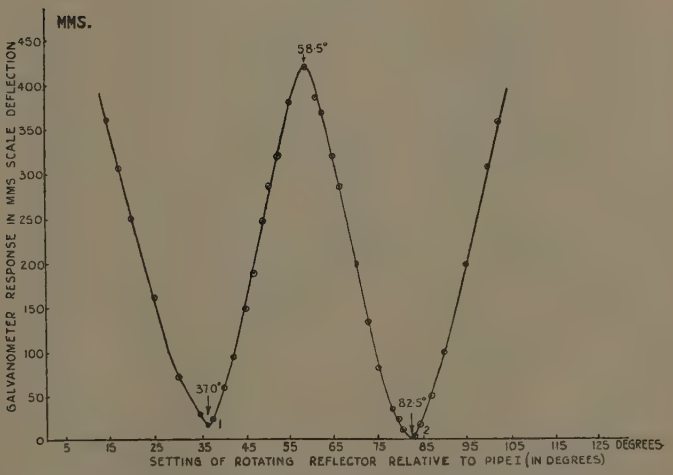

Velocity of sound in air results by rotating reflector—dual telephone method (with pipes).

Angle between pipes = 60°. Distance of open ends of pipes from centre of reflector = 20·75 cm. N = 1000. Temp. = 18° C. (See fig. 22 and Table XI.)

(SO+OR) and SR is equivalent to a whole number of wave-lengths, then both sets of waves arrive at R in phase, and reinforcement takes place. If the paths differ by an odd number of half wave-lengths then neutralization of the waves akset place at R. Now the variation in path difference is produced by keeping the pipes fixed and rotating the reflector about a vertical axis through O. For each

setting of the reflector the corresponding galvanometer deflexion due to rectification of sound effects at R are observed, and provided the frequency is large enough, upon plotting the galvanometer deflexion against the setting of the reflector (in degrees of scale) a response

Fig. 22.

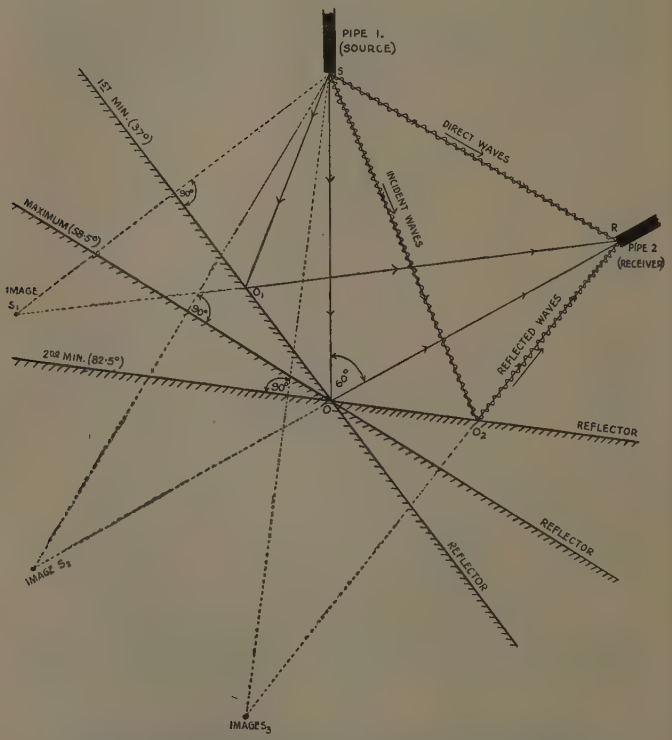

Graphical construction for velocity of sound in air results (fig. 21) by rotating reflector—dual telephone method (with pipes). Angle between pipes = 60°. N = 1000, Temp. = 18·0° C. (See fig. 21 and Table XI.)

curve with several maxima and minima is obtained (figs. 21 & 23). The maxima correspond to positions of the reflector at which the path difference between

(SO+OR) and SR equals a number of whole wave-lengths, and the minima to positions where (SO+OR)−SR is equal to an odd number of half wave-lengths. From such a response curve either the maxima or minima positions are interpolated (preferably the former), and the positions

Fig. 23.

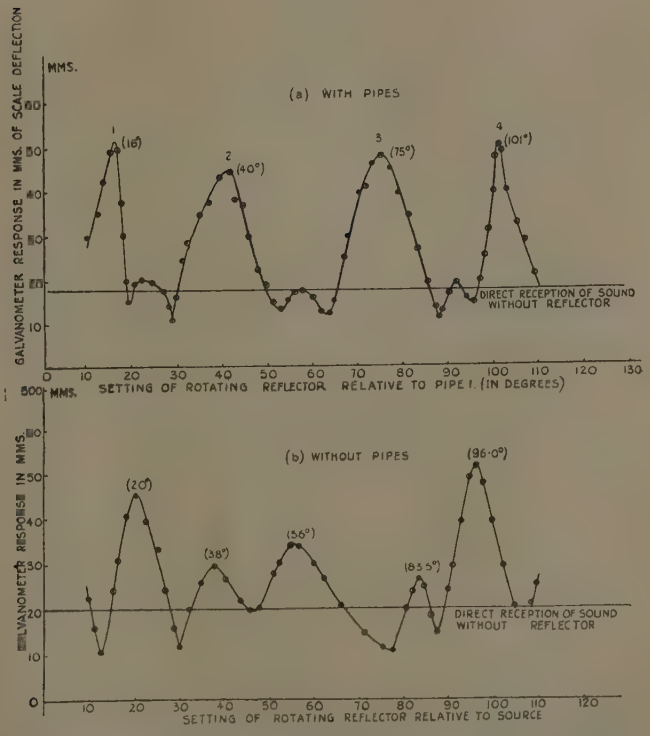

Velocity of sound in air results by rotating reflector—dual telephone method. (With and without pipes.)

(*a*) Angle between pipes = 60°. Distance of open ends of pipes from centre of reflector = 21·0 cm. N = 3532. Temp. = 17·5° C. (See fig. 24 and Table XII.)

(*b*) Angle subtended at centre of reflector by source and receiver. Distance of source and receiver from centre of reflector = 21·5 cm. N = 3412. Temp. = 17·5° C.

of the pipes and reflector drawn accurately (full size) on a large sheet of paper. The paths (SO+OR) and SR

are then measured for each critical setting, and the corresponding path difference finally obtained. Since the pitch of the source is accurately determined by either a monochord and standard fork, or stroboscopically, hence fairly reliable value of the velocity of sound. It is important to prevent waves being reflected from the base of the

Fig. 24.

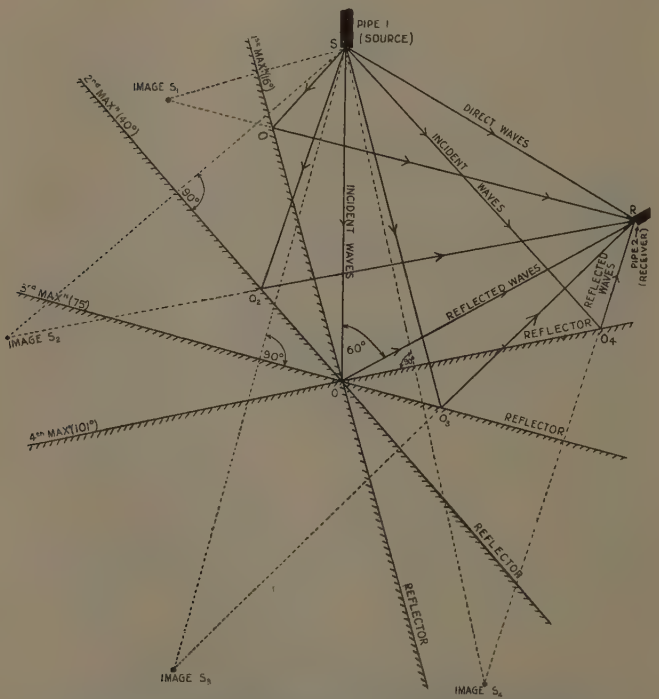

Graphical construction for velocity of sound in air results (fig. 23) by rotating reflector—dual telephone method (with pipes). Angle between pipes = 60°. N = 3523. Temp. = 17·5° C. (See fig. 23 and Table XII.)

turn-table into the open end of the receiver pipe. This is achieved by covering the turn-table with cotton wool. Tests with and without the wool showed very little sound entered the pipe in this way. Movement of the observer

will again vitiate the results, as in the stationary wave method with single telephone.

Specimen Results for the Velocity of Sound in Air by Rotating Reflector—Dual Telephone Method.

Included in figs. 21, 22, 23 *a*, 24 and Tables XI. & XII. are results for frequencies of 1000 and 3523 . The multiple maxima and minima are well in evidence for the higher frequency. By way of comparison, results without the pipes are also shown in fig. 23 *b*. The presence of the pipe increases the sensitivity of the receiver. Although it is possible to interpolate the maxima to within one degree, the method is not one of precision like the other methods described herein, since the errors introduced in computing the path differences are dependent upon the accuracy of drawing the positions of the reflector and pipes. The method does, however, provide an interesting means for lecture purposes of demonstrating the principles of interference and reflexion of sound at a plane barrier. We could alternately keep the reflector and pipes fixed and alter the frequency of the source, observing the corresponding galvanometer responses for each determined frequency. In view of the variation in energy output of the oscillator with change in frequency, it is better to keep to the former method and rotate the reflector instead.

A Further Application of the Pipe Results : Measurement of the Resonant Frequency of a Telephone Diaphragm.

The fundamental frequency * of a telephone diaphragm is expressible as

$$N = 0{\cdot}4745 \frac{h}{a^2} \sqrt{\frac{E}{\rho(1-\sigma)}} \quad \text{or} \quad N = 0{\cdot}4735 \frac{h.c}{a^2},$$

where h is the thickness and a the radius of the diaphragm, E = Young's modulus, ρ the density, and σ Poisson's ratio of the material of the diaphragm, c = the velocity of elastic waves in an infinite thin plate of the same material and thickness.

Confirmation of the validity of this expression is possible using any of the foregoing pipe systems. For a given pipe system a series of different frequencies are used, and the

* A. B. Wood, ' Sound,' p. 158.

Table XI.

Velocity of Sound Results in Air. Rotating Reflector—Dual Telephone Method.

Angle between pipe axes = 60°. Frequency of source = 1000.
Distance between open ends of pipes from centre of reflector = 20·75 cm.
Distance between open ends of pipes = 20·75 cm. Temp. = 18·0° C.

Number of minimum. (Fig. 21.)	Scale-reading in degrees.	Length of paths (cm.).	SR. (cm.).	Path differences. $\lambda/2$ (cm.).	Mean λ (cm.).	V_t metres per sec.	V_0 metres per sec.
1	37·0	$O_1S = 14{\cdot}50$ $O_1R = 23{\cdot}50$	20·75	$O_1S + O_1R - SR$ $= 38{\cdot}0 - 20{\cdot}75$ $= 17{\cdot}25$			
2	82·5	$O_2S = 23{\cdot}50$ $O_2R = 14{\cdot}20$	20·75	$O_2S + O_2R - SR$ $= 37{\cdot}70 - 20{\cdot}75$ $= 16{\cdot}95$ Mean = 17·10	34·20	342·0	331·3

Table XII.

Velocity of Sound Results in Air. Rotating Reflector—Dual Telephone Method.

Angle between pipe axes = 60°. Frequency of source = 3523.
Distance between open ends of pipes from centre of reflector = 21·0 cm.
Distance between open ends of pipes = 21·0 cm. Temp. = 17·5° C.

Number of maximum. (Fig. 24.)	Scale-reading in degrees.	Length of paths (cm.).	SR. (cm.).	Path differences. 2λ (cm.).	Mean λ (cm.).	V_t metres per sec.	V_0 metres per sec.
1	16	$O_1S = 6{\cdot}75$ $O_1R = 33{\cdot}50$	21·0	$O_1S + O_1R - SR$ $= 40{\cdot}25 - 21{\cdot}0$ $= 19{\cdot}25$ $\therefore \lambda = 9{\cdot}62$			
2	40	$O_2S = 16{\cdot}10$ $O_2R = 23{\cdot}90$	21·0	$O_2S + O_2R - SR$ $= 40{\cdot}0 - 21{\cdot}0$ $= 19{\cdot}00$ $\therefore \lambda = 9{\cdot}50$			
3	75	$O_3S = 23{\cdot}45$ $O_3R = 17{\cdot}05$	21·0	$O_3S + O_3R - SR$ $= 40{\cdot}50 - 21{\cdot}0$ $= 19{\cdot}50$ $\therefore \lambda = 9{\cdot}75$	9·67	340·6	330·3
4	101	$O_4S = 23{\cdot}80$ $O_4R = 7{\cdot}00$	21·0	$O_4S + O_4R - SR$ $= 30{\cdot}80 - 21{\cdot}0$ $\therefore \lambda = 9{\cdot}80$			

corresponding changes in galvanometer deflexions are observed between consecutive maxima and minima as the resonating air-column is gradually increased. Plotting such deflexions against the frequency yields a

Fig. 25.

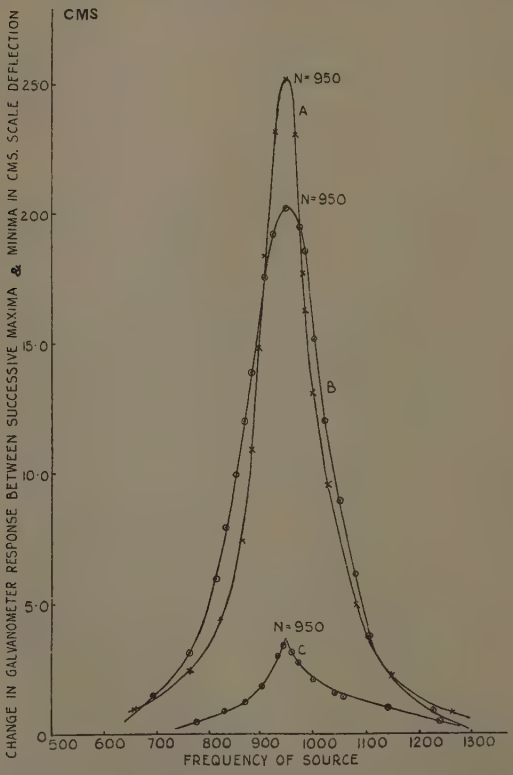

Calibration of detector circuits by resonance tube method (Part I.), and determination of the natural frequency of telephone diaphragm at the source.

A = Two-valve photronic cell and shunted galvo. (Fig. 3.)
B = One valve photronic cell. (Fig. 2.)
C = Oscillating neon. (Fig. 4.)

response curve having a maximum at the fundamental frequency of the diaphragm. Families of such curves

obtained with the resonance tube (Part I.) and sliding pipe arrangement (Part II.) are exhibited in figs. 25 & 26.

Fig. 26.

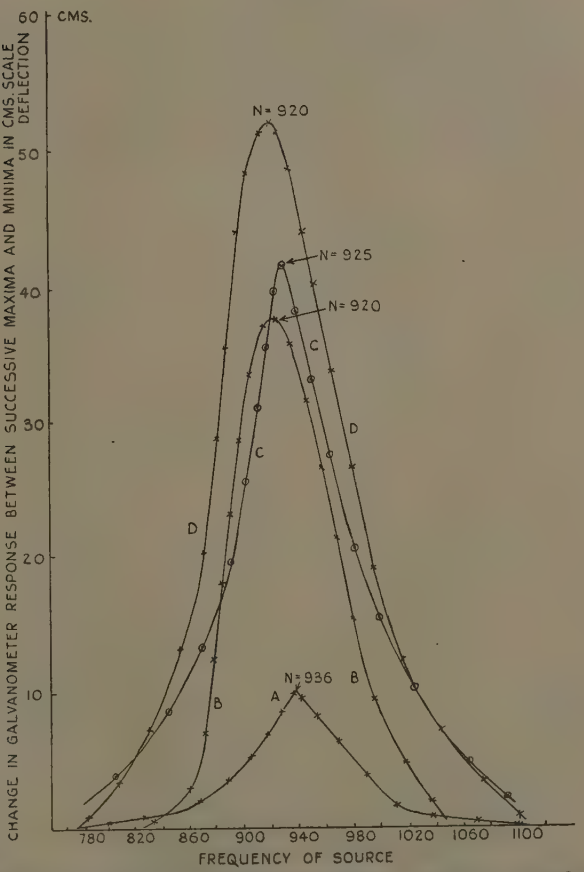

Calibration of receiving circuits by sliding pipe—dual telephone method (Part II.), and determination of the natural frequency of telephone receiver diaphragm.

A = Oscillating neon controlled source, two-valve amplifier, and photronic cell rectifier.

B = Valve oscillator controlled source and receiving circuit of crystal, telephone, and galvanometer in series.

C = One-valve controlled source and receiver circuit comprising "Westinghouse rectifier," telephone, and shunted galvo.

D = One-valve controlled source and receiver circuit comprising one-valve and photronic cell rectifier.

The relative sensitivity of the different methods is at once revealed, likewise maximum galvanometer response at

TABLE XIII.

Calibration of Telephone Diaphragm at the Source by Resonance Tube. Method, as per fig. 1 *a*, Part I. Computation of Resonant Frequency.

$E = 2{\cdot}0 \times 10^{12}$ dynes/cm.^{2}. $\rho = 7{\cdot}80$ gm./c.c. $\sigma = {\cdot}28$ c.g.s.
$h = {\cdot}0235$ cm. $a = 2{\cdot}48$ cm. $c = 5{\cdot}27 \times 10^5$ cm./sec.

$$N = 2{\cdot}50 \times 10^5 . \frac{h}{a^2} = 2{\cdot}50 \times 10^5 \times \frac{{\cdot}0235}{(2{\cdot}48)^2} = 957 \text{ vibs./sec.}$$

Reference curve. (Fig. 25.)	Type of controlled source and detecting circuit.	Interpolated frequency at maximum galvo response.
C	Oscillating neon as per fig. 4.	950
B	One-valve oscillator as per fig. 2.	950
A	Two-valve circuit as per fig. 3.	950

TABLE XIV.

Calibration of Telephone Diaphragm at Receiving End of Sliding Pipe. System as per fig. 11, Part II. Computation of Resonant Frequency.

Theoretical N = 957, same as in Table XIII.

Reference curve. (Fig. 26.)	Type of controlled source.	Type of rectifying circuit.	Interpolated frequency at maximum galvo response.
A	Oscillating neon as per fig. 4.	Two-valve as per fig. 10.	936
B	One-valve oscillator.	Crystal, telephone, and galvo in series	920
C	„ „	Westinghouse rectifier, telephone, and shunted galvo.	925
D	„ „	One valve amplifier and photo cell rectifier.	920

the fundamental frequency of the diaphragm under the experimental conditions. The interpolated frequencies compare well with the theoretical values (Tables XIII. & XIV.). The discrepancies between the theoretical and experimental values of frequency, particularly in the dual telephone sliding pipe system, are due to the varying degrees of clamping of the receiver diaphragm. Better agreement is revealed in the resonance tube results where the clamping remained the same throughout the calibrations.

TABLE XV.

Average Values of Velocity of Sound in Air at 0 C. (Uncorrected).

Method.	Number of tests.	Average value V_0 metres/sec.
Resonance tube.		
Single and dual telephone ...	11	329·5
Diameter of glass tube = 2·50 cm.		
Sliding pipes.		
Open or closed	8	331·6
Diameter of pipe = 3·80 cm.		
Quincke Tube.		
Dual telephone	3	329·2
Diameter of pipe = 1·0 cm.		
Stationary wave.		
Single and dual telephone ...	5	330·6
Rotating Reflector.		
Dual telephone and pipes	2	330·8
Hebb's dual mirror method.	$V_0 = 331·4$ metres sec.	

Discussion of Results and Review of other forms of Experimental Technique.

Comparing the summarized results of the velocity of sound in air at 0° C. for the various methods at sonic frequencies, we observe from Table XV. that substantial agreement is reached. Whereas the single and dual telephone stationary wave methods give an average value of 330·6 metres sec., and the rotating reflector method 330·8 metres sec., most of the narrower pipe results are

slightly lower in comparison with the average value of 331·6 metres/sec. at 0° C. for free air conditions obtained by Hebb *. According to R. C. Parker †, some unpublished pipe results of E. N. da C. Andrade, D. H. Smith, and S. H. Wheeler give a value of 331·74 metres/sec. between 800 and 1400 c./sec.

The Helmholtz-Kirchhoff formula for pipe correction in respect of diameter and nature of gas was not applied to the results in Table XV. owing to the smallness of the corrections involved. The importance and magnitude of such corrections have been critically examined by Henry ‡.

Even in Hebb's dual parabolic mirror method, which is now recognized as a standard method for the determination of the velocity of sound in free air, we could with advantage dispense with the aural method of locating the successive maxima and minima as the distance between the mirrors is gradually varied, and rectify the resulting telephonic currents instead. Graphical representation of the results would then be possible along similar lines to those already described herein. With the aid of a valve amplifier and potentiometer device for balancing out the rectified currents, an extremely accurate null deflexion method might be evolved for computing the wave-length.

Concerning the measurement of the reactive effects at the telephone source when energized by an oscillating neon, this method is believed to be new, and it possesses certain advantages by virtue of the pulsating nature of the controlling frequency despite the richness in harmonics of such a circuit. The sharpness of the peaks on the response curves and the aural warning of change in frequency when approaching the resonant pipe length enhances the possibilities of this method as one of precision.

The dual telephone stationary wave method gives most reliable results, and in view of the elimination of pipe corrections, non-interference due to reflexion from surrounding objects, and the ease of ascertaining both the temperature and humidity of the air within the chamber, its adaption to measurements with other gases available in fairly large quantities is to be recommended.

* Phys. Rev. xx. p. 89 (1905); and xiv. p. 74 (1919).
† Phys. Soc. Proc. xlix. no. 271, p. 103 (March 1st, 1937).
‡ Phys. Soc. Proc. xliii. no. 238 (May 1st, 1931).

Alternate methods employing an additional telephone receiver either as second source or receiver might also be utilized; *e. g.*, two telephone receivers R_1 and R_2 (fig. 27 *a*) functioning purely as detectors of sound are arranged symmetrically with respect to a single maintained source S. Both R_1 and R_2 are coupled to the same amplifier, hence, if R_1 is kept fixed and R_2 traversed away from the source S, positions are obtained for R_2 at which the sound waves received simultaneously by R_1 and R_2 are in phase. Reinforcement takes place with maximum

Fig. 27.

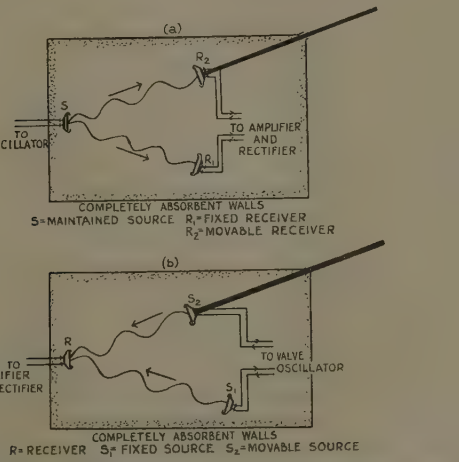

Suggested modified differential methods for determining the velocity of sound in air.

rectification and galvanometer response. When the relative positions of R_1 and R_2 are such that a phase difference of 180° exists between the two sets of waves received simultaneously at R_1 and R_2, neutralization ensues with corresponding minimum rectification and galvanometer response. Thus, as R_2 is gradually moved away from the source, the galvanometer deflexion undergoes alternations for each additional wave-length of path difference between the sets of waves. The distance which R_2 travels between successive maxima or minima is one wave-length.

Conversely, two similar maintained telephone sources S_1 and S_2 and a single receiver R can also be arranged to give a differential electrical method for deducing the wave-length (fig. 27 *b*). By operating S_1 and S_2 from the same valve oscillator and traversing S_2 relative to S_1 away from R, the galvanometer response due to the resulting rectification again exhibits marked alternations and the distance traversed by S_2 between successive maxima or minima is one wave-length.

We must regard the rotating reflector method as an instructional one, suitable for lecture purposes rather than an accurate method for determining the velocity of sound in free air.

The sliding pipe and Kundt's tube arrangements, with certain modifications, also lend themselves ideally to lecture demonstrations. If a light frame be rigidly connected to either the sliding pipe or piston-rod and a large sheet of graph paper fixed to the former, then, by suitable arrangement, the spot of light reflected from the galvanometer mirror can be made to move at right angles to the direction of traverse of the pipe or rod. Thus, as the air column within the pipe is gradually increased, the spot of light travels across the paper and automatically traces out a response curve, the turning points corresponding to maxima and minima. By marking the successive positions of the light spot on the paper for varying pipe-lengths we automatically plot the galvanometer response curve from which the wave-length is interpolated. It is, of course, preferable to traverse with the pipes in the vertical position in order to facilitate easy demonstration to an audience.

Referring to the calibration curves in figs. 25 & 26 it is obvious, with telephone receivers, the sensitivity falls off very rapidly at frequencies not far remote from that natural to the telephone diaphragm. Should it be desirous to operate both the source and receiver at an increased and uniform sensitivity over a wide frequency range, it is better to adopt the method suggested by T. S. Littler * and use the diaphragm of a moving coil loud-speaker unit with special control circuit, such that the e.m.f. generated by the motion of the diaphragm is proportional to the amplitude of the sound wave.

* Journ. Scientific Inst. (Aug. 1927).

In the dual telephone methods with pipes one could also resort to the use of either a condenser or carbon microphone as the receiver instead of the second telephone. Trouble will probably occur with the carbon microphone owing to packing and internal heating, hence preference to the former type of microphone.

Recently, sensitive thermocouples have been employed in pipe work. V. Hardung *, in determining the resonant frequencies of pipes of different length and diameter, measured electrically with a galvanometer the cooling experienced by a thermocouple (energized by a steady current) inserted in a hole at the closed end of the sounding pipe. Johnson † has also directed his attention to the design of a low capacity sensitive thermo-junction which is fixed at one end of a closed pipe with a loud-speaker unit at the other. Such a junction consisted of a cellulose acetate film spread over a mica frame (3×1 cm.) with a central hole 5 mm. diameter. This was sputtered from cathodes of antimony and bismuth so that a covering of metal was formed on either side with the junction at the hole. The average thickness of the couple was $3{\cdot}5 \times 10^{-5}$ cm. Calibraton was effected by means of a condenser microphone. Such a thermo-junction could also be well adapted as a sound detector in any of the foregoing dual telephone methods.

The aural sliding piston device of Pierce ‡ also lends itself for conversion to an all-electrical method. In this method a brass resonance tube (120 cm. long and 4 cm. diameter) is provided with a piston and reference scale. The tube is mounted with the open end inside a felt box. Also in this box is an electrically driven telephone facing the open tube. A microphone is conveniently placed between the open end of the pipe and the telephone, such that the sound received direct by the microphone from the telephone source is just balanced out by that emitted by the pipe at maximum strength. The microphone was coupled *via* a transformer to a pair of head receivers, so that when the piston is traversed along the pipe, sounds with alternate maxima and minima are heard in the head receivers. The distance travelled

* *Helv. Phys. Acta*, ix. 5, pp. 341–366 (1936).
† Phys. Review, xlv. p. 641 (1934).
‡ Proc. Amer. Acad. lx. p. 284 (1925). Also A. B. Wood, ' Sound,' p. 243.

by the piston between successive maxima or minima is a half wave-length. By means of an electric filter the fundamental frequency of the sound (995·88 pps.) was cut out and the harmonic $3\times 995{\cdot}88$ listened to instead. Pierce thus found the velocity of sound in air to be $331{\cdot}94 \pm{\cdot}07$ metres/sec. at 0° C., uncorrected for tube effects. If we substitute any of the foregoing rectifying devices for the head receivers even greater accuracy may be obtained.

Of other electrical methods employed in pipe investigations the hot wire and resistance thermometer methods may be cited. The cooling of an electrically heated wire of small diameter such as platinum (·001″ diam.) by an oscillating current of air is well known *, and the measurement of either its steady drop in resistance or oscillatory change when exposed to such an air current has been successfully employed in the determination of: (*a*) displacement or velocity amplitude of aerial vibrations in a sounding pipe †; (*b*) absorption coefficients of materials by a stationary wave method ‡; (*c*) impedance of air columns in pipes §; (*d*) velocity of sound in gases at ultra-sonic frequencies ‖; (*e*) temperature changes at a node in a sounding pipe ¶. Usually the wire is mounted either in the neck of a resonator, as in a Tucker-Paris hot-wire microphone, or as a straight element at the end of the prongs of a fork. Either form could be employed in any

* Tucker and Paris, Roy. Soc. Phil. Trans. cci. p. 389 (1921). See also R. C. Richards, Phil. Mag. xlv. p. 925 (1923); R. S. Maxwell, Phil. Mag. vi. p. 945 (Nov. 1928).

† Richardson, Proc. Roy. Soc. cxii. p. 522 (1926); Goldbaum, Müller, Waetzmann, *Zeits. f. Phys.* liv. p. 179 (1929), and lxii. p. 167 (1930); also Müller, *Phys. Zeits.* xxxi. p. 350 (1930).

‡ Penman and Richardson, Acoustical Soc. Journ. of America, iv. p. 322 (April 1933); Paris, Phys. Soc. Proc. xxxix. p. 269 (1927); Proc. Roy. Soc. cxv. p. 407 (1927); and Phil. Mag. iv. p. 907 (1927); Richardson, Proc. Roy. Soc. cxlvi. p. 56 (1934).

§ Penman and Richardson, Acoustical Soc. Journ. of America, iv. p. 322 (April 1933); Richardson, Phys. Soc. Proc. xl. p. 206 (1928).

‖ Malov, Hochfreq, xlii. p. 115 (1933); Bucks and Müller, *Zeits. f. Phys.* lxxxiv. p. 75 (1933); Richardson, Proc. Roy. Soc. cxlvi. p. 56 (1934); also Railston and Richardson, Phys. Soc. Proc. xlvii. p. 533 (1935).

¶ K. Neuscheler, *Ann. d. Phys.* xxxiv. p. 131 (1911); K. Heindlhofer, *Ann. d. Phys.* xxxvii. p. 247 (1912), and xlv. p. 259 (1914); J. Friese and E. Waetzmann, *Zeits. f. Phys.* xxix. p. 110 (1924); A. H. Davis, 'Modern Acoustics,' p. 124; Johnson, Phys. Review, xlv. p. 641 (1934); Hippel, *Ann. d. Phys.* lxxv. p. 521 (1924), and lxxvi. p. 590 (1925).

of the foregoing dual telephone arrangements, the second telephone being replaced by the hot wire.

In view of the smallness of the cooling effect produced, in certain cases, it is essential to use either a sensitive Wheatstone bridge network when measuring the steady resistance drop, or an amplifier coupled to the wire when observing the oscillatory changes in resistance. These latter effects can be examined in terms of either the rectified currents or amplitudes of deflexion of an Einthoven galvanometer at the higher frequencies, or tuned vibration galvanometer at frequencies less than 500 per sec.

An electrical visual demonstration of the effects produced on a hot wire when placed at a nodal or antinodal position in a sounding pipe is also possible with the aid of an amplifier and Osglim lamp.

If the pipe is an open one with maintained source at one end, provision should be made for traversing the hot wire down the centre of the pipe while it is sounding. The resulting cooling effects of the wire are then communicated via an amplifier to a neon lamp supplied with the necessary H.T. bias so as to just prevent the lamp from flashing when the hot wire is at a node. When the wire occupies an antinodal position, the oscillating changes in resistance produce corresponding variations in P.D. across the wire which after amplification cause the lamp to flash at a frequency of the aerial vibrations. Thus as the wire travels along the pipe, the lamp will glow intermittently at the antinodes, and fail to light at the nodes With a closed pipe, it is better to mount the wire across the middle section of the pipe and arrange that this section can slide separately inside the main tube. By this means the hot wire can be brought into either a nodal or antinodal position with similar flashing as before.

Comprehensive accounts of non-electrical methods employed in the experimental observation of aerial vibrations in pipes have appeared in most modern text-books * on sound, and these can be consulted if necessary.

* A. H. Davis, ' Modern Acoustics,' chaps. vii. and viii., and pp. 208–213; A. B. Wood, ' Sound,' pp. 178-184, 239–244, 324–325; E. G. Richardson, ' Sound,' pp. 179–186, 287–288.

LXXXI. *On the Structure of Pepsin.* *By* D. M. Wrinch, *M.A., D.Sc.Oxon, Mathematical Institute, Oxford* *.

[Plate VIII.]

Introduction.

It has been established by Svedberg and his school that there exist a number of proteins which have a certain molecular status ; that their molecular weights do not form a random distribution, but fall into a few widely separated classes ; and that proteins falling into one of these classes may yet have very different chemical compositions (Svedberg, 1929 *et seq*).

These results fall easily into place on the cyclol theory of protein structure (Wrinch, 1936, 1937) which implies the existence of " globular " proteins, polycondensation products of the amino acid molecules, which can be built only of certain special numbers of such building blocks. It is suggested that a molecular weight class connotes one of these structures or an association of a number of such units, and that the individual properties of proteins belonging to one such class are due to the individual selections of building blocks and their varying arrangements in the common structure.

Among the closed cyclol molecules which have already been investigated—C_1, C_2, . . . C_n, . . . containing 72, 288, . . . $72n^2$, . . . amino acid residues (Wrinch, 1937 α, γ, δ)—the molecule C_2 has a molecular weight which gives it an *à priori* right to be considered in relation to the class of proteins with molecular weights in the neighbourhood of 36,000. The predicted number of residues is that subsequently given as the number in each egg albumin molecule on the basis of chemical analyses (Bergmann and Niemann, 1937). Further, a case has been made out (Wrinch, 1937 γ) for the suggestion that the insulin molecule has this structure, on the basis of the crystallographic, chemical and physico-chemical facts. In the present communication a similar suggestion is made with regard to the pepsin molecule.

The detailed structure of the C_n molecule has been discussed in earlier publications of this series. The

* Communicated by the Author.

cyclol fabric is shown in fig. 1. For convenience of exposition, the cyclol-6 molecule (fig. 2) may be replaced

Fig. 1.

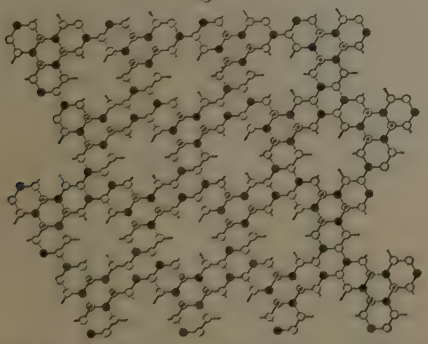

The cyclol fabric. The median plane of the lamina is the plane of the paper. The lamina has its "front" surface above and its "back" surface below the paper. [From Proc. Roy. Soc. A, clx. p. 69, fig. 9.]

- ● =N.
- ◑ =C(OH), peptide hydroxyl upwards.
- ◌ =C(OH), peptide hydroxyl downwards.
- ○– CHR, direction of side chain initially outwards.
- ○– CHR, direction of side chain initially upwards.

Fig. 2.

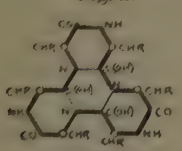

The cyclol-6 molecule. [From Proc. Roy. Soc. A, clxi. p. 506, fig. 1.]

Fig. 3.

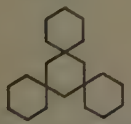

The median network of the cyclol-6 molecule shown in fig. 2.—[From Proc. Roy. Soc. A, clxi. p. 508, fig. 3.]

by its median network (fig. 3) in which the C–C–N atoms of the constituent residues are replaced by points midway

between linked atoms. The median networks of all the C_n molecules lie on the faces of truncated tetrahedra—the " polyhedral frames " of the molecules—and so have four hexagonal faces and four triangular faces. Fig. 4 shows the polyhedral frame of C_2. Fig. 5 shows the detailed structure of one triangular and one hexagonal face of C_2 and so represents one-quarter of the fabric required to build one C_2 molecule. Pl. VIII. fig. 6 shows photographs of a model of the complete median network of a C_2 molecule.

Fig. 4.

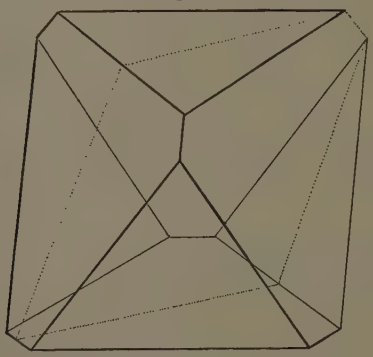

The polyhedral frame of the C_2 molecule.

The Data relating to Pepsin.

The fact has been established that, in appropriate circumstances, pepsin in solution is isodisperse (Philpot and Eriksson-Quensel, 1933). The molecule is found to be " globular " with low asymmetry number and to have the molecular weight of 39,200. Certain data are available as to the chemical composition of pepsin (Calvery, Herriott and Northrop, 1936). Crystalline pepsin contains relatively large amounts of tyrosine (10·3 per cent.), aspartic acid (6·8 per cent.), and glutamic acid (18·6 per cent.). Its content of diamino acids is relatively low. There is at present no indication that any prosthetic group is present.

The first X-ray photographs of crystalline pepsin were taken by Bernal and Crowfoot in 1934, who gave as the dimensions of the unit cell $a=67$ Å. $c=154$ Å. correct to

about 5 per cent., adding that the spots on the c row lines were too close for accurate measurement and that the c-axial length had been derived from the axial ratio $2{\cdot}3 \pm 0{\cdot}1$ of the crystals themselves. For this reason, they pointed out, the c-dimension of the hexagonal cell might still be a multiple of 154 Å. A later report by Crowfoot (1935) states that the most marked periodicity along c is one of only 9·6–10·2 Å., and that the true cell of pepsin has a c-dimension three times as long as that first

Fig. 5.

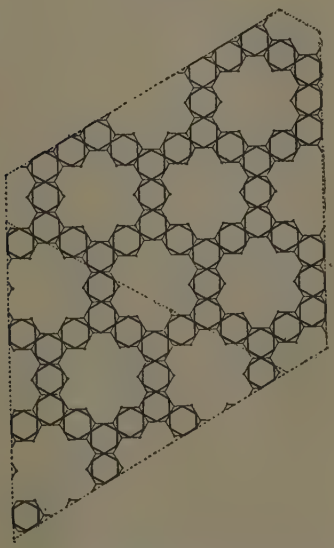

Part of the cyclol fabric (compare fig. 1) which constitutes the molecule C_2. One hexagonal face and one triangular face are shown, comprising one-quarter of the whole molecule. The thin lines join the atoms; the heavy lines represent the median network. The long dashes represent the lines about which the network is folded in order to make a closed cyclol molecule.—[From Proc. Roy. Soc. A, clxi. p. 515, fig. 12.]

suggested, so that the data at the moment are $a = 67$ Å., $c = 462$ Å. It should, however, be noticed that this c-dimension may need further modification.

Now the cell molecular weight for the larger cell, assuming the density of 1·32 is 1,434,000. It was found

that the crystals contain about 50 per cent. of water removable at room-temperature. It then follows (using Svedberg's value of the molecular weight) that the number of molecules per cell is $1{,}434{,}000/2 \nearrow 39200 = 18{\cdot}3$.

The structure proposed by Crowfoot for the molecular lattice consists of "crumpled" layers in which the molecules are arranged in networks of six-sided rings of the non-planar type, which occur, for example, in diamond and wurzite. The side of such a ring projected on to (0001) is $a/\sqrt{3} = 38{\cdot}67$ Å. The fact that there is a periodicity of 9·6 10·2 Å. along the c-axis is interpreted to mean that the thickness of a layer is 9·6 10·2 Å., say 10 Å. Accordingly, associating with each molecule some fixed point in it, say the orthocentre, the molecules in a single layer are so arranged that their orthocentres lie alternately in planes 10 Å. apart along the trigonal axis.

Now the crystallographically possible ways of arranging one layer upon another so that the upper members of the lower layer are uniformly coordinated with the lower members of the upper layers are only two, α and β. α is exemplified in the diamond and β in the wurzite. The α repeat is three layers and the β repeat is two.

With the original dimensions $c = 154$ Å. it was natural, having taken 10 Å. as the thickness of a single layer, to assume a three-layer structure of the type $\alpha\alpha\alpha$ which then gives as the distance between layers $154/3 = 10 = 41{\cdot}34$ Å. The change from this c-dimension to one three times as long, implying that the structure repeats in nine layers, but not in three, makes this structure which repeats in three layers no longer possible. Crowfoot therefore suggested that not all layers are related to neighbouring layers by the α relation, but that there is an alteration of α and β relations between layers. Such alterations have already been used in devising structures. Thus carborundum (Strukturbericht, vol. i. p. 80, 1931) has layer structures of the type $\alpha\beta$, $\alpha\beta$ (carborundum III), of the type $\alpha\beta\alpha$, $\alpha\beta\alpha$ (carborundum II), and of the type $\alpha\beta\alpha\beta\alpha$, $\alpha\beta\alpha\beta\alpha$, $\alpha\beta\alpha\beta\alpha$ (carborundum I). Evidently it is possible also to devise such an alternation which will repeat in nine layers, for example $\alpha\beta\beta\alpha\beta\beta\alpha\beta\beta$. Also it is possible that there is a certain degree of randomness in the α–β alternations.

Each layer contributes two molecules to the unit cell, since a nine layer-cell contains 18 molecules, in agreement

with the number already deduced from the cell molecular weight and the molecular weight of pepsin found by Svedberg. Adopting this result we deduce that in the molecular lattice there are water molecules weighing 1,434,000 18 39,200 40,466 (say 2,350 water molecules) for every molecule of pepsin.

The C_2 Molecule as a Structure for Pepsin.

The first datum to interpret is the fact that pepsin is a molecule which is in some sense "globular," and has molecular weight 39,200. Evidently, as in the case of insulin (Wrinch, 1936 *c*), the only one of the series of space-enclosing cyclol molecules which comes into question is the molecule C_2, which, consisting of 288 amino acid residues, has a molecular weight of the right order of magnitude. We further suggest that its polyhedral configuration is in accordance with, and provides an interpretation of its "globularity" which has been established by Svedberg. Further, this structure, consisting entirely of amino acid residues, does not postulate the existence of a prosthetic group.

We consider next how far the X-ray analysis fits with the geometry of the C_2 structure. In the first place, the structure has a polyhedral frame consisting of four hexagonal and four triangular faces, arranged in four parallel pairs. If normals through the centres of parallel faces be drawn, they intersect in O the orthocentre of the frame. There are, therefore, four tetrahedrally related axes associated with each molecule, and apart from R groups (*i. e.*, the side chains or rings of the amino acids) each is a trigonal axis of the molecule. To build a lattice it is sufficient if the four directions associated with any one molecule are adopted as characterizing the lattice in general, so that the molecules are arranged so that each has one pair of faces normal to each of these four directions.

To build a trigonal lattice, it is sufficient to impose a trigonal R distribution on one hexagonal and one trigonal faces of each molecule and to make the remaining three hexagonal faces and also the remaining three triangular faces—identical in R distributions.

In the lattice, then, each molecule has H, T faces normal to the trigonal axis, and its other three identical pairs *h*, *t* normal to three directions which, with the trigonal axis, make up a tetrahedrally related set.

The C_2 molecules thus lend themselves readily to arrangement in accordance with the X-ray findings. Since there is a 4-coordination pattern, molecules are coordinated by the parallel apposition of H or of T faces. We have selected the case when T faces are apposed for illustration and consideration. The only other arbitrary point is the orientation of the molecules with respect to the hexagonal

Fig. 7.

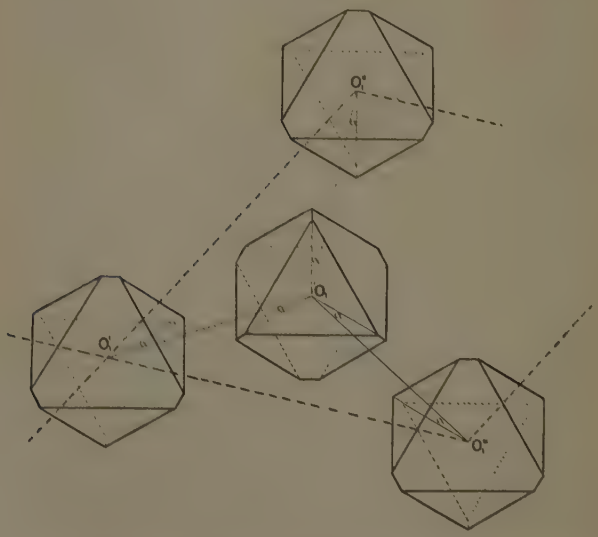

C_2 molecules arranged in the hexagonal cell of the pepsin lattice.

cell, or, in other words, the value of the angle α shown in fig. 7. The value of α should in due course be deducible from X-ray studies of pepsin crystals. Fig. 8 shows the arrangement of molecules belonging to different layers. In view of the proposed alternation of α and β layers, the diagram shows a layer 2 superposed on a layer 1 in the β position and a layer 3 superposed on a layer 2 in the α position. Fig. 8 is drawn for the particular case when α is zero; it can be modified without difficulty to cover the case when α has any specified value.

Using the X-ray measurements and the dimensions of the C_2 molecule we find that the TT interface distance is

$$\begin{aligned} T_1T_2' &= O_1O_2' - O_1T_1 - T_2'O_2', \\ &= 41{\cdot}33 - 2 \times 12{\cdot}75, \\ &= 15{\cdot}83 \text{ Å}. \end{aligned}$$

Fig. 8.

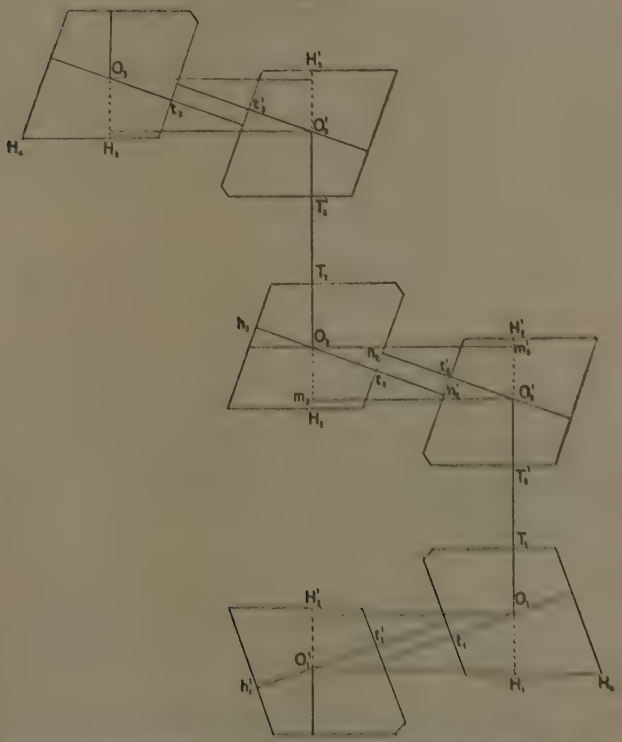

C_2 molecules arranged in the rhombohedral cell of the pepsin lattice.

These faces are centrally aligned. The *tt* faces are not centrally aligned, either along the axes O_2t_2, $O_2't_2'$ or (unless α is zero) along axes perpendicular to these. The *tt* interface distance is

$$\begin{aligned} n_2t_2' &= n_2't_2, \\ &= O_2m_2' \sin\delta - O_2m_2 \cos\delta - O_2t_2 - O_2't_2'. \end{aligned}$$

$=67/\sqrt{3}.\sin\delta\cos\alpha-10\cos\delta-25{\cdot}5,$

$=14{\cdot}30-36{\cdot}47\ (1-\cos\alpha),$

$=14{\cdot}30,\ 14{\cdot}15,\ 13{\cdot}74,\ 13{\cdot}06,\ 12{\cdot}10,\ 10{\cdot}89,\ 9{\cdot}41$ Å.,...

when

$\alpha=0°,\ 5°,\ 10°,\ 15°,\ 20°,\ 25°,\ 30°,\ \ldots$

Evidently, therefore, there is no difficulty in arranging the C_2 molecules in the manner suggested by the X-ray analysis. It remains to consider the interface distances with a view to discovering, if possible, the actual mechanism of coordination in the lattice. As was found in the case of insulin, an interface distance of 6·2 Å fits well with coordination by means of peptide hydroxyls; distances appreciably greater than these indicate that R groups are involved. In pepsin the TT distance is 15·83 Å. and the *tt* distance

$$14{\cdot}30-36{\cdot}47\ (1-\cos\alpha).$$

Both types of coordination, therefore, involve R groups.

The Mechanism of Coordination in the Crystal.

Among the R groups which may be involved are those belonging to tyrosine, glutamic acid, and aspartic acid, and the diamino acids. All the possible mechanisms of coordination can be considered in turn when the chemical composition of pepsin is known more fully. They are strictly limited in number. Obvious possibilities include the following :—

1. Association of the phenolic groups of tyrosine.
2. Dimeric association of glutamine (or aspargine) molecules, similar to the dimeric association of molecules in isatin crystals (Cox, Goodwin and Wagstaff, 1936).
3. Association of glutamic or aspartic acid molecules with water molecules as intermediaries, as in the case of the molecules in crystals of oxalic acid dihydrate (Zachariasen, 1934 ; Bernal and Megaw, 1935).

1. The fact that acetyl pepsins, in which in addition to lysine R groups some tyrosine R groups have been acetylated, form crystals which are indistinguishable from pepsin crystals (Herriott and Northrop, 1934), suggests

that tyrosine residues play no part in coordination mechanisms. This mechanism, otherwise plausible, will not be further considered until an X-ray analysis of the various acetyl pepsins is available. A comparative study of pepsin and the acetyl pepsins will settle the point.

2. In isatin the O—H—N distance is taken to be 2·8 Å., and the distance between the carbon atoms in the apposed HN—C—O groups, measured parallel to the remaining valency bonds of these carbon atoms to be 4·0 Å. To apply these measurements to a similar type of coordination between the δ—$CO.NH_2$ groups of glutamine residues located in the apposed faces, we estimate the distance measured normal to the faces between C_α and C_δ as equal to

$$1{\cdot}54+1{\cdot}54/3+1{\cdot}54=3{\cdot}59 \text{ Å}.$$

giving, if C_α is ·26 Å. from the face, the distance from the face to C_δ equal to 3·85 Å. The distance between faces would then be

$$3{\cdot}85+4{\cdot}0+3{\cdot}85=11{\cdot}7 \text{ Å}.$$

This distance appears to be appropriate for *tt* coordinations and would carry with it the suggestion that α is 20° to 30°.

3. We also suggest for consideration the association of glutamic acid molecules with water, molecules as intermediaries, as in the case of the molecules in crystals of oxalic acid dihydrate. Here the distance between the carbons of the apposed carboxyl groups is (about)

$$5{\cdot}37+2\times1{\cdot}25\cos 63°=6{\cdot}49 \text{ Å}.$$

If the C_β atoms of the glutamic acid molecules are at distances 3·85 Å. from the faces in which they are located, the distance between the faces is

$$3{\cdot}85+6{\cdot}49+3{\cdot}85=14{\cdot}19 \text{ Å}.$$

This distance fits adequately with the given *tt'* interface distance of

$$14{\cdot}30-36{\cdot}47\ (1-\cos\alpha)$$

and carries with it the implication that α is small, say not greater than 5°. It may plausibly be considered in further detail when the exact number of glutamic acid molecules in the molecule of pepsin is known. Such knowledge

necessarily presupposes an estimate of the number of glutamine molecules in the pepsin molecule, since not all the glutamic acid molecules found when the pepsin hydrolysate is analysed represent glutamic acid residues with free carboxyl groups in the molecule.

The greater distance between TT faces (15·83 Å.) implies that the coordination of these faces requires the co-operation of a greater number of water molecules. The apposition of the parallel TT faces will be of two types according to whether the layers stand in the α or β relation. We may picture the apposition being of one or other type according to the way in which one single pair of molecules are apposed. Given an α-situation here, this situation will be maintained throughout the layers. A certain degree of random in the alternations of α and β situations, as is allowed by the X-ray findings, therefore seems quite likely.

It is premature to try to decide between the coordinating mechanisms above suggested for consideration. The important points are that the chemical analysis of pepsin restricts them to a very few alternatives and that only a more complete analysis of pepsin is required to make a decision between them. Great interest attaches to the analysis of egg albumin, hæmoglobin, and fibrinogen by Bergmann and Niemann, in which certain R groups are shown to have characteristic frequencies in these protein molecules. A similar analysis for pepsin is urgently required. An estimate of the number of glutamines in the molecule would be of special interest.

The Water associated with Pepsin in the Crystal.

It will be noticed that the mechanism of TT co-ordination suggested for pepsin on the basis of the X-ray measurements (in contradistinction to those suggested for insulin) involve the cooperation of water molecules. The lattice would therefore collapse if these water molecules were withdrawn. This fits admirably with the well-known fact that pepsin crystals lose their stability on drying. The main factor causing the crystal to collapse on drying must, however, have to do with the disposition in the crystal of the rest of the enormous complement of (say) 2250 water molecules per molecule of pepsin, which is present in the lattice.

Now, of this large number of molecules, some, as suggested, may be used in *tt* and TT′ coordinations. Several hundreds may be needed intramolecularly (this includes those filling spaces in the interior of the molecule), for the cyclol fabric possess one peptide hydroxyl per amino acid residue, and, with the considerable distances apart of molecules in the lattice, no single peptide hydroxyl can form direct links with peptide hydroxyls of neighbouring molecules. It is presumed that blocks of water molecules in orderly array act as intermediaries linking hydroxyl to hydroxyl, however far apart they may be. A few water molecules may also be required for some hydroxyl R groups. But at the most, the intramolecular complement of water molecules can hardly exceed some hundreds, leaving a thousand or two (including the few involved in *tt* and TT coordination) to be used non-intramolecularly.

It seems probable that these water molecules form megaclusters so that there is a severely crystalline arrangement of atoms throughout the lattice. Clusters of water molecules are not unknown in molecular lattices. An interesting precedent is afforded by the beautiful structure recently established for $H_3PW_{12}O_{40}.29\,H_2O$ (Bradley and Illingworth, 1935). This structure consists of two interpenetrating diamond lattices. The one consists of eight anions $PW_{12}O_{40}$, the other of eight clusters of water molecules together with the acidic hydrogens $H_3.29H_2O$, so that the structure may therefore be regarded as a regular alternation of anions and cations. The implications for the structure of pepsin are obvious. We may postulate that megaclusters of water molecules (possibly also containing hydrogen and hydroxyl ions) are located in layers intermediate between the layers of pepsin molecules. When one layer stands to the next in the α relation, each molecule will have a sixth share of six clusters, which will, therefore, each contain the net number corresponding to one molecule of insulin. When the layer stands to the next in the β relation, each molecule has a sixth share of three clusters, which thus contain twice as many water molecules.

Whatever, in fact, is the arrangement of the enormous number of water molecules in the pepsin lattice, it appears from the present investigation that there is an essential difference between pepsin and insulin in regard to the types of intermolecular coordinations involved in the

lattices, in that some water molecules at least appear to be used as intermediaries between the pepsin molecules, whereas few apparently are so used in the insulin lattice.

Conclusions.

In view of the preliminary investigation of the data regarding pepsin which has been given in this communication, the closed cyclol C_2 is proposed as the structure of pepsin. The arguments in favour of this structure for pepsin include the following :—

The C_n molecules have a polyhedral character and so offer an interpretation of the "globular" character of pepsin. They contain no prosthetic group. They explain the 4-coordination pattern in pepsin crystals in terms of the apposition of their four triangular (or hexagonal) faces. The trigonal nature of the lattice is easily translated into terms of the arrangements of the various types of residues in the cyclol fabric.

The molecular weight of pepsin is known sufficiently accurately to disqualify the structures C_1 and C_3, so that only the structure C_2 comes into consideration. This structure has a molecular weight which is of the right order of magnitude. The C_2 molecule fits easily into the carborundum-like structures which have been deduced from the X-ray analysis and in doing so suggests possible mechanisms of coordination in the lattice. These involve the cooperation of water molecules. The presence of mega-clusters of water molecules in the lattice is also implied. In this way the instability of pepsin crystals on drying is explained.

The author offers thanks for advice and criticism to Professor M. Bergmann, to Professor Northrop and R. M. Herriott, to J. D. Bernal and D. Crowfoot, A. J. Bradley, H. D. Megaw and J. M. Robertson, to J. St. L. Philpot, and to E. H. Neville. Thanks are also offered to M. F. Howson who was good enough to draw the diagrams.

References.

M. Bergmann and C. Niemann, J. Biol. Chem. cxviii. p. 301 (1937).
J. D. Bernal and D. Crowfoot, 'Nature,' cxxxiii. p. 794 (1934).
J. D. Bernal and H. D. Megaw, Proc. Roy. Soc. A, cli. p. 384 (1935).
A. J. Bradley and J. W. Illingworth, Proc. Roy. Soc. A, clvii. p. 113 (1935).

H. O. Calvery, R. M. Herriott and J. H. Northrop, J. Biol. Chem. cxiii. p. 11 (1936).
E. G. Cox, T. H. Goodwin, and A. I. Wagstaff, Proc. Roy. Soc. A, clvii. p. 399 (1936).
D. Crowfoot, ' Nature,' cxxxv. p. 591 (1935).
R. M. Herriott and J. H. Northrop, J. Gen. Physiol. xviii. p. 35 (1934).
J. St. L. Philpot and I. B. Eriksson-Quensel, ' Nature,' cxxxii. p. 932 (1933).
J. M. Robertson, *Z. Krist.* lxxxix. p. 318 (1934).
J. M. Robertson, ' Nature,' cxxxvi. p. 755 (1935).
T. Svedberg, J. Amer. Chem. Soc. (1929 *et seq*) ; ' Nature,' cxxxix. p. 1051 (1937).
D. M. Wrinch, ' Nature,' cxxxvii. p. 411 (1936) ; cxxxviii. pp. 241 and 651 (1936).
D. M. Wrinch, ' Nature,' cxxxix. p. 972 (1937 α).
D. M. Wrinch, Proc. Roy. Soc. A, clx. p. 59 (1937 β).
D. M. Wrinch, ' Science,' lxxxv. p. 566 (1937 γ).
D. M. Wrinch, Proc. Roy. Soc. A, clxi. p. 505 (1937 δ).
W. H. Zachariasen, *Z. Krist.*l xxxix. p. 442 (1934) ; Phys. Rev. xlv. p. 755 (1934).

LXXXII. *The Diffraction of Beta-Rays.* *By* Samuel C. Curran, *M.A., B.Sc., Ph.D., Carnegie Research Scholar, Glasgow University.**

Introduction.

THE diffraction of electrons is a subject which has received considerable attention, both theoretical and experimental, in recent years. Since Elsasser [1] suggested that evidence for the wave-nature of electrons would be found in their interaction with crystals considerable attention has been devoted to the matter. The equation of de Broglie, $\lambda=h/mv$ [2], has been verified, λ being the wave-length, h Planck's constant, m and v the mass and velocity of the electron respectively. The experiments of Davisson and Germer [3] and of G. P. Thomson [4] mark the beginning of a long series of investigations in which the diffraction of electrons has been studied by many experimenters, employing both transmission and reflexion methods, for energies of the electrons between 65 and 10^5 electron volts. Little work has been done with electrons of energy greater than 10^5 electron volts, though Rupp [5] has verified the equation $\lambda=h/mv$ up to 250,000 volts. Kosman and Alichanian [6] obtained diffraction patterns

* Communicated by Prof. E. Taylor Jones.

for electrons of 520,000 electron volts energy without verifying the law. The diffraction of the β-particles from radioactive sources is important for two reasons: (1) the velocity of β-particles is greater than that of normal artificially produced cathode rays; (2) it is desirable to co-relate the β-particle with the electron in the property of being diffracted. Hughes [7] has given results for β-rays transmitted through gold films, and the present work gives results for gold and aluminium films. The two methods employed in these experiments are quite different in their nature, the present paper describing a method of more general application.

Preliminary Experiments.

Many technical difficulties are encountered in approaching this problem. In work with cathode rays care is taken to render the beam homogeneous in velocity, and no great difficulty is experienced in this case. The β-rays emitted by radioactive sources are not homogeneous, and it is necessary to adopt some kind of resolving device such as a magnetic field. This results in a beam of very low intensity however. Another complication is introduced by the fact that there is generally a strong γ-radiation present. The measurement of a weak beam of β-particles in the presence of strong γ-radiation is a matter of some difficulty.

Preliminary experiments with strong sources of radon were attempted, the β-rays falling on the photographic plate being rendered homogeneous in a magnetic field. It was found that a beam sufficiently strong to show diffraction effects could not be obtained in this way. The non-homogeneous rays emitted by Ra(B+C) were used in a second attempt in which the rays were simply allowed to pass through a system of collinear apertures before falling on the photographic plate. The reason for trying this method is that a large part of the β-ray intensity from a source of Ra(B+C) lies within fairly narrow energy limits. Thus from the curve due to Chadwick [8] for the number of β-rays emitted by Ra(B+C) [9] we find that 23 per cent. of the total intensity (line and continuous spectrum) has energy limits at $H\rho = 1400$ and $H\rho = 2000$, or 153,000 and 264,000

electron volts respectively. To find the diameter of the diffraction rings we have :

$$eP\ 300 = m.c^2 \sqrt{1 - v^2 c^2} - m_0 c^2. \quad . \quad . \quad . \quad (1)$$

$$\lambda = h \sqrt{1 - v^2 c^2}\, m_0 v; \quad . \quad . \quad . \quad . \quad . \quad (2)$$

$\therefore$ eliminating v and approximating,

$$\lambda = h \sqrt{150\, eP m_0}\ (1 + eP/1200 m_0 c^2). \quad (3)$$

The symbols in (1), (2), and (3) have the usual meanings, and eP is the energy in electron volts.

If D = diameter of ring, L = distance from film to plate, d = spacing between the crystal planes,

$$D = 2\lambda L/d; \quad . \quad . \quad . \quad . \quad . \quad . \quad . \quad . \quad . \quad . \quad (4)$$

$$\therefore \quad D = 2Lh \sqrt{150\, eP m_0}\, d(1 - eP/1200 m_0 c^2). \quad . \quad . \quad . \quad (5)$$

Substitution of the numerical values in equation (5) shows that D = 10·0 mm. for P = 153,000 volts and D = 7·6 mm. for P = 264,000 volts for the (2 0 0) planes of gold. These diffraction rings were expected to appear as the edges of a rather broad diffuse ring round the central spot, but even with extremely dense spots no rings were visible. From this work it appeared that a photographic method would prove difficult and tedious, and the electrical counter was chosen as the detector on account of its extreme sensitivity. Hughes [7] employed a photographic method, and diffracted β-rays from radon for values of the momentum given by $H\rho = 1938$ to $H\rho = 4866$. The diffraction rings obtained agreed to within 5 per cent. with those expected from de Broglie's equation. His method, a modification of one proposed by Lebedeff [10], includes focussing and selection of rays of a particular velocity. It suffers, however, from two defects : (1) β-rays of energy slightly different from those focussed at the centre form a background on the plate ; (2) very large thin films, about 5 cm. diameter, are required. Thus success was achieved only with gold sputtered on a gelatine base.

The first attempt to use an electrical counter with a homogeneous beam proved unsuccessful, largely on account of the strong γ-radiation from the radon source. The background of counts due to γ-rays was of the same

order of magnitude as the counts due to the homogeneous β-rays, even when considerable lead shielding was employed. The action of γ-radiation can be minimized by the choice of material for the counter walls [11] etc., but it cannot be entirely eliminated, since the γ-rays form secondary β-rays in passing through matter, and any counter which responds to β-rays must of necessity respond to γ-rays. It is generally the case that β-rays from radioactive sources are accompanied by γ-rays, but an important exception to this is RaE. This element emits a normal continuous spectrum of β-rays or disintegration electrons [12] whose limits are given by $H\rho=1600$ and $H\rho=5000$ with a single maximum of intensity at $H\rho=2100$. No γ-rays are emitted by this element (actually the extremely small emission can be neglected), and there are no homogeneous groups superimposed in the form of a line spectrum. These unique properties indicated RaE as the most suitable source for the work proposed, and the first successful results were obtained with a specially prepared source of this element.

Apparatus.

The Counter.—The Geiger point counter was used as detector of the β-rays, since these were in the form of a narrow pencil and this type of counter is the most suitable one for work in such circumstances. The effective counting volume in this form of tube is limited to a small narrow cone [13] with its apex at the point and its base on the metal front if the piont is nearer the front than the sides. In this tube the natural count is small, an important thing when counting small intensities of β-radiation. The efficiency of such a tube may be made very small, but this is not important where the source is of RaE. The dimensions of the tube were: length of cylinder, 6 cm.; diameter of cylinder, 2 cm.; distance of point from face, 0·8 cm. A copper rod, 0·5 cm. diameter, supported in an ebonite insulating plug corrugated along the surface to increase the resistance, bore the point electrode which was made of steel and ground to the form suggested by Emeléus [14]. Before assembly the point was washed in alcohol and slightly heated. The hemispherical tip was of diameter

0·01 cm. The vessel was of copper, and it was heated and immersed in alcohol in order to obtain a clean smooth surface. The counter was filled with dried air or argon to a pressure of about 10 cm. Hg, the drying being carried out by passing the gas from a vessel immersed in liquid air. Before readings were taken the tube was allowed to count steadily for a few days. Contrary to usual procedure the cylinder was maintained at a potential negative with respect to the point, since greater efficiency in β-ray detection was secured in this way. The counting voltage was determined by graphing counts per minute against applied voltage, and setting the voltage at the middle of the plateau on the curve. This eliminated any tendency on the part of the counter to show instability or to pass spurious discharges. The potential was supplied by dry batteries and was steady over long periods. It was determined experimentally that the statistical variation in a total count of the order of 3000 was less than 0·6 per cent.

The Amplifier and Register.—Several good amplifiers for use in counting experiments have been described [15]. The amplifier used in the present work differed in some ways from these. It was a three-stage resistance capacity coupled amplifier with high voltage magnification. The first valve was a screened-grid valve, the second and third being triode and pentode valves respectively. The amplifier was enclosed in an earthed metal screen, and decoupling was made as complete as possible. The output of the amplifier was fed into a loudspeaker, a thyratron valve circuit controlling an automatic register, and a cathode ray oscillograph, all connected in parallel. The first and last formed an effective check on the action of the counter. The automatic recording device was that of Wynn-Williams [16].

The Experimental Arrangement.

The arrangement is indicated in fig. 1. A Pyrex glass tube was closed at both ends by ebonite plugs with central apertures covered by thin mica films. The source-holder was mounted in the tube at one end. The source of β-rays was of Ra(D+E+F) in equilibrium, and it was prepared from old radon tubes which had decayed for periods of between two and three years. It was

mounted at A in the source-holder, and held in position by the cap B. The source was on the axis of a cylinder S, 2·4 cm. external diameter, 1·5 cm. internal diameter. The cylinder was in two sections, and directly opposite the source was a small aperture D of diameter 0·5 mm. The distance from A to D was 7 cm. The film-holder E was immediately in front of D. Between the film and the counter a small electromagnet was mounted, so that

Fig. 1.

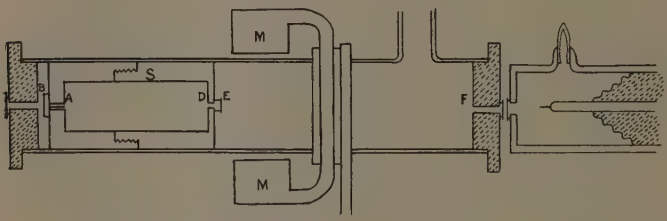

The camera and counter.

Fig. 2.

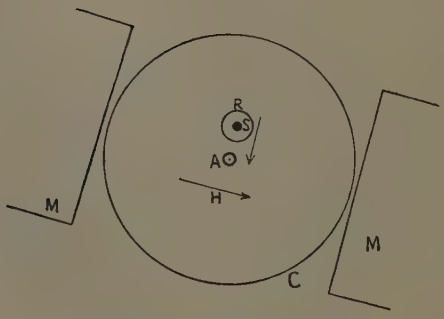

Magnetic analysis of pattern.

it could be rotated round the axis of the tube. The rays through the tube left it by an aperture F of 1 mm. diameter, and immediately behind this was placed the counter aperture of 2 mm. diameter. The tube was connected to a pumping system. The air equivalent of the two mica windows between source and counter was 1·8 cm. The distance from film to F was 10 cm.

The source prepared from old radon tubes was of Ra(D+E+F), the quantities of the last two being to within 2 per cent. in their equilibrium ratio [17]. The β-rays of RaD are very soft [18] and are absorbed by the mica films, so that they can be neglected. Emeléus [19] has shown that there are 24·5 β-particles to every 17·1 α-particles from RaF with this source. The α-rays were usually absorbed by putting a thin mica film between camera and counter to increase the air equivalent of the films to 4 cm. When the α-rays were not so absorbed they formed a constant background to the total count. The principle of the method is indicated in fig. 2. Suppose M represents the poles of the magnet producing a field H across the tube whose section is indicated by circle C. The aperture F of fig. 1 is indicated by A. Suppose the β-ray beam falls at S; in that case β-rays will not be detected. With the poles in the setting shown and at a certain value of the field H the beam S will coincide with A and the β-rays will pass into the counter. Any diffraction ring R formed round S will likewise be deviated by the magnetic force, and will be observed as an increase in the β count. From the values of H required to produce the displacements of the rays the diameter of the ring may be calculated. It may be noted that the method depends on the fact that RaE has no line spectrum, as this would complicate results. RaE has a single maximum of intensity at $H\rho=2100$. The magnetic control does not lend itself to accurate determination of ring diameters, but since the rays were not homogeneous this is not of great importance. Only approximate values can be expected, but the actual results obtained show fairly good agreement with the theoretical values.

Discussion of Results.

Consider an electron moving across the magnetic field whose area is bounded by the circle ACD of fig. 3. Let AB be the undeflected path of the electron along a diameter of the circle, and suppose the lines of force of the magnetic field, of strength H, are perpendicular to the plane of the figure. Let the diameter $AC=2a$. The displacement $x=BE$ of the electron from B, at distance b from C, where BE is $\perp^r$ AB, is required. The electron describes

the arc of the circle AD and leaves in the direction DE. The radii AO $\perp^r$ AB and DO $\perp^r$ DE meet in O. Let ED meet AC in G. Then G is the centre of the circle ACD, since AG=GD and G is on a diameter.

$$\therefore \quad GB=GC+CB=b+a.$$

$x=$GB tan θ, where $\theta=\angle$ AOD$=\angle$ BGE and tan $\theta/2=a/\rho$, where $\rho=$radius AO;

$$\therefore \quad x=(a+b)2a/\rho(1-a^2/\rho^2). \quad . \quad . \quad . \quad . \quad . \quad (6)$$

Fig. 3.

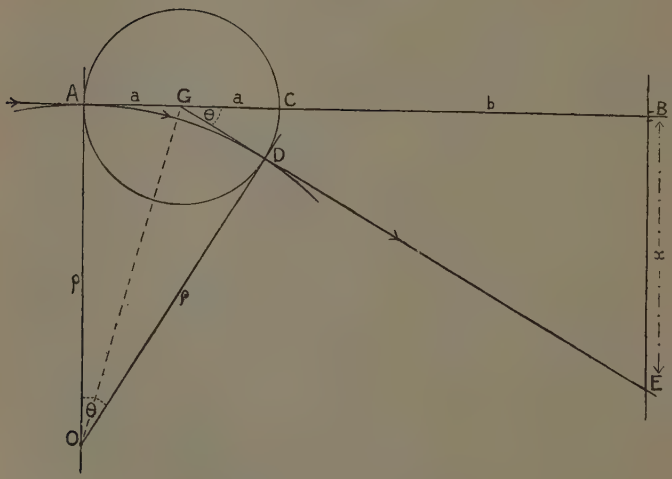

Magnetic deviation of electron.

For this particular experiment $H\rho=2100$, $b=5{\cdot}6$ cm., $a=1{\cdot}0$ cm.

$$\therefore \quad x=0{\cdot}0063H/[1-(H/2100)^2].$$

Since H is seldom greater than 40 a good approximation is

$$x=0{\cdot}0063 \text{ H or}$$

$$\delta x=0{\cdot}0063\ \delta H \quad . \quad . \quad . \quad . \quad . \quad . \quad (7)$$

for displacements corresponding to variations in H. Equation (7), though proved for the case of a ray passing along a diameter, can be shown to be approximately

true for adjacent rays. The small change δH is found in practice from a calibration curve connecting field strength H with current i through the windings of the magnet.

In tracing any actual diffraction curve counts were taken at different settings of the magnet and at different values of H till the particular setting and value of H

Fig. 4.

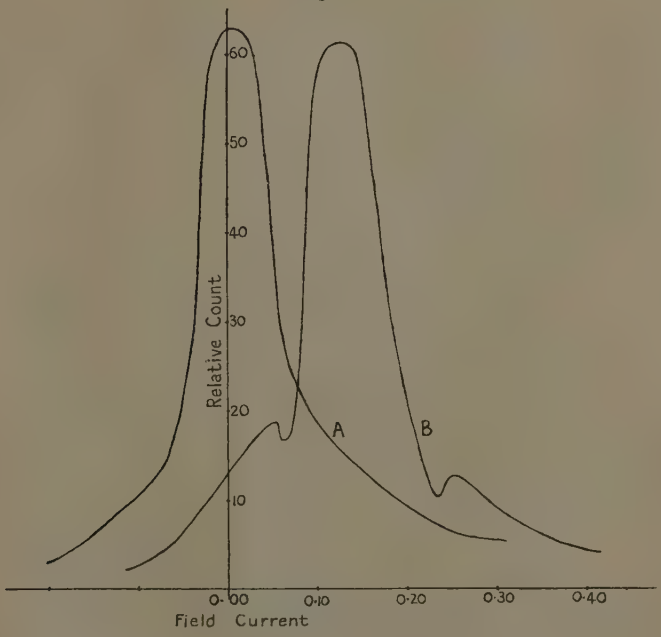

Curve A. No film. Curve B. Aluminium film.

giving a maximum count were obtained. In many cases where careful alignment of source, aperture at film, and window at counter end had been carried out the maximum count was at $H=0$, or, in other words, the beam fell directly on the counter window. When the maximum was obtained the magnet was clamped in position and counts were taken for various values of H in the neighbourhood of the particular value at the maximum. The different values of total count

so obtained were then plotted against corresponding field currents. Each count plotted was the mean of a number of experimental values. When no diffracting film was present the curves took the form shown in fig. 4, curve A, a smooth curve with a single large maximum. With a film present two small maxima could be detected on the curve, as shown in fig. 4, curve B, which gives a result for an aluminium film. The two

Fig. 5.

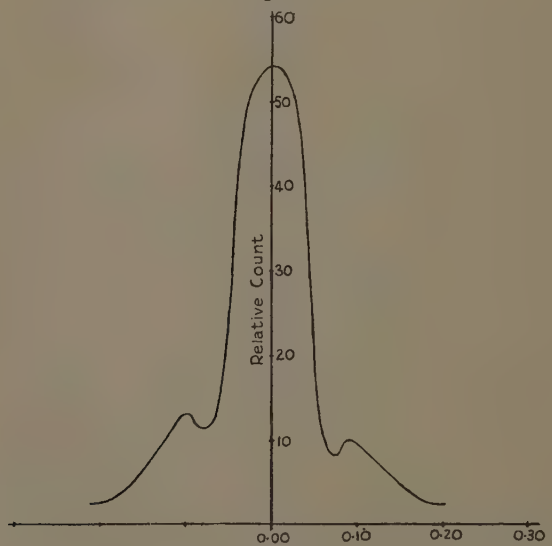

Gold film.

small maxima indicate the presence of a diffraction ring formed round the primary beam. Consider curve B. The small maxima are at $i_1 = 0{\cdot}25$ amp., $i_2 = 0{\cdot}05$ amp. Thus the change in field current $= \delta i = 0{\cdot}20$ amp. From the calibration curve of the magnet $\delta H = 34{\cdot}6$ gauss for this value of δi. Hence $\delta x = 0{\cdot}0063\ \delta H$ cm. by equation (7) $= 0{\cdot}22$ cm. The diameter D of the diffraction ring is given then by $D = 0{\cdot}22$ cm. Now from equation (5) we find by calculation that for rays of $H\rho = 2100$ (or

P=300,700 volts) D for the (2 0 0) ring of aluminium =0·193 cm. The agreement between the theoretical and experimental values is very satisfactory when it is remembered that the β-rays are not homogeneous and the magnetic field is not uniform over its whole effective area. It is assumed that the diffraction maxima correspond to rays in the large maximum that have suffered diffraction in passing through the film—that is, to rays of $H\rho=2100$ or of wave-length $\lambda=h/mv=$ 19·6 X.U.

The curve of fig. 5 gives a typical curve obtained with a gold film. From the figure the diameter of the ring=0·21 cm. The diameter of the (2 0 0) ring for gold for P=300,700 volts is, by equation (5), =0·192 cm. This is, again, satisfactory agreement between theory and experiment. Diffraction experiments with celluloid films failed to produce definite results. The smallness of the pattern to be expected in this case would explain the failure, since the instrument is not capable of resolving maxima which occur very close to the main beam. Narrower apertures and source giving greater resolving power would at the same time add considerably to the experimental difficulties. The smallness of the diffraction maxima with β-rays as compared with cathode rays is a notable feature of the experiments. One reason for this may be found in the greater velocity of the β-particle. The diffraction curves are the result of careful counting of a very large number of rays, and it was verified thoroughly that the maxima occurred only when the diffracting films were present.

The writer is much indebted to Professor E. Taylor Jones for his helpful advice and interest in the work. The experiments were carried out in the Research Laboratories of the Natural Philosophy Department at Glasgow University. Part of the research was done by the author during his tenure of a Carnegie Research Scholarship, for which he expresses his thanks.

References.

(1) W. Elsasser, *Naturwissenschaften*, xiii. p. 711 (1925).
(2) De Broglie, ' Dissertation ' (Masson, Paris, 1924); Phil. Mag. xlvii. p. 446 (1924).
(3) Davisson and Germar, Phys. Rev. xxx. p. 707 (1927).
(4) G. P. Thomson, Proc. Roy. Soc. A, cxvii. p. 600 (1927).

(5) Rupp, *Ann. Physik*, lxxxv. p. 981 (1928) ; l. p. 773 (1929).
(6) Kosman and Alichanian, *Naturwissenschaften*, xxi. p. 250 (1933).
(7) Hughes, Phil. Mag. xix. p. 129 (1935).
(8) Chadwick, *Verh. d. d. Phys. Ges.* xvi. p. 383 (1914).
(9) ' Radiations from Radioactive Substances' (Rutherford, Chadwick, and Ellis), p. 400.
(10) Lebedeff, ' Nature,' cxxviii. p. 491 (1931).
(11) Myers and Cox, Phys. Rev. xxxiv. p. 1067 (1929).
(12) Madgwick, Proc. Camb. Phil. Soc. xxiii. p. 982 (1927) ; Hahn and Meitner, *Phys. Z.* cccxxi. p. 697 (1908).
(13) ' Conduction of Electricity through Gases ' (Sir J. J. Thomson and G. P. Thomson), 3rd ed. vol. ii. p. 176.
(14) Emeléus, Proc. Camb. Phil. Soc. xxxii. p. 576 (1923–25).
(15) Locher, Phys. Rev. xlii. p. 528 (1932) ; Van den Akker and Watson, Phys. Rev. xxxvii. p. 1631 (1931) ; De Bruyne and Webster, Proc. Camb. Phil. Soc. xxvii. p. 113 (1931).
(16) C. E. Wynn-Williams, Proc. Roy. Soc. A, cxxxii. p. 295 (1931).
(17) St. Meyer and E. v. Schweidler, ' Radioaktivität,' p. 365.
(18) Meitner, *Phys. Z.* xvi. p. 272 (1915).
(19) Emeléus, Proc. Camb. Phil. Soc. xxii. p. 400 (1923–25).

LXXXIII. *The Theory of Elastic Scattering of a Beam of Particles by Atoms. By* Profs. K. C. Kar, *D.Sc.*, M. Ghosh, *M.Sc.*, *A.Inst.P.*, *and* K. K. Mukherjee, *M.Sc.**

THE wave-theory of elastic scattering was first developed in a general form by Born † and Elsasser ‡. Wenzel § and Bethe and Mott ‖ have used the above method of Born up to first approximation only, and derived formulæ which reduce to the well-known Rutherford formula of scattering, if the perturbing potential is supposed to be Coulombian. Thus, according to Wenzel, the intensity of scattering (I) of a beam of electron (e) at an angle θ per unit solid angle and per unit distance from the scattering centre, is given by

$$I = \left(\frac{Ze^2}{mv^2}\right)^2 \cdot \frac{1}{\left(\sin^2\frac{\theta}{2} + \beta^2\right)^2}, \quad \ldots \quad (1)$$

* Communicated by Prof. K. C. Kar, D.Sc.

† M. Born, *Gött. Nachr.* p. 146 (1926) ; also *Zs. f. Phys.* vol. xxxvii. p. 863 (1926) ; vol. xxxviii. p. 803 (1926).

‡ W. Elsasser, *Zs. f. Phys.* vol. xlviii. p. 522 (1927).

§ Wenzel, *Zs. f. Phys.* vol. xl. p. 590 (1927).

‖ H. Bethe, *Ann. d. Phys.* vol. v. p. 325 (1930) ; he uses Schrödinger's perturbation method. Mott, Proc. Roy. Soc. A, vol. cxxvii. p. 658 (1930).

where z is the atomic number of the scattering atom, v the velocity of the incident electrons, and $\beta=\frac{z}{ak}$ in which a is the radius of the first Bohr orbit of hydrogen and $k=\frac{2\pi mv}{h}$. The other symbols have their usual meaning. It should be noted that if the perturbing potential is taken to be Coulombian, then $\beta=0$ and so (1) becomes the same as Rutherford's formula obtained from classical dynamics.

According to Bethe and Mott, the intensity of scattering is given by

$$I=\left(\frac{e^2}{mv^2}\right)^2 \operatorname{cosec}^4\frac{\theta}{2}(Z-f(\theta))^2, \quad . \quad . \quad . \quad (2)$$

where $f(\theta)$ is the atomic "structure factor." If the interaction between the orbital electrons of the atom and the incident electron is neglected, then $f(\theta)=0$. So that (2) at once reduces to Rutherford-Born formula. It is evident that $f(\theta)$ is of the nature of screening constant, depending on the angle of scattering (θ). A similar correction, it may be noted, is made in the formula for the X-ray scattering.

Now, of the two formulæ quoted above, the first gives too low a value for the intensity, especially at small angles. As regards formula (2) of Bethe and Mott, it may be mentioned that recently Hughes, McMillen, and Webb * have made an attempt to verify it by first determining, for a given velocity of the bombarding electrons, a set of fitting values of $f(\theta)$ for different angles of scattering and then using this set of values to evaluate the intensity of scattering at different angles for other velocities of incidence of the beam of electrons. Since the structure factor $f(\theta)$ depends on θ only, there should be good agreement between the theoretical values thus determined and those observed. But actually it is found otherwise. This obviously goes against the theory of Bethe and Mott.

Thus a substantial improvement of the theory of elastic scattering is called for. Faxen and Holtzmark †

* Hughes, McMillen, and Webb, Phys. Rev. vol. xli. p. 154 (1932).
† Faxen and Holtzmark, *Zs. f. Phys.* vol. xlv. p. 307 (1927).

have, however, made an important advance in this direction. According to them

$$I = \left\{ \frac{1}{2ik} \Sigma_s (2s+1) P_s(\cos\theta)[e^{2i\eta_s} - 1] \right\}^2, \quad . \quad . \quad (3)$$

where $k = \frac{2\pi mv}{h}$ and

$$\eta_s = -\frac{\pi}{2} \cdot \frac{8\pi^2 m}{h^2} \int_0^\infty v(r) J_{s+\frac{1}{2}}^2(kr) r\, dr.$$

In deriving the above formula Faxen and Holtzmark have generally followed Rayleigh's * classical theory of scattering. However, it appears to us that if Rayleigh's theory is completely followed, the limit of the integral for η_s should be r_0 instead of zero. This is also evident from the fact that the incident electron can never approach the centre of the scattering atom. The minimum distance of approach should be, according to the classical mechanics, the distance of the vertex of the hyperbolic path from the centre of the atom. The wave-statistical value of this critical approach will, however, be derived in a different paper by one of the writers †.

Møller ‡ and Distel § have studied the limits of validity of the higher approximations of Born. According to them the series of approximations is convergent only when $\frac{u}{v} \leqslant 1$, where u is the velocity of the electron in the first Bohr orbit for hydrogen and v the velocity of the incident electron. A very rigorous treatment of the problem of scattering is also given by Gordon ‖, Temple ¶, and Sommerfeld **. But their formulæ cannot be expressed in terms of experimentally determinable quantities, and so are practically useless.

In the present paper we shall deduce a perfectly general formula of elastic scattering, somewhat similar to that of Faxen and Holtzmark, by considering the higher approximations of Born.

* Rayleigh, ' Theory of Sound,' vol. ii. art. 323.
† K. C. Kar, Phil. Mag. xxiv. p. 971 (1937).
‡ Møller, *Zs. f. Phys.* vol. lxvi. p. 513 (1930).
§ Distel, *Zs. f. Phys.* vol. lxxiv. p. 785 (1932).
‖ Gordon, *Zs. f. Phys.* vol. xlviii. p. 180 (1928).
¶ Temple, Proc. Roy. Soc. A, vol. cxxi. p. 673 (1928).
** Sommerfeld, *Ann. d. Phys.* vol. xi. p. 257 (1931).

We have for the incident wave equation

$$\Delta\chi_0 - k^2\chi_0 = 0. \quad . \quad . \quad . \quad . \quad . \quad . \quad (4)$$

since

$$\frac{8\pi^2 m}{h^2} E = k^2,$$

where

$$k = \frac{2\pi}{\lambda} = \frac{2\pi mv}{h}.$$

On coming within the potential field V the perturbed wave function must satisfy the equation

$$\Delta\chi + k^2\left(1 - \frac{V}{E}\right)\chi = 0. \quad . \quad . \quad . \quad . \quad . \quad (5)$$

where

$$\chi = \chi_0 + \lambda_1\chi_1 + \lambda_2\chi_2 + \ldots, \quad . \quad . \quad . \quad . \quad (6)$$

in which λ_1, λ_2, etc. are the coefficients of the different order scattering functions χ_1, χ_2, ... etc. On substituting (6) in (5) we have

$$\Delta\chi_0 + k^2\chi_0 + \lambda_1(\Delta\chi_1 + k^2\chi_1) + \lambda_2(\Delta\chi_2 + k^2\chi_2) + \ldots$$
$$= \frac{k^2 V}{E}(\chi_0 + \lambda_1\chi_1 + \lambda_2\chi_2 \ldots) \quad . \quad . \quad . \quad (7)$$

Remembering that the perturbing potential is small we equate the same order and get

$$\left.\begin{aligned}
&\Delta\chi_0 + k^2\chi_0 = 0 \text{ (incident).}\\
&\Delta\chi_1 + k^2\chi_1 = \frac{1}{\lambda_1}\cdot\frac{k^2 V}{E}\chi_0 \text{ (scattered).}\\
&\Delta\chi_2 + k^2\chi_2 = \frac{\lambda_1}{\lambda_2}\cdot\frac{k^2 V}{E}\chi_1 \text{ (scattered).}\\
&\quad\ldots\ldots\ldots\ldots\ldots\ldots\\
&\qquad\qquad\text{and so on.}
\end{aligned}\right\} \quad . \quad . \quad (8)$$

Let the incident wave be supposed to move along the x-axis, therefore $\chi_0 \sim e^{ikx}$. Hence, from (8) we have

for the well-known solution, taking the origin at the centre of force,

$$\chi_1(r_2, \theta_2) = -\frac{1}{4\pi\lambda_1} \cdot \frac{k^2}{E} \int V(r_1) e^{ikr_1} \frac{e^{ikr_{12}}}{r_{12}} d\tau_1, \quad . \quad . \quad . \quad . \quad (9)$$

where

$$r_{12}^2 = r_1^2 + r_2^2 + 2r_1 r_2 \cos \Theta \quad . \quad . \quad . \quad . \quad . \quad . \quad . \quad (9.1)$$

$$\cos \Theta = \cos \theta_1 \cos \theta_2 - \sin \theta_1 \sin \theta_2 \cos (\phi_1 - \phi_2) \quad . \quad (9.2)$$

As the incident and perturbed waves are symmetrical about the x-axis, we have $\phi_1 = \phi_2 = 0$. Thus (9.2) becomes

$$\cos \Theta = \cos \theta_1 \cos \theta_2 - \sin \theta_1 \sin \theta_2. \quad . \quad . \quad (9.3)$$

Again we have *

$$e^{ikx_1} = \sum_s^{0, \infty} (2s+1)\, i^s \sqrt{\frac{\pi}{2kr_1}}\, J_{s+\frac{1}{2}}(kr_1) P_s(\cos \theta_1), \quad (10)$$

and for $r_1 \gtrless r_2$

$$\sin \frac{kr_{12}}{r_{12}} = \pi \sum_n^{0, \infty} (n+\tfrac{1}{2}) \frac{J_{n+\frac{1}{2}}(kr_1)}{\sqrt{r_1}} \frac{J_{n+\frac{1}{2}}(kr_2)}{\sqrt{r_2}} P_n(\cos \Theta) \quad . \quad (11)$$

Supposing that there is an essential singularity at $r_{12} = 0$, we have

$$\frac{e^{ikr_{12}}}{r_{12}} \sim \frac{\sin kr_{12}}{r_{12}} \quad . \quad . \quad . \quad . \quad . \quad . \quad . \quad (12)$$

On substituting (12), (11), and (10) in (9) we get for the scattering function at r_2, since $\frac{k^2}{E} = \frac{8\pi^2 m}{h^2}$,

$$\chi_1(r_2, \theta_2) =$$

$$-\frac{2\pi mk}{\lambda_1 h^2} \int V(r_1) \left\{ \sum_s (2s+1) i^s \sqrt{\frac{\pi}{2kr_1}}\, J_{s+\frac{1}{2}}(kr_1) P_s(\cos \theta_1) \right.$$

$$\times \left. \left\{ \sum_n (2n+1) \sqrt{\frac{\pi}{2kr_1}}\, J_{n+\frac{1}{2}}(kr_1) \sqrt{\frac{\pi}{2kr_2}}\, J_{n+\frac{1}{2}}(kr_2) \right. \right.$$

$$\left. \left. P_n(\cos \Theta) \right\} d\tau_1 \quad . \quad . \quad . \quad (13)$$

* Watson, 'Bessel Functions.'

Again we have, since $m=0$, on account of axial symmetry,

$$P_n(\cos\Theta)=\sum_{m=-n}^{m=+n}\frac{(n-m)!}{(n+m)!}P_n^m(\cos\theta_1)P_n^m(\cos\theta_2)e^{im(\phi_1-\phi_2)}$$
$$=P_n^0(\cos\theta_1)P_n^0(\cos\theta_2)\quad\ldots\ldots\quad(14)$$

On substituting (14) in (13) and remembering that θ_1- integration vanishes unless $n=s$, we get

$$\chi_1(r_2,\theta_2)=-\frac{2\pi mk}{\lambda_1 h^2}\int_{r_0}^{\infty}V(r_1)\sum_s(2s+1)^2 i^s\cdot\frac{\pi}{2kr_1}J_{s+\frac{1}{2}}^2(kr_1)r_1^2dr_1$$
$$\times\int P_s^2(\cos\theta_1)\sin\theta_1\,d\theta_1\,d\phi_1\cdot\sqrt{\frac{\pi}{2kr_2}}J_{s+\frac{1}{2}}(kr_2)P_s(\cos\theta_2),$$

and since

$$\int P_s^2(\cos\theta_1)\sin\theta_1\,d\theta_1\,d\phi_1=\frac{4\pi}{2s+1},$$

$$\chi_1(r_2,\theta_2)=\frac{1}{k}\sum_s\sqrt{\frac{\pi}{2kr_2}}J_{s+\frac{1}{2}}(kr_2)(2s+1)i^sP_s(\cos\theta_2).\eta_s\quad(15)$$

where

$$\eta_s=-\frac{\pi}{2}\cdot\frac{8\pi^2m}{h^2}\int_{r_0}^{\infty}V(r_1)J_{s+\frac{1}{2}}^2(kr_1)r_1dr_1\quad\ldots\quad(16)$$

Substituting (15) in (8) we get in the same way the second order scattering function χ_2 and so on. Thus we have at r :—

$$\chi_0(r)=\sum_s\sqrt{\frac{\pi}{2kr}}J_{s+\frac{1}{2}}(kr)(2s+1)i^sP_s(\cos\theta),$$

$$\lambda_1\chi_1(r)=\sum_s\sqrt{\frac{\pi}{2kr}}J_{s+\frac{1}{2}}(kr)(2s+1)i^sP_s(\cos\theta).\eta_s,$$

$$\lambda_2\chi_2(r)=\sum_s\sqrt{\frac{\pi}{2kr}}J_{s+\frac{1}{2}}(kr)(2s+1)i^sP_s(\cos\theta).\eta_s^2,$$

. . . . . .

and so on.

Hence the total scattering is

$$\chi(r,\theta)=\lambda_1\chi_1+\lambda_2\chi_2+\ldots.$$
$$=\sum_s\sqrt{\frac{\pi}{2kr}}J_{s+\frac{1}{2}}(kr)(2s+1)i^sP_s(\cos\theta)\{\eta_s+\eta_s^2+\ldots\}$$

and if $\eta_s << 1$

$$= \Sigma_s \sqrt{\frac{\pi}{2kr}} J_{s+\frac{1}{2}}(kr)(2s+1)i^s P_s(\cos\theta) . \frac{\eta_s}{1-\eta_s} . \quad (17)$$

Now the asymptotic value of

$$\sqrt{\frac{\pi}{2kr}} J_{s+\frac{1}{2}}(kr) \sim \frac{\sin(kr - \frac{1}{2}s\pi)}{kr} \sim \frac{e^{ikr}}{kr} . i^{-s} \quad . \quad (18)$$

On substituting the above value in (17) we get

$$\chi(r, \theta) = \frac{e^{ikr}}{r} f(\theta), \quad . \quad . \quad . \quad . \quad . \quad . \quad (19)$$

where

$$f(\theta) = \frac{1}{k} \Sigma_s (2s+1) P_s(\cos\theta) . \frac{\eta_s}{1-\eta_s} \quad . \quad . \quad (19.1)$$

Hence we have, for the intensity of scattering,

$$I = \left\{ \frac{1}{k} \Sigma_s (2s+1) P_s(\cos\theta) . \frac{\eta_s}{1-\eta_s} \right\}^2 . \quad . \quad (19.2)$$

It should be noted that η_s of Faxen-Holtzmark (*vide* (3)) differs from η_s of ours (*vide* (16)) in so far as they have taken the lower limit of the integral involved to be zero instead of r_0. If this difference is ignored then evidently both (3) and (19.2) give the same value for I up to the first approximation only. It is well known that this approximate value may be easily reduced to Rutherford-Born form, on transforming after substituting the value of η_s. We shall not, however, do it here.

Now the higher approximations, discussed above form a series in η_s, which is convergent only if $\eta_s < 1$. Let us, therefore, evaluate η_s and find the conditions for the convergency. We have from (16) on using the asymptotic value in (18)

$$\eta_s = -\frac{8\pi^2 m}{kh^2} (-1)^s \int_{r_0}^{\infty} V(r) \, e^{2ikr} \, dr. \quad . \quad . \quad (20)$$

Taking the potential to be Coulombian and the incident particle to be an electron, we have, since $k = \frac{2\pi mv}{h}$,

$$\eta_s = \frac{2zu}{v} (-1)^s \int_{r_0}^{\infty} \frac{\sin 2kr}{r} \, dr, \quad . \quad . \quad (20.1)$$

where $u=\dfrac{2\pi e^2}{h}$ being the velocity of the electron in the first Bohr orbit for hydrogen.

If the lower limit is taken to be zero then the integral in (20.1) has the value $\pi/2$. Thus we have

$$\eta=\frac{\pi z u}{v}(-1)^s. \quad . \quad . \quad . \quad . \quad . \quad (20.2)$$

Hence the power series in η_s giving the higher approximations of scattering is convergent if $\dfrac{u}{v}<<1$. This is the condition obtained by Møller and Distel (*l. c.*). It may, however, be pointed out that the wave-statistical value of r_0 depends on the incident velocity v. In fact, it increases with the decrease of velocity. Thus the integral in question is much less than $\pi/2$ for low velocity, and so η_s may be less than unity even for low velocity of the incident electron, *i. e.*, even if $\dfrac{u}{v}>1$.

Physical Laboratory,
Presidency College, Calcutta.
March 1937.

LXXXIV. *On the Elastic Scattering by Hydrogen and Helium.* *By* Prof. K. C. Kar, *D.Sc.**

IT may be shown † that to a first approximation the scattering function for elastic collision is given by (*vide* (16))

$$\chi_1(r_2,\theta_2)=\mathrm{A}\sum_s\sqrt{\frac{\pi}{2kr_2}}\mathrm{J}_{s+\frac{1}{2}}(kr_2)(2s+1)i^s\mathrm{P}_s(\cos\theta_2).\eta_s, \quad (1)$$

where

$$\left.\begin{aligned}\eta_s&=-\frac{\pi}{2}\cdot\frac{8\pi^2m}{h^2}\int_{r_0}^{\infty}\mathrm{V}(r)\mathrm{J}^2_{s+\frac{1}{2}}(kr)r\,dr,\\ k&=\frac{2\pi mv}{h},\end{aligned}\right\} \quad . \quad . \quad (1.1)$$

* Communicated by the Author.
† Kar, Ghosh, and Mukherjee, Phil. Mag. xxiv. p. 964 (1937).

v being the velocity of the incident particle, m its mass, and A the averaging factor being equal to $\frac{1}{\sqrt{v}}$ if it is supposed that one electron crosses unit area in one second.

Now, it is well known * that for $r_1 \gtrless r_2$

$$\frac{\sin kr_{12}}{r_{12}} = \pi \sum_{s}^{0,\infty} (s+\tfrac{1}{2}) \frac{J_{s+\frac{1}{2}}(kr_1)}{\sqrt{r_1}} \cdot \frac{J_{s+\frac{1}{2}}(kr_2)}{\sqrt{r_2}} P_s(\cos\theta_1) P_s(\cos\theta_2). \quad (2)$$

If we take $r_1 = r_2$ and also r_1 along the axis of x being the direction of the incident wave, and so $\theta_1 = 0$, we have

$$\frac{\sin k'r_1}{k'} = \frac{\pi}{2k} \sum_{s} (2s+1) J^2_{s+\frac{1}{2}}(kr_1) P_s(\cos\theta_2), \quad . \quad (2.1)$$

where

$$k' = 2k \sin\frac{\theta_2}{2}. \quad . \quad . \quad . \quad . \quad . \quad . \quad (2.2)$$

Again, we have for the asymptotic value

$$\sqrt{\frac{\pi}{2kr_2}} J_{s+\frac{1}{2}}(kr_2) \sim \frac{\sin(kr_2 - \frac{1}{2}s\pi)}{kr_2} \sim \frac{e^{ikr_2}}{kr_2} \cdot i^{-s}. \quad . \quad (3)$$

Using the above value in (1) and substituting for η_s we get

$$\chi_1(r_2, \theta_2) = -\frac{\pi}{2k} \cdot \frac{8\pi^2 m}{h^2} A \cdot \frac{e^{ikr_2}}{r_2} \int_{r_0}^{\infty} \sum_{s} (2s+1) P_s(\cos\theta_2) V(r) J^2_{s+\frac{1}{2}}(kr_1) r_1 \, dr_1,$$

and from (2.1) after a little transformation

$$= -\frac{k \operatorname{cosec}\frac{\theta}{2}}{mv^2} A \cdot \frac{e^{ikr_2}}{r_2} \int_{r_0}^{\infty} \sin k'r V(r) \, dr. \quad . \quad (4)$$

In case we are considering the scattering of a beam of electrons we may take

$$V(r) = -z'eU(r), \quad . \quad . \quad . \quad . \quad . \quad . \quad (5)$$

* Watson, 'Bessel Functions.'

where z' is the atomic number of the scattering atom. Thus (4) becomes at r

$$\chi_1(r,\theta) = \frac{z'e^2}{2mv^2} \cdot \operatorname{cosec}^2\frac{\theta}{2} A \cdot \frac{e^{ikr}}{r} F(r_0), \quad . \quad (6)$$

where

$$F(r_0) = k' \int_{r_0}^{\infty} \sin k'r\, U(r)\, r\, dr. \quad . \quad . \quad . \quad (6.1)$$

Hence we have for the relative intensity of scattering for helium $z'=2$, per unit solid angle and at unit distance from the scattering centre

$$I = \left(\frac{e^2}{mv^2}\right)^2 \operatorname{cosec}^4\frac{\theta}{2}\{F(r_0)\}^2. \quad . \quad . \quad . \quad . \quad (7)$$

If we assume Coulomb potential, we have $U(r)=\frac{1}{r}$ and so from (6.1), $F(r_0)=\cos k'r_0$. Therefore (7) becomes

$$I = \left(\frac{e^2}{mv^2}\right)^2 \operatorname{cosec}^4\frac{\theta}{2} \cos^2 k'r_0, \quad . \quad . \quad (7.1)$$

which is the formula deduced by Mukerjee * and Ghosh †. For $r_0=0$, $F(r_0)=1$; so that (7) reduces to Rutherford-Born formula. It may be noted that Ghosh (*l. c.*) has taken the dynamical value of r_0 in the absence of the wave-statistical value which should have been used.

We now proceed to find the wave-statistical value of r_0. We have for the incident wave along the x-axis

$$\chi_0 = Ae^{ikx} = Ae^{ikr\cos\theta}, \quad . \quad . \quad . \quad . \quad . \quad . \quad . \quad . \quad (8.1)$$

and expanding in terms of Bessel function ‡

$$= A \sum_{s}^{0,\infty} (2s+1) i^{-s} \sqrt{\frac{\pi}{2kr}} J_{s+\frac{1}{2}}(kr) P_s(\cos\theta),$$

and using the asymptotic value of $J_{s+\frac{1}{2}}(kr)$ (*vide* (3))

$$= A \frac{e^{ikr}}{kr} \sum_{s}^{0,\infty} (2s+1) P_s(\cos\theta). \quad . \quad . \quad . \quad . \quad . \quad (8.2)$$

Now at $r=r_0$ we have for the boundary conditions :

$$\left.\begin{aligned} \frac{d\chi_0}{dr} + \frac{d\chi_1}{dr} &= 0, \\ \chi_0 + \chi_1 &= 0. \end{aligned}\right| \quad . \quad . \quad . \quad . \quad . \quad (9)$$

* K. K. Mukherjee, *Phys. Zeit.* vol. xxxiv. p. 175 (1933).
† M. Ghosh, Phil. Mag. vol. xx. p. 234 (1935).
‡ Watson, *l. c.*

From the first condition and on using the values in (6) and (8.2) we get

$$\frac{d}{dr}\left(\frac{e^{ikr}}{r}\right)\left[\frac{1}{k}\sum_{s}^{0,\infty}(2s+1)P_s(\cos\theta)+\frac{e^2}{mv^2}\operatorname{cosec}^2\frac{\theta}{2}F(r_0)\right]=0\Big|_{r=r_0},$$

giving

$$\frac{d}{dr}\left(\frac{e^{ikr}}{r}\right)=\frac{d}{dr}\left(\frac{\sin kr}{r}\right)=0\Big|_{r=r_0}.$$

Or we have

$$\tan kr_0=kr_0 \quad . \quad . \quad . \quad . \quad . \quad . \quad . \quad (10)$$

Again, from the second condition and on using the values in (6) and (8.1) we get

$$e^{ikr\cos\theta}=-\frac{e^2}{mv^2}\operatorname{cosec}^2\frac{\theta}{2}\frac{e^{ikr}}{r}F(r_0)\Big|_{r=r_0}$$

or

$$1=-\frac{e^2}{mv^2}\operatorname{cosec}^2\frac{\theta}{2}\,e^{\frac{2ikr\sin^2\frac{\theta}{2}}{r}}.k'\int_{r_0}^{\infty}e^{ik'r}U(r)r\,dr\Big|_{r=r_0}. \quad (11)$$

Since $-\sin\left\{2kr\sin^2\frac{\theta}{2}\right\}=\sin\left\{-2kr\sin^2\frac{\theta}{2}\right\}$, *i. e.*,

$-e^{2ikr\sin^2\frac{\theta}{2}}=+e^{-2ikr\sin^2\frac{\theta}{2}}$, we have from (11),

$$1=\frac{e^2}{mv^2}\operatorname{cosec}^2\frac{\theta}{2}\frac{e^{2ikr_0\left(\sin\frac{\theta}{2}-\sin^2\frac{\theta}{2}\right)}}{r_0}G(r_0), \quad . \quad . \quad (12)$$

where

$$G(r_0)=k'\int_{r_0}^{\infty}\sin k'(r-r_0)U(r)r\,dr. \quad . \quad . \quad (12.1)$$

Again, since $e^{-in\pi}=1$, where n is an even number, (12) may be written as

$$r_0=\frac{e^2}{mv^2}\operatorname{cosec}^2\frac{\theta}{2}\left\{e^{i(2kr_0-n\pi)}\right\}^{\left(\sin\frac{\theta}{2}-\sin^2\frac{\theta}{2}\right)}G(r_0)$$

$$=\frac{e^2}{mv^2}\operatorname{cosec}^2\frac{\theta}{2}\sin\left\{(2kr_0-n\pi)\left(\sin\frac{\theta}{2}-\sin^2\frac{\theta}{2}\right)\right\}G(r_0).$$

$$. \quad . \quad . \quad (12.2)$$

If n is given the highest value so that $2kr_0-n\pi$ lies

in the first quadrant, then (12.2) may be reduced to the simple form *, since $G(r_0)=1$ for Coulomb potential,

$$r_0=\rho\cdot\frac{2e^2}{mv^2}\left(\operatorname{cosec}\frac{\theta}{2}-1\right), \quad . \quad . \quad . \quad (12.3)$$

where

$$\rho=\tfrac{1}{2}(2kr_0-n\pi). \quad . \quad . \quad . \quad . \quad (12.31)$$

On graphically solving (10), it may be found that kr_0 has the possible values $1{\cdot}43\pi$, $2{\cdot}459\pi$, $3{\cdot}471\pi$, $4{\cdot}4774\pi$, and so on. Assuming first order diffraction only, we must take $kr_0=1{\cdot}43\pi$. And so $n=2$. Thus from (12.31) we have $\rho=1{\cdot}35$. We have, then, from (12.3)

$$r_0=1{\cdot}35\times\frac{2e^2}{mv^2}\left(\operatorname{cosec}\frac{\theta}{2}-1\right). \quad . \quad . \quad . \quad (13)$$

It is interesting to note that the classical dynamics gives for the critical approach exactly the above formula, except, of course, the numerical formula factor 1·35. The above numeral factor may, therefore, be taken as a measure of the dynamical defect.

In a more rigorous treatment of the problem one should use the wave-statistical potential rather than the Coulomb potential as above. It is well known that the wave-statistical potential $V(r)$ is given by (5) with $z'=1$ for hydrogen and $z'=2$ for helium, and where

$$U(r)=\left(\frac{1}{r}+\frac{z}{a}\right)e^{-\frac{2zr}{a}}, \quad . \quad . \quad . \quad . \quad (14)$$

in which $z=1$ for hydrogen and $z=1{\cdot}69$ for helium †, a being the radius of the first Bohr orbit for hydrogen. With the above value of $U(r)$ in (6.1), we get

$$F(r_0)=\frac{e^{-\frac{2zr_0}{a}}}{\operatorname{cosec}^2\frac{\theta}{2}}\left[\frac{\cos k'r_0}{\sin^2\frac{\theta}{2}+\beta^2}\left\{\left(1+\frac{zr_0}{a}\right)+\frac{\beta^2}{\sin^2\frac{\theta}{2}+\beta^2}\right\}\right.$$

$$\left.+\frac{\beta\operatorname{cosec}\frac{\theta}{2}}{2}\,\frac{\sin k'r_0}{\sin^2\frac{\theta}{2}+\beta^2}\left\{\left(1+\frac{2zr_0}{a}\right)+\frac{2\beta^2}{\sin^2\frac{\theta}{2}+\beta^2}\right\}\right], \quad . \quad . \quad . \quad (15)$$

* In case of positron $(+e)$ we have evidently $r_0=\rho\cdot\frac{2e^2}{mv^2}\left(\operatorname{cosec}\frac{\theta}{2}+1\right)$.

† Hyllaraas, *Zs. f. Phys.* vol. liv. p. 347 (1929).

where $\beta = \frac{z}{ak}$. Hence from (7) we have, for the relative intensity of scattering,

$$I = \left(\frac{e^2}{mv^2}\right)^2 e^{-\frac{4zr_0}{a}} \left[\frac{\cos k'r_0}{\sin^2\frac{\theta}{2}+\beta^2} \left\{ \left(1+\frac{zr_0}{a}\right) + \frac{\beta^2}{\sin^2\frac{\theta}{2}+\beta^2} \right\} + \tfrac{1}{2}\beta \operatorname{cosec}\frac{\theta}{2} \frac{\sin k'r_0}{\sin^2\frac{\theta}{2}+\beta^2} \left\{ \left(1+\frac{2zr_0}{a}\right) + \frac{2\beta^2}{\sin^2\frac{\theta}{2}+\beta^2} \right\} \right]^2. \quad . \quad . \quad . \quad (16)$$

Again, on substituting in (12.1) the value of $U(r)$ from (14) we get, after integrating,

$$G(r_0) = \frac{e^{-\frac{2zr_0}{a}}}{1+\beta^2 \operatorname{cosec}^2\frac{\theta}{2}} \left\{ \left(1{\cdot}5+\frac{zr_0}{a}\right) - \frac{\frac{1}{2}\beta\left(\sin\frac{\theta}{2}-\beta\right)}{\sin^2\frac{\theta}{2}+\beta^2} \right\}. \quad . \quad . \quad . \quad (17)$$

Hence from (12.2) we get

$$r_0 = \frac{\rho \cdot \frac{2e^2}{mv^2}\left(\operatorname{cosec}\frac{\theta}{2}-1\right)}{1+\beta^2 \operatorname{cosec}^2\frac{\theta}{2}} e^{-\frac{2zr_0}{a}} \times \left\{ \left(1{\cdot}5+\frac{zr_0}{a}\right) - \frac{\frac{1}{2}\beta\left(\sin\frac{\theta}{2}-\beta\right)}{\sin^2\frac{\theta}{2}+\beta^2} \right\}, \quad (18)$$

where the defect factor $\rho = 1{\cdot}35$. On solving (18) graphically for a given angle of scattering and a given velocity of the bombarding electrons, we get the value of r_0. Substituting the value of r_0 thus determined, in (16) we get readily the corresponding relative intensity of scattering (I). In Tables I. and II. the values of I calculated in this way (*vide* column 3) are compared with the experimental values of Hughes, McMillen, and Webb *

* Hughes, McMillen, and Webb, Phys. Rev. vol. xli. p. 154 (1932).

(*vide* column 2) for electrons bombarding with 700 and 25 volts. The corresponding values from Rutherford-Born formula is given in column 5. Mukherjee and

TABLE I.

Bombarded by 700-volt Electrons.

Angle of scattering.	$I \times 10^{22}$ (Expt.).	$I \times 10^{22}$ (Kar).	$r_0 \times 10^{10}$ cm. (Kar).	$I \times 10^{22}$ (Rutherford, Born).	$I \times 10^{22}$ (Mukherjee, Ghosh).
7	15·97	10·98	4·09	755·8	439·7
9·5 ...	13·07	9·27	4·81	232·5	158·5
12	9·14	7·66	5·05	50·49	35·59
17	5·41	4·82	5·39	21·94	14·14
22	2·72	2·87	5·44	7·89	5·53
27	1·82	1·71	5·35	3·53	2·48
37	0·658	0·673	4·54	1·01	0·791
47	0·307	0·318	3·32	0·41	0·34
57	0·155	0·161	3·01	0·20	0·17
72	0·0812	0·0752	2·14	0·088	0·0795
87	0·0510	0·0424	1·44	0·047	..
102	0·0397	..	..	0·029	..
117	0·0356	0·0191	0·61	0·020	..
132	0·0344	..	..	0·015	..
147	0·0154	..	..	0·012	..

TABLE II.

Bombarded by 25-volt Electrons.

Angle of scattering.	$I \times 10^{22}$ (Expt.).	$I \times 10^{22}$ (Kar).	$r_0 \times 10^{10}$ cm. (Kar).	$I \times 10^{22}$ Rutherford, Born).
15	24·30	12·08	7·51	28230
20	18·52	11·28	8·79	9012
25	13·25	10·67	9·77	3729
35	10·12	9·37	10·98	1001
45	7·91	8·18	11·36	381·3
55	6·93	7·26	11·36	180·0
65	5·83	6·43	10·93	98·17
75	5·60	5·74	10·23	59·54
85	5·13	5·23	9·25	39·26
95	5·13	4·76	8·15	27·67
105	5·23	4·41	6·97	20·65
115	5·45	4·14	5·67	16·17
125	5·76	3·92	4·34	13·22
135	6·09	3·73	3·11	11·23

Ghosh's theoretical values are given in column 6 for 700 volt electrons only. Now in calculating I Ghosh (*l. c.*) has made a mistake in taking $z' = 1{\cdot}69$ instead of 2. This

has been corrected, and instead of the dynamical value of r_0 used by Ghosh, the wave-statistical value (*vide* (13)) for Coulomb potential is taken.

The curves showing the variation of I with θ are given in figs. 1 and 2. Although usually the theoretical and the experimental values of scattering are compared by curves only, it must be mentioned that such a com-

Fig. 1.

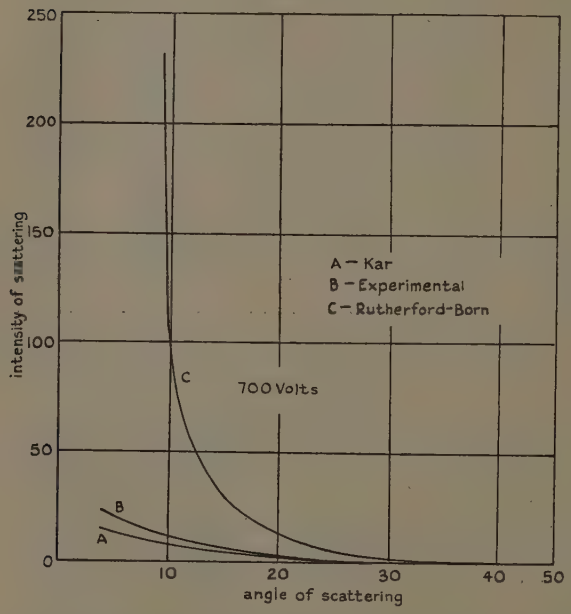

parison is often misleading. For, by reducing the scale, the agreement may be made to look decidedly better. We, therefore, give Tables I. and II. for accurate comparison. It is clear from Table I. that for high velocity of incidence Rutherford-Born formula fails at small angles of scattering. Again, from Table II. it is evident that for low-velocity electrons the formula is hopelessly inadequate at all angles of scattering.

However, the theoretical values given by formula (16)

are in decidedly better agreement at all angles, and at high and low velocities of incidence. The agreement is undoubtedly worse at small angles. But even here there is agreement in the order. This appears to be highly encouraging. One important drawback of the formula proposed is that it does not explain the minimum observed in the I—θ curve for helium at low velocities. Experimentally it is found that the minimum is more prominent

Fig. 2.

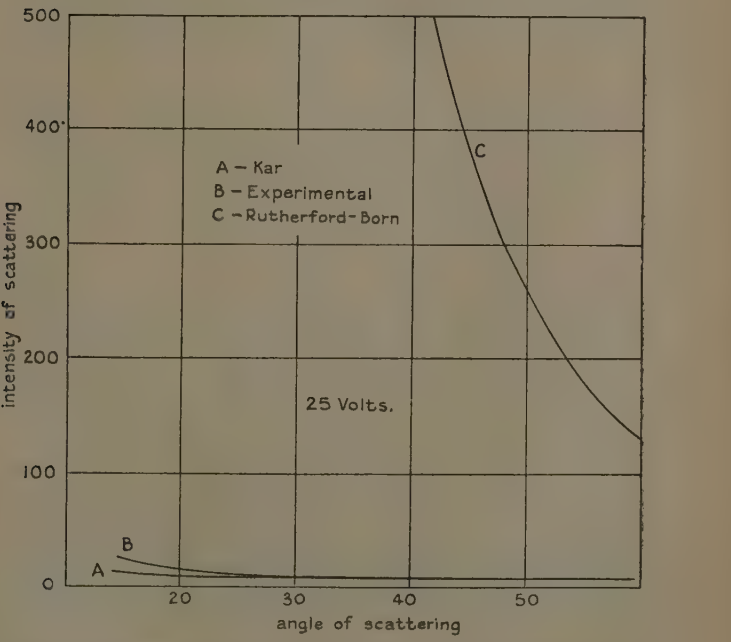

at low velocity of incidence, but appears nearly at the same angle of scattering, viz., 90°. It is interesting to note in this connexion (*vide* fig. 3) that r_0 calculated from (18) shows a maximum which is shifted towards larger angles of scattering as the velocity of the bombarding electrons is decreased. At low velocity, however, the maximum appears nearly at the same angle, viz., 55°.

A line of improvement of the formula (16) suggests itself at this stage, which may explain the minimum

observed at 90°. It is shown in the previous paper * that when the higher approximations are considered, we have the additional factor $\frac{1}{1-\eta_s}$. This factor, when taken, will have the effect of increasing the value of I at small angle. Again, since $\eta_s \rightarrow$ min. when $r_0 \rightarrow$ max., the correction-factor attains a minimum value at (r_0) max. Thus, the oscillatory change of the intensity of scattering may be explained.

Lastly, we must note that the Mukherjee-Ghosh formula is not appreciably better than that of Rutherford and

Fig. 3.

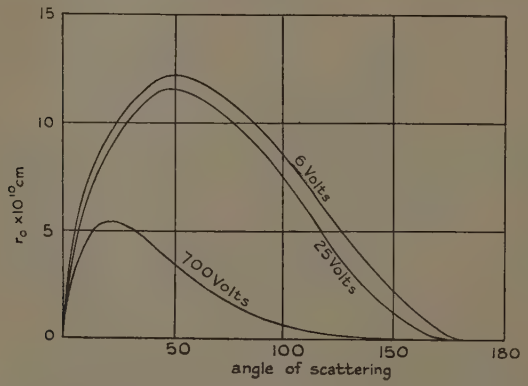

Born (*vide* Table I.), because the formula is based on Coulombian potential, which is not valid in the case of a helium or hydrogen atom. For collision between a proton and an electron the formula may be justified, provided the wave-statistical r_0 given in (13) is used.

Note added in Proof.—Due to an algebraic mistake, which has unfortunately crept in, the expression for r_0 given in (18) is somewhat wrong. It should be

$$r_0 = \frac{\rho\left(\frac{2e^2}{mv^2}\right)\left(\operatorname{cosec}\frac{\theta}{2}-1\right)}{1+\beta^2\operatorname{cosec}^2\frac{\theta}{2}}\left\{\left(1+\frac{zr_0}{a}\right)+\frac{\beta^2}{\sin^2\frac{\theta}{2}+\beta^2}\right\}.$$

* Kar, Ghosh, and Mukherjee, Phil. Mag. xxiv. p. 964 (1937).

However, the values of r_0 calculated from the above formula are found to be practically the same as before for low velocity of incidence. For high velocity, there is a slight difference which, however, makes the calculated value of the intensity of scattering agree still more closely with the experimental.—K. C. K.

Physical Laboratory,
Presidency College, Calcutta.
April 1937.

LXXXV. *Fluctuations of Composition in a System of Molecules in Chemical Equilibrium.* *By* F. G. Donnan, E. Teller, *and* B. Topley *.

1. *Introduction*

In discussions on the problem of fluctuations in a system in equilibrium, comparatively little attention has been paid in the past to the case of fluctuations of chemical composition in a system of molecules in chemical equilibrium. An important exception must be made, however, in the case of Professor R. H. Fowler's standard work on 'Statistical Mechanics.' The comparatively simple treatment given in the present paper is restricted to cases where the physical interaction between the molecules is sufficiently small and the state of dilution sufficiently large to allow them to be treated independently, and where the method employed may be that of classical statistics. Concerning the applicability of this method to the present case, some remarks will be made at a later stage.

We deal with an assembly of molecules $(n_1, n_2, \ldots n_i \ldots)$ enclosed in a constant volume V (of the container) and immersed in a thermostat of constant temperature T. Thus the symbol n_i denotes the number of molecules of the ith sort, so that $(n_1, n_2, n_3 \ldots n_i \ldots)$, which may be briefly written (n_i), denotes a specific distribution of the

* Communicated by the Authors.

molecules over the various possible sorts which take part in the chemical reaction considered, *i. e.*, a specified accessible *chemical state*.

In the first part (A) of the following discussion we deal with the fluctuations of composition occurring in the *enclosed* volume (V), whereas in the second part (B) we consider fluctuations occurring in an *open* volume-element, *i. e.*, in a small volume forming part of a very much larger enclosed system of the same sort.

A. Enclosed Systems.

2. *Simple Isomeric Equilibrium.*

Consider chemical equilibrium between two isomeric sorts of molecules, A_1 and A_2, of equal molecular mass. The total number, n, of molecules will remain constant in this case. Since the two sorts of molecules contain the same numbers of each sort of atom, a very simple treatment suffices. The number of complexions corresponding to any specific macroscopic (chemical) state (n_1, n_2) will be equal to $\frac{n!}{n_1!\,n_2!}$, but the various sets of complexions corresponding to different specified macroscopic states will not possess equal probabilities. We shall call the probability of a molecule chosen at random, *i. e.*, with respect to both position and time, being in the A_1 state, w_1, and in the A_2 state, w_2, where $w_1+w_2=1$, and we shall assume that these *a priori* probabilities are constant with respect to both time and position, but will in general vary with the temperature T of the thermostat.

The statistical probability, W, corresponding to any specified chemical state (n_1, n_2), will then be given by the equation

$$\mathrm{W}=\frac{n!}{n_1!\,n_2!}w_1^{n_1}.w_2^{n_2}. \quad . \quad . \quad . \quad . \quad (1)$$

Thus, in any Gibbsian or any time (Einstein) ensemble of the molecular assembly considered, the quantity W gives the fraction of all the accessible chemical states (molecular distributions) which corresponds to the specified chemical state (n_1, n_2), so that $(\Sigma \mathrm{W})_{\text{all states}}=1$. Assuming that the chemical state which we call the state of chemical equilibrium is that particular chemical state which occurs most frequently in the Gibbsian or in the

time ensemble, we obtain for this state the two conditions $d \log W = 0$, and $dn_1 + dn_2 = 0$. Putting

$$\log (n_i !) = (n_i + \tfrac{1}{2}) \log n_i - n_i + \tfrac{1}{2} \log 2\pi,$$

equation (1) leads to the result

$$\frac{n_1}{n_2} = \frac{w_1}{w_2} = \text{a constant (K)}. \quad . \quad . \quad . \quad . \quad (2)$$

Equation (2) is the law of chemical equilibrium applicable to the case considered, the constant K being the chemical equilibrium constant.

Denoting now the chemical equilibrium (most frequent) distribution by (n_1, n_2), we shall consider a chemical composition deviation (fluctuation) from this state, denoted by $(n_1 - x, n_2 + x)$. Calling the statistical probability (frequency fraction) of this deviating state W_x, and that of the chemical equilibrium (most frequently occurring) state W_0, we obtain by division

$$\frac{W_x}{W_0} = \frac{n_1 !}{(n_1 - x) !} \cdot \frac{n_2 !}{(n_2 + x) !} \cdot \frac{1}{K^x} \cdot \quad . \quad . \quad . \quad . \quad (3)$$

If we take the logarithms of both sides of equation (3), use the approximate form of Stirling's theorem for the logarithms of the factorials, and expand the logarithmic series, it is easily shown that

$$\log \frac{W_x}{W_0} = -\frac{nx^2}{2n_1 n_2} = -\frac{1}{2}\left(\frac{x^2}{n_1} + \frac{x^2}{n_2}\right), \quad . \quad . \quad (4)$$

provided that both $\frac{x}{n_1}$ and $\frac{x}{n_2}$ are sufficiently small in comparison with unity. Since $n_1 + n_2 = n$, and $\frac{n_1}{n_2} = K$, it follows that $n_1 n_2 = \frac{K}{(1+K)^2} n^2$. Defining the chemical fluctuation by D, where $D = \frac{x}{n}$, we obtain

$$\log \frac{W_D}{W_0} = -\tfrac{1}{2} n \frac{(1+K)^2}{K} D^2,$$

or

$$W_D = W_0 \exp \left\{ -\tfrac{1}{2} n \frac{(1+K)^2}{K} D^2 \right\}. \quad . \quad . \quad (5)$$

The sum of all possible values of W_D is unity, so that

$$\frac{1}{n} = W_0 \sum_{(D)} \exp\left\{ -\tfrac{1}{2}n \frac{(1+K)^2}{K} D^2 \right\} \frac{1}{n} \quad . \quad . \quad . \quad (6)$$

Since successive values of D differ by $\frac{1}{n}$, we may, for sufficiently large values of n, replace equation (6) by

$$\frac{1}{n} = W_0 \int_{-\infty}^{+\infty} \exp\left\{ -\tfrac{1}{2}n \frac{(1+K)^2}{K} D^2 \right\} dD \quad . \quad . \quad (7)$$

Hence

$$\frac{1}{n} = W_0 \frac{1}{1+K} \sqrt{\frac{K}{n}} \sqrt{2\pi}$$

or

$$W_0 = \frac{1+K}{\sqrt{2\pi n K}}, \quad . \quad . \quad . \quad . \quad . \quad . \quad (8)$$

and therefore

$$W_D = \frac{1+K}{\sqrt{2\pi n K}} \exp\left\{ -\tfrac{1}{2}n \frac{(1+K)^2}{K} D^2 \right\} \quad . \quad . \quad (9)$$

This equation may be written in the form

$$W_D = A \exp(-aD^2), \quad . \quad . \quad . \quad . \quad (10)$$

where

$$A = \frac{1+K}{\sqrt{2\pi n K}}, \quad a = \tfrac{1}{2}n \frac{(1+K)^2}{K}.$$

The probability that D lies in a small range (D, D+dD), dD being, nevertheless, large in comparison with $\frac{1}{n}$, is $W_D n dD$, because the range dD comprises $n d$D possible statistical states.

Since $\sum_D W_D = 1$, the mean value of D^2 is given by

$$\overline{D^2} = \sum_{(D)} D^2 W_D = \int_{-\infty}^{+\infty} D^2 n W_D dD. \quad . \quad . \quad (11)$$

In the integration, n is a constant, its value being given by equation (7), *i. e.*,

$$\frac{1}{n} = A \int_{-\infty}^{+\infty} \exp(-aD^2) dD,$$

whilst, from equation (10),

$$W_D = A \exp(-aD^2).$$

Hence equation (11) takes the form

$$\overline{D^2}=\frac{\int_{-\infty}^{+\infty}\exp(-aD^2)D^2dD}{\int_{-\infty}^{+\infty}\exp(-aD^2)dD}. \quad . \quad . \quad . \quad (12)$$

Integrating the denominator by parts,

$$\int_{-\infty}^{+\infty}e^{-aD^2}dD=\int_{-\infty}^{+\infty}1.e^{-aD^2}dD$$

$$=\left[De^{-aD^2}\right]_{-\infty}^{+\infty}+2a\int_{-\infty}^{+\infty}D^2e^{-aD^2}dD.$$

Since $\left[De^{-aD^2}\right]_{-\infty}^{+\infty}=0$, we obtain, finally,

$$\overline{D^2}=\frac{1}{2a}=\frac{K}{(1+K)^2n}, \quad . \quad . \quad . \quad . \quad (13)$$

and for the root mean square value of D we have

$$\sqrt{\overline{D^2}}=\frac{\sqrt{K}}{1+K}\cdot\frac{1}{\sqrt{n}}. \quad . \quad . \quad . \quad . \quad . \quad (14)$$

It follows from equation (14) that for constant n and variable K the maximum value of $\overline{D^2}$ corresponds to $K=1$. In this special case, which applies at all temperatures to the chemical equilibrium of "optical isomers" (*d* and *l* forms), equation (14) reduces to the form

$$\sqrt{\overline{D^2}}=\frac{1}{2\sqrt{n}}. \quad . \quad . \quad . \quad . \quad . \quad (15)$$

For example, if $n=250{,}000$, the r.m.s. value of the fluctuation D will be 0·001, or 0·1 per cent. Since $D=\frac{x}{n}=\frac{x}{250{,}000}$, the corresponding value of x will be 250. Fluctuations from the state of optical inactivity towards the *d*- or *l*-sides will occur with equal frequency, but the frequency-distribution will be such that $\sqrt{x^2}=250$ and $\sqrt{\overline{D^2}}=0{\cdot}001$. This result applies, of course, only to the type of systems considered in this paper.

3. *The General Case of Chemical Equilibrium.*

Let the chemical reaction considered be written in the form

$$p_1A_1+p_2A_2+\ldots+p_iA_i\ldots,$$

where p_i denotes a molecular reaction-coefficient, and of the members of the group (p_i) some will be positive and some negative. We cannot write, in analogy with equation (1), for the statistical probability $W_{(n_i)}$ of a specified molecular distribution (n_i)

$$W_{(n_i)}=n!\prod_i \frac{w_i^{n_i}}{n_i!}, \quad . \quad . \quad . \quad . \quad . \quad (16)$$

with the condition $\sum_i w_i=1$, nor even in the special case $\sum_i p_i=0$, where $n!$ is now a constant,

$$W_{(n_i)}=C\prod_i \frac{w_i^{n_i}}{n_i!}, \quad . \quad . \quad . \quad . \quad . \quad (17)$$

where C is a constant.

It will be shown, however, in the present section that an equation similar in form to (17) can be obtained, in which the *a priori* probabilities (w_i) employed previously are replaced by other quantities of a more general character. From the equation so obtained a generalized form of equation (4) can be deduced.

We begin by considering a system consisting of various sorts of atoms, namely, ν_1 atoms of the first sort, ν_2 atoms of the second sort, ν_λ atoms of the λ-th sort . . . ., where each member of the group (ν_λ) is constant. The probability of finding these atoms in a certain volume-element $dq_1 \ldots dp_n$ of phase space (where $dq_1 \ldots . dp_n$ is a product of *all* dq_λ and *all* dp_λ) is proportional to the expression

$$\exp\left(-\frac{E}{kT}\right).dq_1 \ldots . dp_n, \quad . \quad . \quad . \quad (18)$$

where E denotes the energy of the *whole* system.

Now consider the case where these atoms form molecules, the interaction of which may be neglected. By this we mean that the probability of finding the atoms *in any other states than as constituting certain kinds of molecules* may be neglected. The molecules may chemically react with each other, but the probability that any molecule is just in the state of chemically reacting will be neglected, and so will all physical interactions between the molecules. This means that the reaction takes place comparatively slowly, but that does not impair the validity of any considerations concerning the equilibrium state or concerning the magnitude of the fluctuations. We now make arbitrarily a difference between identical atoms, numbering

them in a definite way. Furthermore, we assume that we know how these atoms form the molecules, so that not only the numbers of different kinds of molecules are given, but it is also known which are the *particular* atoms to be found together in any *particular* molecule. Finally, we shall also attach numbers to all the molecules, not paying attention to the question whether two molecules are similar or not. For example, in an $H_2+O_2+H_2O$ mixture, we may take as molecule No. 1 an H_2, as No. 2 an H_2O, as No. 3 again an H_2, and so on in any order until all the molecules are disposed of. We shall denote by $dQ_1^1 \ldots dP_{n_1}^1$ the element of content in the phase space for our first molecule, where $Q_1^1 \ldots P_{n_1}^1$ denote coordinates and momenta of the translational, rotational, and internal motions of the molecule, and n_1 its number of degrees of freedom. We shall denote by E^1 the energy for this molecule*. Similarly, $dQ_1^h \ldots dP_{n_h}^h$ will denote the element of content in the phase space for the h-th molecule, n_h its number of degrees of freedom, and E^h the energy for this molecule. If we now disregard the possibility of reaction and of exchange of atoms between different molecules, we shall have, for the probability of finding the molecules in a definite element of content of the phase space, the expression

$$\exp\left(-\frac{E}{kT}\right) \prod_h dQ_1^h \ldots dP_{n_h}^h. \quad . \quad . \quad (19)$$

Since, in the absence of physical interaction energy between the molecules, we can write $E = \sum_h E^h$ where E_h is now the energy of the h-th molecule, the expression (19) becomes

$$\prod_h \exp\left(-\frac{E^h}{kT}\right) . dQ_1^h \ldots dP_{n_h}^h. \quad . \quad . \quad (20)$$

This expression consists of a product of factor F_h where

$$F_h = \exp\left(-\frac{E^h}{kT}\right) . dQ_1^h \ldots dP_{n_h}^h. \quad . \quad . \quad . \quad (21)$$

Integrating the expression (20) over the whole phase space, we might expect to obtain a measure for the relative probability of finding the particular atoms

* This means that E^1 is the increase of the energy of the system on addition of a molecule 1.

associated in the definite way described previously. Thus the ratio of the integrals

$$\int_{\text{phases}}^{\text{all}} \cdots \int \Pi_{\hbar} \exp\left(-\frac{E^{\hbar}}{kT}\right) . dQ_1^{\hbar} \ldots . dP_{n_{\hbar}}^{\hbar} \quad . \quad . \quad (22)$$

for two specified ways of associating the atoms into molecules might be expected to give the ratio of the probabilities for the occurrence of these specified associations. It would, however, be erroneous to calculate from (20) and (22) the relative probabilities of different molecular distributions, because (20) differs from (18) not only formally, but also essentially, inasmuch as in (18) any atoms of the same sort may be substituted into any molecule, whereas in (20) *particular* molecules are composed of *particular* atoms. To obtain the correct probability we must multiply by the number of different ways in which the atoms may build up the molecules. We shall see presently that if the number of molecules is changed by a chemical reaction the number of these possible distributions is also changed. In order to take account of these exchange effects, we may permute all similar atoms, which will have the effect of multiplying (22) by a product of factorials, thus giving us the expression

$$\Pi_{\lambda} \nu_{\lambda} ! \int_{\text{phases}}^{\text{all}} \cdots \int \Pi_{\hbar} \exp\left(-\frac{E^{\hbar}}{kT}\right) . dQ_1^{\hbar} \ldots . dP_{n_{\hbar}}^{\hbar}. \quad (23)$$

Proceeding in this way, however, we shall count certain configurations in phase space too often. Such " multiple " countings occur in two different ways :—(*a*) in integrating over all phases of *one* molecule, configurations in phase space occur which differ only in so far as similar atoms are interchanged within the molecule. The number of ways in which with the help of internal degrees of freedom such interchanges may be produced is the symmetry number $\sigma_{\hbar}$ of the molecule in question. Hence the first sort of overcounting will be corrected if we divide (23) by the symmetry numbers, obtaining thus the expression

$$\Pi_{\lambda} \nu_{\lambda} ! \int_{\text{phases}}^{\text{all}} \cdots \int \Pi_{\hbar} \frac{1}{\sigma_{\hbar}} \exp\left(-\frac{E^{\hbar}}{kT}\right) dQ_1^{\hbar} \ldots dP_{n_{\hbar}}^{\hbar}. \quad (24)$$

(*b*) in integrating over all phases of *all* molecules in phase space, configurations occur which differ only in that similar molecules have been interchanged. This second sort of overcounting will be corrected if we divide by the number of permutations of similar molecules. Denoting by $n_1, n_2, \ldots n_i \ldots$ the numbers of molecules of the different kinds in a particular distribution (n_i), we obtain, finally, the expression

$$\frac{\Pi \nu_\lambda !}{\Pi n_i !} \int_{\text{phases}}^{\text{all}} \ldots \int \Pi_h \frac{1}{\sigma_h} \exp\left(-\frac{E^h}{kT} \right) dQ_1^h \ldots dP_{n_h}^h. \quad (25)$$

Now F_h, as defined by (21), is independent of the number of atoms present and is the same for all molecules of the same kind. Also the quantity

$$\int_{\text{phases}}^{\text{all}} \ldots \int \frac{1}{\sigma_h} \exp\left(-\frac{E^h}{kT} \right) dQ_1^h \ldots . dP_{n_h}^h,$$

which is equal to

$$\int_{\text{phases}}^{\text{all}} \ldots \int \frac{F_h}{\sigma_h},$$

will depend only upon the *kind* of molecule in question and upon the *volume* of the container. We shall therefore put

$$\int_{\text{phases}}^{\text{all}} \ldots \int \frac{F_h}{\sigma_h} = y_i. \quad . \quad . \quad . \quad . \quad (26)$$

for a molecule of the i-th kind.

Since y_i occurs n_i times in (25) ,we obtain for the probability $W_{(n_i)}$ the expression

$$W_{(n_i)} \sim C_1 \frac{\Pi y_i^{n_i}}{\Pi n_i !}, \quad . \quad . \quad . \quad . \quad . \quad . \quad . \quad (27)$$

where $\sim$ denotes proportionality, and C_1 is written for the fixed number $\Pi \nu_\lambda !$ Introducing a proportionality

factor C_2 into (27) and writing C for C_1C_2, we obtain, finally,

$$W_{(n_i)}=C\Pi_i \frac{y_i^{n_i}}{n_i!} \quad . \quad . \quad . \quad . \quad . \quad . \quad (28)$$

The quantity w_i employed in the case of simple isomeric equilibrium denoted the probability that a molecule selected at random may be of the i-th kind. It is seen that in the general case w_i defined in this way will depend on the "initial conditions," *i. e.*, on the numbers $\nu_1, \nu_2, \ldots \nu_\lambda \ldots$ of atoms, whereas the quantity y_i defined by (26) will depend only on the properties of the molecule i and the volume of the container.

According to the principles of quantum mechanics, the foregoing *classical* treatment is subject to two changes, which will not in general affect the final result. In the first place, the integrals which occur in the definition of y_i must be replaced by sums as soon as the quantisation of the different degrees of freedom becomes important. Moreover, the translational motion of any molecule i may be treated classically if the cube of the corresponding de Broglie wave-length is very small compared with $\frac{V}{n_i}$. For the temperature T the average translational energy is $\frac{1}{2}kT$ and the corresponding momentum $\sqrt{m_i kT}$, where m_i is the molecular mass. The corresponding de Broglie wave-length is then $\frac{h}{\sqrt{m_i kT}}$. The condition for the applicability of classical statistics to the translational motion of any molecule i is therefore

$$\frac{V}{n_i} >> \frac{h^3}{(m_i kT)^{\frac{3}{2}}} \quad . \quad . \quad . \quad . \quad . \quad . \quad (29)$$

For gases this condition is practically fulfilled in nearly all cases, because, as soon as we try to make the right-hand side large by making T small, then the left-hand side also becomes large in consequence of the low vapour-pressures at low temperatures. The only known cases, *i. e.*, of gases, where the criterion (29) is not sufficiently satisfied are those of hydrogen and helium at low temperatures. Even here the application of quantum statistics

possesses an importance about equal to that of a consideration of the van der Waals forces.

In the second place, according to the Fermi-Dirac or Bose-Einstein statistics the factor $\Pi_\lambda \nu_\lambda !$ must be cancelled. This does not, however, affect the *relative* probabilities, which alone are of interest in the present discussion. We remark finally that, when the translational motion of any molecule i may be treated classically, the quantity y_i will depend only on the properties of the molecule i and the volume V of the container.

Equation (28) may now be employed to obtain the desired generalized form of equation (4). For *any* specified molecular distribution $n_1, n_2, n_3 \ldots n_i \ldots$ we write

$$W = C \Pi_i \frac{y_i^{n_i}}{n_i !},$$

where W is the probability of this distribution. Putting $\log n_i ! = (n_i + \frac{1}{2}) \log n_i - n_i + \frac{1}{2} \log 2\pi$, we obtain

$$\log W = \Sigma_i n_i \log y_i - \Sigma_i (n_i + \tfrac{1}{2}) \log n_i + \Sigma_i n_i + \text{constant}.$$

Hence

$$d \log W = \Sigma_i \log y_i \, dn_i - \Sigma_i \log n_i \, dn_i - \Sigma_i (n_i + \tfrac{1}{2}) \frac{dn_i}{n_i} + \Sigma_i dn_i,$$

or

$$d \log W = \Sigma_i \log y_i \, dn_i - \Sigma_i \log n_i \, dn_i. \quad . \quad . \quad (30)$$

Denoting now the most probable (equilibrium) state by (n_i), and a fluctuation from this by $(n_i + x_i)$, we may replace dn_i by x_i. Putting $d \log W = 0$ as the condition for the most probable state, (30) gives the equation

$$\Sigma_i x_i \log y_i = \Sigma_i x_i \log n_i. \quad . \quad . \quad . \quad . \quad (31)$$

Calling W_0 the probability of the most probable (equilibrium) molecular distribution (n_i), we have

$$W_0 = C \Pi_i \frac{y_i^{n_i}}{n_i !}. \quad . \quad . \quad . \quad . \quad . \quad (32)$$

For the probability of the deviating distribution $(n_i + x_i)$ we have

$$W_{(xi)} = C \Pi_i \frac{y_i^{(n_i + x_i)}}{(n_i + x_i) !}. \quad . \quad . \quad . \quad . \quad (33)$$

Hence from (31), (32), and (33) it follows that

$$\begin{aligned}\log W_{(x_i)} - \log W_0 &= \sum_i x_i \log n_i - \sum_i (n_i + x_i + \tfrac{1}{2}) \log (n_i + x_i) \\ &\quad + \sum_i (n_i + \tfrac{1}{2}) \log n_i + \sum_i x_i \\ &= \sum_i x_i \log n_i - \sum_i (n_i + x_i + \tfrac{1}{2}) \log \left(1 + \frac{x_i}{n_i}\right) \\ &\quad - \sum_i (n_i + x_i + \tfrac{1}{2}) \log n_i + \sum_i (n_i + \tfrac{1}{2}) \log n_i + \sum_i x_i \\ &= \sum_i (n_i + x + \tfrac{1}{2}) \left\{ \frac{x_i}{ni} - \tfrac{1}{2} \left(\frac{x_i}{n_i}\right)^2 \right\} + \sum_i x_i.\end{aligned}$$

For deviating states (x_i), such that $\frac{x_i}{n_i} << 1$, we obtain finally,

$$W_{(x_i)} = W_0 \exp\left(-\tfrac{1}{2} \sum_i \frac{x_i^2}{n_i}\right). \quad . \quad . \quad . \quad (34)$$

Equation (34) is the required generalized form of (4).

Let us now consider the equation of chemical equilibrium for the chemical reaction $\sum_i p_i A_i = 0$. The chemical equilibrium state corresponds to the most probable (n_i) molecular distribution. For a variation of this state we see from (30) that

$$\sum_i \log n_i \, dn_i = \sum_i \log y_i \, dn_i. \quad . \quad . \quad . \quad (35)$$

Since any variation (dn_i) of the equilibrium state (n_i) is subject to the conditions $\frac{dn_i}{p_i}$ = a common value, equation (35) gives

$$\sum_i p_i \log n_i = \sum_i p_i \log y_i, \quad . \quad . \quad . \quad . \quad (36)$$

whence

$$\prod_i n_i^{p_i} = \prod_i y_i^{p_i}. \quad . \quad . \quad . \quad . \quad . \quad (37)$$

For any y_i we may write in the limiting case $y_i = y_i' V$, where V is the volume of the container and y_i' is a quantity which now depends solely on the properties of the molecule i. Hence, for constant temperature, equation (37) may be written in the form

$$\prod_i \left(\frac{n_i}{V}\right)^{p_i} = \prod_i (y')^{p_i} = \text{a constant (K)}. \quad . \quad (38)$$

This is the equation of chemical equilibrium which we shall use in the following illustration.

The meaning of the word "limiting" may be explained as follows:—In the case considered in this paper, y can be expressed as

$$\iiint dQ_1^h\, dQ_2^h\, dQ_3^h \int \ldots \int \frac{1}{\sigma_h} \exp\left(-\frac{E^h}{kT}\right) dQ_4^h \ldots dP_{n_h}^h,$$

where Q_1^h, Q_2^h, Q_3^h denote the (Cartesian) positional co-ordinates of the centre of mass of the molecule h. The reason for this is that E_h does not depend on these positional coordinates. If now (as a further approximation) we neglect the volume of the molecules, we may put the triple integral equal to the volume V of the container, whilst the second integral will depend only on the internal properties of the molecule (at the temperature T). Hence in this "limiting" case we may write $y_i = y_i' V$, as explained above. Of course, other more exact forms of the equation of chemical equilibrium may be used.

We now proceed to apply (34) to a definite specified chemical reaction

$$\sum_i (p_i A_i) = 0.$$

Since $\frac{x_1}{p_1} = \frac{x_2}{p_2} = \ldots \frac{x_i}{p_i} =$ a common value δ (independent of i), we may specify the fluctuation (x_i) by means of δ, since the group (p_i) is known.

Thus we may write (34) in the form

$$W_{(x_i)} = W_\delta = W_0 \exp\left(-\tfrac{1}{2}\delta^2 \sum_i \frac{p_i^2}{n_i}\right). \quad . \quad . \quad . \quad (39)$$

Let the initial state (molecular distribution) be denoted by (N_i), then

$$\frac{N_1 - n_1}{p_1} = \frac{N_2 - n_2}{p_2} = \ldots \frac{N_i - n_i}{p_i} = \ldots$$

a common value r (the reaction stage parameter).

The series of equations

$$N_i - n_i = r p_i \quad . \quad . \quad . \quad . \quad . \quad . \quad . \quad (40)$$

defines the equilibrium state (n_i) in terms of the known initial state (N_i), the reaction stage parameter r, and the known molecular reaction-coefficients (p_i). The value of r is now determined by substituting the values of n_i from the equation (40) into (38). With this value of r

we can now substitute the values of n_i from equations (40) into (39), and obtain

$$W_{(x_i)}=W_\delta=W_0 \exp\,[-\tfrac{1}{2}\delta^2\phi\{(N_i),\,(p_i'),\,K,\,V\}]. \quad (41)$$

We cannot, however, in general write down the explicit algebraic form of the function ϕ, since the substitution of the values of n_i from (40) into (38) might yield an equation for r of an insoluble order. In particular cases this difficulty may not arise, as may be shown by the following example.

We consider the simple chemical dissociation equation

$$A_1=A_2+A_3, \quad \text{or} \quad A_1-A_2-A_3=0.$$

The specification for this case is

Values of p_i	$+1$,	-1,	-1,
Initial state	N_1,	0,	0,
Equilibrium state	n_1,	n_2,	n_3.

The equations (40) become now

$$\left.\begin{aligned} N_1-n_1&=r,\\ n_2&=r,\\ n_3&=r. \end{aligned}\right\} \quad . \quad . \quad . \quad . \quad . \quad (42)$$

The equation of chemical equilibrium may be written

$$Kn_1=\frac{n_2n_3}{V}, \quad . \quad . \quad . \quad . \quad . \quad . \quad . \quad (43)$$

where K is the reciprocal of the K used in equation (38). Substitution in (43) of the values of n_1, n_2, n_3, from the equations (42) gives $K(N_1-r)=\frac{r^2}{V}$,

whence

$$r=\tfrac{1}{2}KV\left(\sqrt{1+\frac{4N_1}{KV}}-1\right). \quad . \quad . \quad . \quad (44)$$

This determines r as an explicit algebraic function of K, N_1, and V.

We have also

$$\Sigma_i\frac{p_i^2}{n_i}=\frac{1}{n_1}+\frac{1}{n_2}+\frac{1}{n_3}=\frac{2N_1-r}{(N_1-r)r},$$

and therefore

$$W_\delta=W_0 \exp\left\{-\frac{1}{2}\frac{2N_1-r}{(N_1-r)r}\,\delta^2\right\} \quad . \quad . \quad . \quad (45)$$

Putting

$$D=\frac{\delta}{n_1+n_2+n_3}=\frac{\delta}{N_1+r},$$

we obtain

$$W_D=W_0\exp\left\{-\frac{1}{2}\cdot\frac{(2N_1-r)(N_1+r)^2}{(N_1-r)r}D^2\right\}. \quad . \quad (46)$$

Hence

$$\overline{D^2}=\frac{(N_1-r)r}{(2N_1-r)(N_1+r)^2}, \quad . \quad . \quad . \quad . \quad (47)$$

where r has the value given by (44).

Thus, being given the values of K, N_1, and V, the values of D^2 and $\sqrt{\overline{D^2}}$ are easily computed.

From the equations ($x_i=p_i\delta$) we have, in the present case, $x_1=p_1\delta$, $x_2=p_2\delta$, $x_3=p_3\delta$, or since $\delta=(N_1+r)D$,

$$x_1=p_1(N_1+r)D, \quad x_2=p_2(N_1+r)D, \quad x_3=p_3(N_1+r)D.$$

These equations enable us to calculate the values of $\overline{x_1^2}$, $\overline{x_2^2}$, and $\overline{x_3^2}$ from the value of $\overline{D^2}$, since for the specified reaction and the specified initial state (specified values of K, V, and N_1) the quantities $p_1(N_1+r)$, $p_2(N_1+r)$, and $p_3(N_1+r)$ are determinate and known.

B. Open Systems.

4. *Simple Isomeric Equilibrium.*

We return now to the case of isomeric equilibrium considered previously. If we consider in a large (constant) volume V a definite small volume-element v, and if we suppose that we find within this volume-element n molecules (*i. e.*, if we consider only the occasions when the number of molecules in v has a specified value n), then the probability of finding (n_1-x) molecules of the one isomer and (n_2+x) molecules of the second isomer, where $n_1+n_2=n$, is the same as for a closed system, *i. e.*,

$$W_x=W_0\exp\left\{-\frac{1}{2}\left(\frac{x^2}{n_1}+\frac{x^2}{n_2}\right)\right\}, \quad . \quad . \quad (48)$$

where W_0 is the (maximum) probability corresponding to the chemical equilibrium distribution (n_1, n_2) of the n molecules.

The proof of (48) is exactly the same as in the case of a closed volume, and is not altered by the fact that the composition of the volume-element (always supposed to

contain n molecules) will vary not only because of chemical change, but also by reason of molecular diffusion.

If, now, we consider *all* states of the definite small volume-element v, and if we denote now by n the *most probable number* of molecules present in v, then we have, instead of (48),

$$W_{(x,y)}=W_0'W_0''\exp\left\{-\frac{1}{2}\left(\frac{x^2}{n_1}+\frac{y^2}{n_2}\right)\right\}, \quad . \quad (49)$$

where x and y are now *independent* deviations of the numbers of molecules of the first and second kinds from the equilibrium distribution (n_1, n_2), where $n_1+n_2=n$, and $W_0'W_0''$ is written for the (maximum) probability corresponding to the distribution (n_1, n_2) of n. Let us denote by N the number of molecules in the large volume V *minus* the most probable number (n) of molecules in v. We shall begin the proof of (49) by calculating the probability of finding $n+z$ molecules in v. This problem is quite analogous to that of isomeric chemical change. We may call the molecules in v "the one isomer," and those in $V-v$ "the other isomer." Hence we have

$$W_z=W_0'\exp\left\{-\frac{1}{2}\left(\frac{z^2}{n}+\frac{z^2}{N}\right)\right\}, \quad . \quad . \quad (50)$$

where W_0' is the (maximum) probability corresponding to $z=0$.

If $N>>n$, we may write, instead of (50),

$$W_z=W_0'\exp\left(-\frac{1}{2}\frac{z^2}{n}\right). \quad . \quad . \quad . \quad . \quad (51)$$

Equation (51) is an expression for the probability of a fluctuation z in the small volume element v, from the most probable number of molecules, n, in V, and W_0' is the maximum probability corresponding to $z=0$. It may be remarked here that $\overline{n+z}$, *i. e.*, the average value of $n+z$, is equal to the most probable number n. For

$$\overline{n+z}=\frac{\Sigma W_z(n+z)}{\Sigma W_z}=\frac{n\Sigma W_z+\Sigma W_z z}{\Sigma W_z}=n+\frac{\Sigma W_z z}{\Sigma W_z}=n+z.$$

But

$$\Sigma W_z=1, \quad \text{and} \quad \Sigma W_z z=W_0'\Sigma\exp\left(-\frac{1}{2}\frac{z^2}{n}\right).z=0,$$

since for every value of $e^{-\frac{z^2}{n}}$ there correspond equal

positive and negative values of z. Hence $\bar{z}=0$ and therefore $\overline{n+z}=n$. Let N_1 denote the total number of molecules in the constant volume V. The above reasoning shows that we may write $n=\frac{v}{V}N_1=vd$, where d is the constant " overall " density in V.

Let us now suppose that $n+z$ molecules are present in v and proceed to calculate the probability $W_{(x,y)}$ that n_1+x molecules of the first kind and n_2+y molecules of the second kind will be found present, where $x+y=z$ and $n_1+n_2=n$. The most probable distribution of $n+z$ into the two kinds of molecules is $\frac{n_1}{n}(n+z)$ of the first kind and $\frac{n_2}{n}(n+z)$ of the second kind. The deviation δ from the most probable distribution will be given by

$$\delta=n_1+x-\frac{n_1}{n}(n+z)=-(n_2+y)+\frac{n_2}{n}(n+z)=\frac{n_2x-n_1y}{n}. \quad . \quad . \quad . \quad (52)$$

Applying again (48) for the probability of distributing $n+z$ into n_1+x and n_2+y, we obtain

$$W_{(x,y)}=W_zW_0''\exp\left\{-\frac{1}{2}\left(\frac{\delta^2}{\frac{n_1}{n}(n+z)}+\frac{\delta^2}{\frac{n_2}{n}(n+z)}\right)\right\},$$

$$\text{or}\qquad W_{(x,y)}=W_zW_0''\exp\left\{-\frac{1}{2}\frac{n}{n+z}\cdot\frac{n}{n_1n_2}.\delta^2\right\}, \qquad (53)$$

where W_0'' is the probability of the most probable distribution of $(n+z)$ molecules into the two possible kinds of molecules. Substituting from (50) into (53), we obtain

$$W_{(x,y)}=W_0'W_0''\exp\left\{-\frac{1}{2}\left(\frac{1}{n}+\frac{1}{N}\right)z^2\right\}$$
$$\cdot\exp\left(-\frac{1}{2}\frac{n}{n+z}\cdot\frac{n}{n_1n_2}\delta^2\right). \quad . \quad . \quad (54)$$

In (54) $z=x+y$ and $n=n_1+n_2$. Neglecting in the first exponent $1/N$ in comparison with $1/n$ and in the second exponent z in comparison with n, and introducing the value of δ from (52), we obtain

$$W_{(x,y)}=W_0'W_0''\exp\left\{-\frac{1}{2}\left(\frac{x^2}{n_1}+\frac{y^2}{n_2}\right)\right\}, \quad . \quad (55)$$

where (n_1, n_2) is the equilibrium (most probable) distribution of the most probable number n, and (x, y) is a deviation (n_1+x, n_2+y) from this distribution.

The explicit expression for W_0' follows from the consideration that the sum of all probabilities W_2 in (50) must be unity if all possible values of z are included. Successive values of z differ by 1; hence, replacing the sum by an integral,

$$1=W_0'\int_{-\infty}^{+\infty}\exp\left\{-\tfrac{1}{2}z^2\left(\frac{n+N}{nN}\right)\right\}.dz,$$

so that

$$W_0'=\frac{1}{\sqrt{2\pi\dfrac{nN}{n+N}}}\simeq\frac{1}{\sqrt{2\pi n}}. \quad . \quad . \quad (56)$$

Similarly, if all probabilities $W_{(x,y)}$ in (53) are counted which satisfy the condition that the total number of molecules in the open volume element δ is $n+z$, the sum must be W_z. Successive values of δ differ by 1; hence, replacing the sum by an integral,

$$W_z=W_zW_0''\int_{-\infty}^{+\infty}\exp\left\{-\tfrac{1}{2}\delta^2\frac{n}{n+z}\left(\frac{1}{n_1}+\frac{1}{n_2}\right)\right\}d\delta,$$

so that

$$W_0''=\sqrt{\frac{n}{2\pi n_1n_2}}\cdot\sqrt{\frac{n}{n+z}}\simeq\sqrt{\frac{n}{2\pi n_1n_2}}. \quad . \quad (57)$$

Employing the exact forms for W_0' and W_0'' given by (56) and (57), we obtain

$$W_{(x,y)}=\frac{1}{\sqrt{2\pi n_1}}\exp\left(-\frac{1}{2}\frac{x^2}{n_1}\right)\cdot\frac{1}{\sqrt{2\pi n_2}}\exp\left(-\frac{1}{2}\frac{y^2}{n_2}\right)$$
$$. \quad . \quad . \quad (58)$$

Putting $\delta_1.=\dfrac{x}{n}$, $\delta_2=\dfrac{y}{n}$, (58) becomes

$$W_{(\delta_1,\delta_2)}=\frac{1}{\sqrt{2\pi n_1}}\exp\left(-\frac{1}{2}\frac{n^2}{n_1}\delta_1{}^2\right)\cdot\frac{1}{\sqrt{2\pi n_2}}\exp\left(-\frac{1}{2}\frac{n^2}{n_2}\delta_2{}^2\right).$$
$$. \quad . \quad . \quad (59)$$

5. *The General Case of Chemical Equilibrium.*

We consider, now, a general chemical reaction $\sum_i p_iA_i=0$ and a small open volume-element v in a large closed volume V, where $V>>v$. We shall denote the most probable (equilibrium) distribution in the small element by (n_i).

Just as in the simple case, already treated, of isomeric equilibrium and the open volume-element, we may first calculate the probability that a number $(n+z)$ molecules of all kinds will be present in the volume-element v (where $n=\sum_i n_i$ is the *most probable* number of molecules), and then multiply by the independent probability of these $n+z$ molecules being distributed in a specified manner characterized by (x_i), where x_i is the difference between the number of molecules of species i present in v in the deviating state considered, and the most probable number n_i. Thus the deviating state is denoted by (n_i+x_i), and we have the relation $n+z=\sum_i (n_i+x_i)=n+\sum_i x_i$. By equation (51) we have, for the probability of finding $(n+z)$ molecules in v,

$$W_z=W_0' \exp\left(-\frac{1}{2}\frac{z^2}{n}\right). \quad . \quad . \quad . \quad (51)$$

Also, given that v contains $n+z$ molecules, we have, from equation (34),

$$W=W_0''' \exp\left\{-\tfrac{1}{2}\sum_i \frac{(x_i-n_i z/n)^2}{n_i(1+z/n)}\right\}. \quad . \quad . \quad (60)$$

The exponent argument in (60) *has the same meaning* as in equation (34), namely, $(x_i-n_i z/n)$ is the deviation of the number of molecules of species i from the most probable number of that species *when it is known that* $n+z$ *molecules are present in all, i. e.,* $n_i\left(1+\frac{z}{n}\right)$. We obtain $(x_i-n_i z/n)$, since the number of the species i actually present in the deviating state (x_i) is (n_i+x_i), so that the deviation is equal to $(n_i+x_i)-n_i(1+z/n)$. The probability we require is $W_{(x_i)}=WW_z$; hence

$$W_{(x_i)}=W_0'W_0''' \exp\left[-\tfrac{1}{2}\sum_i\left\{\frac{(x_i-n_i z/n)^2}{n_i\left(1+\frac{z}{n}\right)}+\frac{z^2}{n}\right\}\right]. \quad (61)$$

Observing, now, that $\sum_i n_i=n$, and $\sum_i x_i=z$, the exponent argument in (61) reduces to

$$-\frac{1}{2}\frac{\sum_i \frac{x_i^2}{n_i}+\frac{z^3}{n_2}}{1+z/n}.$$

Now $\frac{z}{n} << 1$ and $\frac{z^2}{n}$ is of the same order as $\sum_i \frac{x_i^2}{n_i}$.

Hence

$$W_{(x_i)} \simeq W_0' W_0'' \exp\left(-\tfrac{1}{2} \sum_i \frac{x_i^2}{n_i}\right),$$

so that we obtain the sufficiently approximate equation

$$W_{(x_i)} = W_0 \exp\left(-\tfrac{1}{2} \sum_i \frac{x_i^2}{n_i}\right), \quad . \quad . \quad . \quad (62)$$

where W_0 means the probability of the most probable (equilibrium) state (n_i), and $W_{(x_i)}$ the probability of the deviating state $(n_i + x_i)$.

Concerning equation (62) the following general remarks may be made :

(1) The values (x_i) are independent.

(2) $\sum_i n_i = n$, where n is the *most probable* number of molecules in the volume-element v.

(3) Given an arbitrary defined *initial* molecular distribution $(\bar{N}_i)$ in the given closed and constant volume V (at the given temperature T of the thermostat), then the most probable (equilibrium) distribution (N_i) in V will be determined by the values of K (the chemical equilibrium-constant at T) and V. Hence the value of $\sum_i N_i$ is definite, and determined by K, V, and $(\bar{N}_i)$. Then n is determined by the equation $n = \frac{v}{V} \sum_i N_i$.

(4) (n_i) means the most probable (equilibrium) distribution of n in the volume-element v. This distribution (n_i) is defined by $(n_i) = \left(\frac{v}{V} N_i\right)$. Thus we have

$$\sum_i n_i = \frac{v}{V} \sum_i N_i = n.$$

(5) Thus, knowing T, V, v, K, $(\bar{N}_i)$ and the molecular chemical reaction-coefficients (p_i), we can calculate the set of values (n_i) which appear in equation (62). Hence, knowing W_0, we can calculate the probability $W_{(x_i)}$ of any deviating state $(n_i + x_i)$ specified by the set of values

(x_i); or, without knowing W_0, we can calculate the relative probabilities of different fluctuating states (n_i+x_i). Thus the frequency-distribution curve in i-dimensional space can be defined, for given values of T, V, v, K, and $(\bar{N}_i)$, since we can determine relative values of $W_{(x_i)}$ for any point (n_i+x_i) in this space.

Conclusion.

In the treatment given in this paper no attention has been paid to the question of fluctuations of temperature in the chemical reacting system. It is assumed, therefore, that in the type of systems considered such temperature fluctuations may be regarded as sufficiently smoothed out (by the action of the thermostat at T) to be of negligible importance.

The Sir William Ramsay Laboratories of
Inorganic and Physical Chemistry,
University College, London, W.C. 1.
May 1937.

LXXXVI. *Crystal Growth in Wires of Nickel and Tungsten.*

By James A. Darbyshire, *M.Sc.*, *Ph.D.*, *A.Inst.P.*
(Communicated from the Research Department of Ferranti, Ltd.*)

[Plate IX.]

THE development of large grains in wires of nickel and tungsten has been a source of considerable difficulty in the various industrial applications of these materials. Thus, if the grains are too large a rupture can easily occur across the grain boundary, and the wire will fail. The crystallites must be sufficiently large for a reasonable amount of interlocking to occur, but not so large that a straight fracture is possible. The question of grain growth in tungsten has been studied and described in considerable detail by Smithells † and also by Burgers ‡.

If the filaments are made from pure tungsten the wire is initially composed of long crystals of fibrous nature

* Communicated by the Author.
† J. Smithells, ' Treatise on Tungsten,' p. 90.
‡ W. G. Burgers, 'Philips Technical Review,' vol. ii. no. 1, p. 32 (1937).

running along the length of the wire. As the wire is heated this fibrous structure breaks down at a certain temperature called the "equiaxing" temperature and changes over to a granular type of structure. The grains then tend to grow progressively, and may finally become so large that the crystals slip over each other along their boundary faces, and the wire is liable to give trouble by "off-setting." This off-setting effect creates a local increase in resistance, and the wire may become particularly hot at these points and then fuse. It has been found possible to prevent excessive grain growth by adding small amounts of other substances known as "additives." These are generally salts or oxides, and modify the structure developed in the wire on recrystallizing from the fibrous form to the granular form. Thoria ThO_2 (approximately ·5 per cent.) and Al_2O_3 (·1 per cent.) are often used. The development of large particle size in nickel has not been so thoroughly studied.

The object of the present work was to follow the changes in various types of wire by means of X-ray diffraction patterns. The X-ray method is ideal for this investigation, because any tendency to aggregate is readily visible in the photographs. The specimen, in the form of a wire, is mounted at the centre of a circular camera of the standard type now used for powder work by X-ray diffraction *. Copper radiation was used for both nickel and tungsten. The filter of nickel foil which is normally used to cut off the β-rays was not used for the nickel photographs, but occasionally used for the tungsten photographs. The specimens were not rotated unless very accurate values of lattice constants were required. If the crystallites in the wire are very fine and are distributed at random it can be shown mathematically † that the diffraction lines on the film should be quite uniform and continuous and free from discontinuities or spots on the lines. If the crystallites are extremely fine the resolving power for the X-rays of normal wavelength (1·000 to 1·500 Å.) is very low and the diffraction spectra are broad. If the crystallites are of appreciable size the lines lose their smooth uniform structure and spots appear superposed on the lines. As the crystallites

* A. J. Bradley and A. H. Jay, Proc. Phys. Soc. xliv. p. 563 (1932).
† A. H. Compton, 'X-Rays and Electrons' (Macmillan & Co., Ltd.).

get still larger the spots will appear without the continuous lines at all. Finally, when we have really large crystals, several spots may appear off the lines altogether. This is due to the fact that the crystal is reflecting the general radiation of the target from planes suitably situated, and ignoring in general the characteristic homogeneous component of the radiation from the X-ray tube. The crystal or crystals are so large that it is rather improbable that they should have planes suitably disposed to reflect the homogeneous beam, but some region of the general X-ray spectrum is of suitable wave-length to be reflected by certain crystal planes. These reflexions then appear on the film at positions often far removed from the usual lines due to the diffraction pattern of the material taken with the characteristic radiation of the target. Crystallites in the wires often show considerable preferred orientation, and in many cases the crystallites are distorted. The preferential orientation is clearly revealed by the relative intensities, and also to some extent by the peculiar shape of the lines. The distortion is revealed by the degree of resolution of the α_1 α_2 doublets towards the outer edge of the film.

Experiments on Nickel Wire.

The first series of experiments consisted of heating up nickel wire ·0019 in. diameter *in vacuo* for 100 seconds at various constant temperatures ranging from 100° C. to 1200° C. The specimens of nickel wire consisted of (*a*) bare nickel wire, (*b*) nickel wire coated with the standard carbonate mixture. The carbonate coating (which becomes an oxide coating if the nickel reaches temperatures above 700° C.) is a much better radiator than bare nickel. This is indicated by the corresponding temperatures given in columns 2 and 4 of Table I., which indicate the difference in temperature for the same heater input voltage.

It will be seen from the results given in Table I., columns 3 and 5, that the nickel wire begins to show signs of crystal growth at 900° C. for the uncoated wire and at 950° C. for the coated wire. The time of heating (100 seconds) corresponds approximately to the time for which the filaments are heated during the activation schedule for standard type valves.

Crystal Growth of Nickel Wire during Processing.

In a second series of experiments a reel of nickel wire (diameter ·0019 in.) was followed through the complete processing schedule, and the crystal growth was observed at each stage by means of X-ray diffraction. In the first place the wire was photographed before use. The specimen was not rotated during these experiments, and the original pattern given by the wire is reproduced in fig. 1 (Pl. IX.); the lines were quite fine and continuous and the doublets well resolved. This indicates that there are no large crystal groups and that there is very little

TABLE I.

Temperature of Coated and Uncoated Nickel Wire and Observation on Crystal Growth.

Applied volts.	Coated.	Crystal growth.	Uncoated.	Crystal growth.
·1	20° C.	No.	20° C.	No.
1·0	280° C.	,,	520° C.	,,
2·0	600° C.	,,	740° C.	,,
3·0	788° C.	,,	895° C.	Trace.
4·0	835° C.	,,	945° C.	,,
5·0	952° C.	Trace.	1020° C.	Yes.
6·0	1000° C.	Yes.	1110° C.	,,
7·0	1070° C.	,,	1210° C.	,,
8·0	1100° C.	,,		
9·0	1140° C.	,,		
10·0	1200° C.	,,		

distortion. The wire was then coated with a mixture of strontium and barium carbonates. This process involved heating up the nickel wire to a temperature of approximately 500° C. for two minutes. The X-ray photograph still gave fine and continuous lines with well-resolved doublets (Pl. IX. fig. 2). Thus so far as this stage in the processing operations the filament is fine-grained and free from lattice distortion or excessive crystal aggregation.

Fig. 3 (Pl. IX.) is a photograph taken from a filament of a valve just after activation according to a production schedule with lighting as given in Table I. at 6 volts. On comparing this with fig. 1 (Pl. IX.), which is a photograph of the original nickel wire before activation, it is seen that a certain amount of aggregation has occurred. A photo-

graph was taken after the valve had been aged after activation, and the crystal size apparently did not increase appreciably during ageing. Some battery filaments which had failed on life test were then examined by X-ray methods, and it was always found that the crystals had grown to a very great extent. This can be readily seen in fig. 4 (Pl. IX.), which is a reproduction of a photograph of a failed nickel filament. The filaments which run quite successfully on life or in service nearly always gave a pattern indicating much finer grain size. A photograph of such a filament is reproduced in fig. 5 (Pl. IX.), and it will be seen that the lines are much more uniform and continuous than those in Pl. IX. fig. 4. The good filaments occasionally gave rather broken lines. Presumably these filaments were in danger of fracture, or may be a certain degree of crystal growth has no detrimental effect on the life of the wire.

The general evidence from X-ray examination indicates that the chief cause of considerable crystal growth is too high temperature during activation and pumping. After this stage has been passed there is definitely a slow progressive crystal growth during life, in many cases often without any serious consequences to the reliability of the filament. In other cases, where the crystal aggregation during activation has not been very marked, there is practically no increase in grain size during life, It seems possible that the initial aggregation which occurs on activation may form some kind of nucleus about which the crystal growth continues throughout life, whereas if there is no appreciable nucleus at the commencement there will be no growth during life.

In another series of experiments a length of nickel wire was mounted on a special frame in such a manner that it could be inserted in the X-ray camera for examination and then mounted in a highly evacuated vessel whilst it was heated. This wire was photographed in its initial state before any heating, and then it was heated to a temperature of 220° C. for 1 minute. After being photographed it was heated to 600° C. for another minute, and so on until the wire was finally fused at a temperature of approximately 1400° C. The results of these experiments are given in Table II. Column 1 gives the temperature at which the wire was heated for 60 seconds and column 2 the results of the X-ray examination.

Nickel Wire taken to the Fusing-point.

In this experiment small lengths of nickel wire were taken to their fusing-point by increasing the temperature uniformly throughout. In the first place the wire was raised to its fusing-point very rapidly and broke approximately one second after switching on the current. All these specimens after failure were photographed by the X-ray method at a distance of approximately 3 mm. from the point of failure. The filaments were assembled

TABLE II.

Temp.	X-ray pattern and conclusions.
25° C.	Lines continuous. No crystal growth.
220° C.	,, ,, ,, ,,
600° C.	Trace of spots on lines.
900° C.	Many spots on lines.
1000° C.	Very considerable amount of crystal growth.

TABLE III.

Time (seconds).	Type of pattern and conclusions.
1.....	Trace of crystal growth.
5.....	Spots on lines. Def. evidence of crystal growth.
10.....	,, ,, ,, ,, ,,
15.....	,, ,, ,, ,, ,,
20.....	,, ,, ,, ,, ,,
25.....	,, ,, ,, ,, ,,

in highly evacuated glass bulbs before heating. The results of these experiments are collected in Table III. Column 1 gives the time during which the filament was heated before it collapsed, and in column 2 the results of the X-ray examination of that wire are given.

There is another factor which has some influence on the growth of nickel crystallites in nickel valve filaments ; this is the tension which it is necessary to introduce at the points of support in order to hold

the filament rigid relative to the rest of the assembly. This rigid construction is essential in order to avoid the parasitic noises which are otherwise likely to be very troublesome. The tension is introduced by means of small springs of molybdenum wire. If this tension is too great it appears that the tendency for single crystal growth is considerably accelerated. The influence of tension on the aggregation of the crystallites has not yet been completely followed by X-ray examination, and will form the subject of future work. It is interesting to mention one further experiment in which a piece of nickel wire ·0042 in. diameter was stretched under a gradually increasing force until it snapped. An X-ray photograph was taken 2 mm. from the point of fracture and the lines were again fine and continuous. The spectra, however, were considerably improved in sharpness, indicating some alteration in the preferred orientation of the crystallites in the wire.

Nickel Alloys.

As regards other alloys of nickel we have initiated a series of experiments with :—

(*a*) Ni–Mn–Al–Si. 2 per cent. Mn, 1·5 per cent. Al, 1 per cent. Si, remainder Ni.
(*b*) Ni–Mg ..... ·48 per cent. Mg.
(*c*) Ni–Fe ..... 1·14 per cent. Fe.

The alloys (*a*) and (*b*) were more brittle than pure nickel even at the early stage of assembly before any heat treatment according to activation schedule. The alloy (*b*) gave good emission and was rather easier to assemble than (*a*). The filaments of alloy (*b*) behaved quite well on life test, and after 1000 hours successful running the X-ray patterns still gave fairly uniform lines (see Pl. IX. fig. 6) indicating relatively little crystal aggregation. The behaviour of filaments of the alloy (*a*) on life test was no better than those of pure nickel, and the emission was less than that from pure nickel. The emission from alloy (*c*) was so low initially that no further tests were carried out. X-ray photographs of the three alloys were taken before the filaments were heated, but a complete record throughout the life test run has not yet been obtained for alloy (*a*). Initial photographs indicated fine-grain crystallines just as in the case of the

pure nickel wire. The Ni–Mn–Al–Si alloy, however, gave just a slight indication of aggregation, whereas the other two alloys could not be distinguished from pure nickel as regards their initial texture.

Experiments on Tungsten Wire.

As in the case of nickel the first series of experiments consisted of heating up fine tungsten wire *in vacuo* for 100 seconds at various constant temperatures ranging from 20° C. to 1800° C. These experiments were carried out on uncoated tungsten wire and on tungsten wire which had been coated with alumina just as in the case of the standard valve heaters. In both cases the tungsten wire showed no tendency at all to recrystallize into larger agglomerates. The α_1 α_2 doublets sharpened up considerably, indicating that some lattice distortion had been removed by heating. Although tungsten does not form large grains when heated to 1800° C. for 100 seconds, nevertheless, as will be seen later, it can develop very large crystals if heated at 1600° C. for a suitable length of time under intermittent conditions. If tungsten is heated at 2500° C. for 100 seconds crystal growth is appreciable and the diffraction lines begin to break up into spots. We are now approaching the region in which tungsten tends to recrystallize and grow larger units just as nickel wire does round about 1000° C. Fortunately it is not often necessary to take tungsten up to such high temperatures, and therefore it is not likely to develop large grain size as readily as nickel during ordinary processing operations.

Tungsten Wire taken to the Fusing-point.

Small filaments of tungsten wire were taken to their fusing-point in highly evacuated glass bulbs just as in the case of the nickel filament described on page 1004. The temperature was increased uniformly from 25° C. up to the melting-point, and the time interval from the commencement of heating until the final breakdown varied from 1 second to 60 seconds. The specimens were then photographed in the X-ray camera, and the results of this examination are given in Table IV.

Crystal Growth of Tungsten Wire during Processing.

The photographs of tungsten wire before any heating experiments had been carried out always showed fine

continuous lines belonging to the α tungsten structure (cubic body centred, with lattice constant 3·1583 Å.). A typical photograph of tungsten wire is reproduced in fig. 7 (Pl. IX.). This was taken with Cu Kα radiation, using the nickel foil to filter off the β-components. The wire was next coated with alumina—this process involved heating the wire up to a temperature of 1200° C. in an atmosphere of hydrogen for an interval of approximately 200 seconds. This is the standard coating process involved in the preparation of the wire for use as heater

TABLE IV.

Time (seconds).	Observations.
1.....	Several spots. Large crystals.
10.....	Very many spots. „ „
20.....	„ „ „ „ „
30.....	„ „ „ „ „
60.....	„ „ „ „ „

in an indirectly heated valve cathode. The X-ray photograph of tungsten wire after this operation always gave fine and continuous lines as in fig. 7 (Pl. IX.). There was no evidence of crystal aggregation in this process. There may have been some slight crystal growth, but in view of the fact that the X-ray pattern is not altered crystal size is still within the range 10^{-3}, 10^{-5} cm. After this operation the wire was still quite ductile. The coated wire was then cut up into heaters of required size.

The next operation involves furnacing the completed heaters in

(a) dry hydrogen at 800° C. for 5 minutes,

or (b) moist hydrogen at 1750° C. for 15 seconds.

The heaters are still quite ductile after operation (a) or (b), and the X-ray photograph still indicated fine crystallites. There was, however, a decided indication of a slight beadiness developing in the diffraction lines from the (a) sample, but not sufficient to enable the pattern to be placed in a different class from (b). The pattern from the (b) sample was indistinguishable from

that of the tungsten wire initially. The next operation involves activating the cathode of the complete assembly on the automatic pumping machine. In this operation the temperature schedule of the tungsten wire would be approximately as follows :—

Position	1.	2.	3.	4.	5.	6.	7.	8.	9.
Seconds	0	0	16	16	16	16	16	16	16
Temp. °C.	0	0	700	800	800	1000	1100	1300	1000

This is the operation in which appreciable grain growth occurs in the case of the nickel filaments for battery valves if the heating schedule is too high. In the case of the tungsten heaters, however, the wire did not exhibit any appreciable increase in grain size after this operation, even if the lighting schedule was 30 per cent. higher than normal. Experiments were carried out on both unannealed and annealed tungsten wires, and no difference could be seen in the X-ray photographs as far as this operation. A photograph of a tungsten heater which has been overheated very considerably on the automatic pump is reproduced in fig. 8 (Pl. IX.). It will be seen that there is no evidence of spots developing on the lines. The lines are quite uniform and continuous, and indicate the fine crystalline structure of the wire even after considerable overheating.

The next step is the ageing of the valves after pumping. This involves running the heater of the cathode at approximately 900° C. for 5 minutes, then at 1100° C. for 1 minute, and then 800° C. for 25 minutes. The latter temperature is the normal running temperature of the heater during life. Ageing does not give any observable grain growth as revealed by the X-ray patterns.

At this stage the valves are ready to commence life, and we proceeded to examine the heaters from time to time to see how they were behaving under normal working conditions. In most cases, of course, valves having heaters made of tungsten as used for standard production would carry on throughout life test without failure occurring, but occasionally routine life tests revealed batches of heaters that were unreliable, and these were made the subject of special study by X-ray methods. Until the commencement of the life test run the X-ray patterns indicated no difference at all between batches

of heaters which were subsequently unreliable and those which were quite reliable. In both cases the lines were fine and continuous and the doublets equally well resolved.

Also experiments were carried out with unannealed and annealed pure tungsten wire in batches which were treated to precisely the same conditions during coating, activation, and ageing. No difference could be detected between annealed and unannealed tungsten as far as the commencement of life test. On actual intermittent life test the unannealed were slightly better statistically than the annealed, and in normal cases when the heaters ran satisfactorily on life test the wire gave X-ray patterns showing continuous unbroken lines, indicating very little crystal growth. In the case of heaters which broke down on life, the lines were broken and discontinuous in every case (Pl. IX. fig. 9).

One particular batch of unreliable tungsten heaters which failed on intermittent life test were put on continuous life test under precisely the same running conditions. The wires were examined as usual before commencing life test, and gave continuous fine lines in their diffraction patterns. X-ray photographs were taken of sample heaters from this batch every fortnight. The diagrams remained as they were originally, the diffraction lines being continuous and indicating no appreciable aggregation of crystallites. This state of affairs went on until the heaters had run for more than twice the normal life test period. On continuous life test these heaters had shown less than half a per cent. failures, although on intermittent life test approximately 10 per cent. had failed. This experiment indicates that the intermittent life test is absolutely essential for test purposes, and that the repeated cooling and heating of the tungsten wire is one of the prime factors in aggregation. Also it indicates once again that aggregation is the chief cause of failure on life.

Tungsten Wire taken to Fusing-point.

It has been seen that the tendency for nickel wire to develop large grains during actual pumping and activation is much greater than in the case of tungsten wire. This is not due to a fundamental physical difference between tungsten and nickel, but to the fact that the nickel wire is working relatively much nearer to its melting-point

than tungsten and because its equiaxing temperature is lower than that of tungsten. It has been seen that in the flashing experiments the tungsten wire developed very large crystals even more readily than the nickel wire.

Discussion.

As to the reason why some batches of tungsten become unreliable and exhibit progressive recrystallization during life, whereas other batches remain finely crystalline and fairly malleable throughout life, the X-ray investigation does not give a direct answer.

Recent experiments tend to indicate the cause of such differential behaviour, and there are many processing factors which have to be taken into consideration, especially those connected with the coating of the heater with alumina. A series of comparison experiments of crystal growth in uncoated and coated tungsten wire is the subject of further investigation.

In conclusion, the author would like to thank Ferranti, Ltd., for providing facilities for this research and for permission to publish the results. In particular my thanks are due to Mr. A. L. Chilcot for initiating this work, and to Mr. L. F. Berry for assistance in a number of experiments.

Ferranti, Ltd.,
Hollinwood and Moston.
July 1937.

LXXXVII. *A Note on the Definition and Determination of Mass in Newtonian Mechanics. By* C. G. Pendse *.

IT is a matter of common agreement that classical mechanics, founded by Galileo and Newton, and developed by generations of astronomers, mathematicians, and physicists in its diverse aspects, is a logically self-consistent and elegant mathematical science. Though the science was mainly formulated during the seventeenth and the eighteenth centuries, its postulates began to be examined critically during the last century. Particularly the notion of mass was examined very carefully by Ernst

* Communicated by the Author.

Mach, who interpreted mass in terms of Newton's Second and Third Laws of Motion. The object of this note is to show that, though Mach's definition of mass may be a dynamical one, it does not enable an observer to determine the ratios of the masses of a system—an "isolated" system—of bodies (particles) from his observations if the system be composed of more than a certain number of bodies (particles)—*seven* being the absolutely maximum limit for observed accelerations taken at an arbitrary number of instants, and four in case the observer seeks to find the ratios of the masses from the observed accelerations at one instant.

The note consists of four sections. In § 1 the necessary well-known portions of mechanics are stated. In § 2 Mach's definition of mass is stated, and in § 3 it is examined from a theoretical point of view. In § 4 the question of the determination of masses is considered.

§ 1. *A Brief Statement of the well-known Portions of Mechanics.*

It is necessary to state very briefly the well-known portions of mechanics; a thoroughgoing account is not attempted here. A succinct discussion of the principles of Newtonian Mechanics is given by Filon [3].

The theoretical abstractions with which we are concerned in Newtonian Mechanics are "particles" and "continuous media." In the present note we shall be concerned with particles alone.

In the background we have the notions of space and absolute time and mass. (Newton postulated also the existence of absolute directions.) It is assumed that space is Euclidean and that "particles" are mathematical points, each of which is endowed with a constant positive number called its "mass" and defined in terms of some unit.

The positions of points (or particles) are referred to a frame of reference $Oxyz$; and it is postulated that corresponding to every point or particle there exists a unique Cartesian vector function of t (time), called its position vector, which is assumed to be a continuous function of t. Fixing our attention on a definite point or particle, let $\overrightarrow{OP}$ be its position vector. $\overrightarrow{OP}$ is assumed to be a diffe-

rentiable function of t. $\dot{\overrightarrow{OP}}$ is defined to be the velocity of the point or particle relative to the frame $Oxyz$. $\overrightarrow{OP}$ is also assumed to possess a derivative $\ddot{\overrightarrow{OP}}$ (except possibly at a finite number of points as in the case of impulsive motion). $\ddot{\overrightarrow{OP}}$ is called the acceleration of the point or particle relative to the frame $Oxyz$. From the hypothesis of absolute time and the hypothesis that the position of a point or particle relative to a frame of reference is represented by a vector, it is easy to deduce the parallelogram law connecting the velocities (or accelerations) of a point or particle relative to two frames of reference and the relative velocity (or acceleration) of the origins of the frames of reference, on the assumption that the orientation of one of the frames of reference does not change relative to that of the other with time. From this point onwards we assume that the orientation of any one of the frames of reference does not change with time relative to that of any other frame among the frames of reference in question, and we shall speak of the velocity (or acceleration) of a point relative to an origin O.

Now we come to the Laws of Motion and the corollary to the Second Law.

Law I.—Every body continues to be in a state of rest or of uniform motion in a straight line unless it is compelled by force to change that state.

Law II.—Change of motion is proportional to the force applied and takes place in the direction in which the force acts.

Corollary.—Every force produces independently its own acceleration.

Law III.—To every action there is an equal and opposite reaction, or the mutual reactions of two bodies are equal and opposite.

It is necessary to make certain assumptions concerning the meaning of some phrases in the laws as stated.

A "body" is taken to mean a "particle"; the "motion of a body" is taken to mean "mass of the body" $\times$ its velocity (momentum), and the change of motion is assumed to mean the rate of change of the momentum

with respect to time. Assuming that the mass remains constant

$$\frac{d}{dt}(\text{mass} \times \text{velocity}) = \text{mass} \times \text{acceleration}.$$

Assuming that the forces have been correctly prescribed in relation to the frame of reference *, we have, for the motion of the particle, mass × acceleration of the particle = the force acting on the particle.

We consider now a system of n particles P_α of mass $m_\alpha (\alpha, \beta = 1, \ldots, n)$. Let $\overrightarrow{E_\alpha}$ be the "external" force on the particle P_α, and let $\overrightarrow{I_{\alpha\beta}}$ be the force on it due to the particle P_β. Then

$$m_\alpha \ddot{\overrightarrow{OP}}_\alpha = \overrightarrow{E_\alpha} + \sum_{\substack{\beta=1 \\ \neq}}^{n} \overrightarrow{I_{\alpha\beta}},$$

and $\overrightarrow{I_{\alpha\beta}} = -\overrightarrow{I_{\beta\alpha}}$ by the third law. It is further assumed that $\overrightarrow{I_{\alpha\beta}}$ is parallel to the straight line $P_\alpha P_\beta$.

It is only in the second law that the notion of mass comes in. Newton defined the "mass of a body" as "the volume of the body multiplied by its density," as he believed density to be an inherent property of a body. A commonplace definition of mass is: "the mass of a body is the quantity of matter contained in the body." The two definitions have no empirical—dynamical—significance. It was Ernst Mach [1] who pointed out that the definition of mass is contained in the second and third laws of motion. Mach was supported by Pearson [2] and others.

§ 2. *Mach's Definition of Mass.*

Suppose we have a pair of particles forming an "isolated" system relative to the frame of reference, which is a Newtonian frame.

Let m_1 and m_2 be the masses of the particles P_1 and P_2.

Then $m_1 \ddot{\overrightarrow{OP}}_1$ = force on the particle P_1 due to the particle P_2,

= − force on the particle P_2 due to the particle P_1, by the third law of motion,

$= -m_2 \ddot{\overrightarrow{OP}}_2$,

since the particles form an "isolated" system.

* Such a frame is called a Newtonian frame.

Therefore

$$m_1\ddot{\overrightarrow{OP}}_1 = -m_2\ddot{\overrightarrow{OP}}_2.$$

Consequently Mach defined the ratio of the masses of two particles as the negative inverse ratio of their mutually produced accelerations, and he postulated that this ratio was a constant. It is further necessary to postulate that if m_{12} is the ratio of the mass of particle 1 to that of particle 2, m_{23} is the ratio of the mass of particle 2 to that of particle 3, and m_{13} is the ratio of the mass of particle 1 to that of particle 3, as defined above,

$$m_{13} = m_{12} \times m_{23}.$$

Filon [3] has described an ingenious experiment to demonstrate the rôle played by the second and third laws of motion in the definition of mass. It is possible to verify the rule $m_{13} = m_{12} \times m_{23}$, stated above, by Filon's experiment

§ 3. *A Critique of Mach's Definition.*

In Mach's definition of the ratio of the masses of *two* bodies (particles), stated above, it is assumed that the bodies (particles) form an "isolated" system relative to the frame of reference. Hence it is necessary to examine Mach's definition from a theoretical standpoint when the system is composed of more than two bodies (particles).

We consider a system of $n\,(>2)$ particles $P_\alpha(\alpha, \beta = 1, \ldots, n)$, moving relative to a Newtonian frame $Oxyz$, the forces being assumed to be correctly prescribed. It is desired to give a meaning to the term "the acceleration of the particle P_α due to the particle $P_\beta(\beta \neq \alpha)$."

We imagine the particle P_α to move without the action of the particle P_β on it, and denote its position at any instant t by $P_{\alpha\beta}$; it is assumed that when the particle P_α is at $P_{\alpha\beta}$ it is acted on by all the forces actually acting on it at that instant (in its real position) except the action of the particle P_β on it (the particle P_α) at that instant. The point $P_{\alpha\beta}$ will describe an orbit; the velocity and acceleration of the particle P_α relative to $P_{\alpha\beta}$ will be quite definite, and

$$\ddot{\overrightarrow{OP}}_\alpha = \ddot{\overrightarrow{OP}}_{\alpha\beta} + \ddot{\overrightarrow{P_{\alpha\beta}P_\alpha}}.$$

Moreover, by the corollary to the second law of motion, the acceleration of the particle P_α due to the action of the particle P_β is produced independently of other forces.

$\overrightarrow{\ddot{P_{\alpha\beta}P_{\alpha}}}$ can, therefore, be called the acceleration—the additional acceleration, to use an expression due to Filon[3], —of the particle P_α produced by the action of the particle P_β.

Hence it is possible to argue that if the ratio of the masses of two bodies (particles) be defined as the "negative inverse ratio of mutually induced accelerations" the ratios of the masses of all pairs of bodies (particles) in a system thereof are *conceptually* perfectly definite, though the observable acceleration of a body (particle) P_α is its cumulative acceleration $\overrightarrow{\ddot{OP_{\alpha}}}$, due to all the forces relative to the Newtonian frame. The main feature of Mach's definition is that it is dynamical.

§ 4. *Determination of Masses by Observation.*

Now, however, arises the following question: Given a system containing more than two particles, will it be possible for an observer fixed in a Newtonian frame for the system of particles—called for the sake of brevity a Newtonian observer—to determine the ratios of the masses of the particles by observing their motions? It is assumed that the observer can record the path of each particle. Consequently the observer is supposed to know the motion of every particle in the system. He cannot observe the ratios of the masses of the particles or the reactions between them: he can only aspire to infer them.

If a Newtonian observer were given two particles forming an "isolated" system he could immediately assume that the acceleration of one of the particles is induced by the other and find the ratios of the masses of the particles.

We consider now an "isolated" system containing $n(>2)$ particles. Using the suffixes λ, $\mu=1, \ldots, n$, let $\vec{f_\lambda}$ be the Newtonian acceleration of the particle P_λ. We have to consider two cases: (I), in which the accelerations of the particles at one instant are considered, and (II), in which the accelerations of the particles at several instants are taken into account.

(I.) The observer will not be able to say always that a certain portion of $\vec{f_\lambda}$ is due to the action of a certain particle P_μ. To make the matter clear, suppose that

$\overrightarrow{f_{\lambda\mu}}$ is the part of the acceleration of the particle P_λ due to the action of the particle P_μ, and let $\overrightarrow{e_{\lambda\mu}}$ be the unit vector in the direction $P_\lambda \rightarrow P_\mu$. By the axiom that the action between two particles is parallel to the straight line joining them, $\overrightarrow{f_{\lambda\mu}} = \phi_{\lambda\mu}\overrightarrow{e_{\lambda\mu}}$, where $\phi_{\lambda\mu}$ is a scalar quantity. Then

$$\overrightarrow{f_\lambda} = \sum_{\substack{\mu=1 \\ \mu\neq\lambda}}^{n} \phi_{\lambda\mu}\overrightarrow{e_{\lambda\mu}}.$$

The above vector equation is equivalent to not more than three distinct linear algebraic equations for the $(n-1)$ unknown quantities $\phi_{\lambda\mu}(\mu=1, \ldots, n \text{ and } \mu\neq\lambda)$ in connexion with the acceleration of the particle P_λ.

If $n=3$ and if the particles are not collinear there will be two distinct equations for the pair of ϕ's associated with each particle and the ϕ's for each can be determined uniquely. Thus the ratios of the masses of the particles can be determined. If, however, the particles remain always collinear there will be only one equation for the pair of ϕ's associated with each particle; the values of the ϕ's for each particle will not be known uniquely, and the ratios of the masses of the particles cannot be determined.

If $n=4$ and if the particles are not in one plane there will be three distinct equations for the three ϕ's associated with each particle. The ϕ's and consequently the ratios of the masses of the particles can be determined uniquely. If, however, the particles are always coplanar or collinear, there will be less than three distinct equations for the three unknown ϕ's associated with each particle; and the values of the ϕ's and consequently the ratios of the masses of the particles will be indeterminate.

If $n>4$ there will be not more than three distinct equations for the $(n-1)$ unknown ϕ's associated with each particle, and the values of the unknown ϕ's and hence the ratios of the masses of the particles cannot be found uniquely.

To express the above results in an alternative way, it is possible to express uniquely the acceleration of a particle as the sum of vectors parallel to the straight lines joining the particle to the other particles, when the particles are not collinear in the case of three particles and when the particles are neither collinear nor coplanar in the case of four particles; and it is impossible to do

so when the system is composed of more than four particles *.

(II.) Now we consider the case in which the Newtonian observer seeks to find the ratio of the masses of the particles of the system with the aid of the observed accelerations at *several instants*.

In case (I.) we have had three equations for the $(n-1)$ ϕ's for each particle, *i. e.*, $3n$ equations for the $n(n-1)$ unknown ϕ's associated with the whole system.

Now suppose that the observer employs the accelerations of the particles at r instants. The masses (m_λ's) of the particles remain unaltered throughout the motion, but the $\overrightarrow{e_{\lambda\mu}}$'s and the reactions between the particles and consequently the $\phi_{\lambda\mu}$'s in the above case (I.) would generally vary with time. Let $F_{\lambda\mu}\overrightarrow{e_{\lambda\mu}}$ be the reaction of the particle P_μ on the particle P_λ at any instant. Then, since $\overrightarrow{e_{\lambda\mu}}=-\overrightarrow{e_{\mu\lambda}}$ and $F_{\lambda\mu}\overrightarrow{e_{\lambda\mu}}=-F_{\mu\lambda}\overrightarrow{e_{\mu\lambda}}$ (by the third law of motion), $F_{\lambda\mu}=F_{\mu\lambda}$ and $\phi_{\lambda\mu}=F_{\lambda\mu}/m_\lambda$ at that instant; and there will be r sets of n vector equations

$$m_\lambda\overrightarrow{f_\lambda}=\sum_{\substack{\mu=1\\ \mu\neq\lambda}}^{n} F_{\lambda\mu}\overrightarrow{e_{\lambda\mu}},\ (\lambda=1,\ \ldots,\ n),$$

each set of n equations corrseponding to observed accelerations at one of the instants in question.

The number of $F_{\lambda\mu}$'s corresponding to any instant is $\frac{1}{2}n(n-1)$. Hence the total number of unknown quantities for observations at r instants is $n-1+\frac{1}{2}rn(n-1)$, as the masses remain unchanged, and only the ratios of the unknowns enter into the equations.

The rn vector equations stated above are equivalent to not more than $3nr$ distinct linear algebraic equations. The solution of these not more than $3nr$ equations will be indeterminate if

$$n-1+\tfrac{1}{2}rn(n-1)>3nr,$$

i. e., if $$n-1>\frac{6rn}{rn+2},\quad \textit{i. e.},\ >6-\frac{12}{rn+2},$$

i. e., if $$n>7-\frac{12}{rn+2}.$$

* Compare this statement with the following view of Pearson :— "The manner in which the part of A's acceleration due to B might be separated from that due to other corpuscles in the same field cannot be fully discussed in the present work. In many cases it could be discriminated by the aid of the parallelogram of accelerations (p. 236)." 'The Grammar of Science,' ed. 2, p. 300, footnote 2.

Hence we conclude that if there be more than *seven* particles in the system the observer will be unable to determine the ratios of the masses of the particles or the forces between them, however large the number of instants, the accelerations pertaining to which are considered, may be. An observer cannot dissect a given " isolated " system into smaller "isolated" systems ; he can only observe the motions.

It may be possible, in some particular cases, to determine the law of force between the particles of an " isolated" system and the ratios of masses by a process of approximation and subsequent induction. This process would be possible when it is permissible to single out one of the particles as the " dominating " particle for one or some of the particles of the system.

It would be interesting to consider a few examples.

(1) In Filon's " Fletcher-trolley " experiment [3] the experimenter can regard the two interacting bodies as forming an " isolated " system, the walls of the laboratory constituting a Newtonian frame for the problem.

(2) A binary star may be regarded as an " isolated " system of two bodies, and by treating each component as a particle a Newtonian observer for the system can determine uniquely and exactly the ratio of their masses by observing their motions.

(3) The solar system may also be regarded an " isolated " system ; but, strictly speaking, a Newtonion observer for the system would be unable to determine *uniquely* and *exactly* the ratios of the masses of the members of the system (which contains more than seven bodies) by observing their motions. He has to assume, as a first approximtion, that the sun and one of the planets form an " isolated " system, and has to use the law of gravitation formulated from the orbit of the planet. He has to create mentally artificial " isolated " systems as a first approximation.

The procedure is permissible only because it is fortunately possible to ignore the interactions between the planets in comparison with the gravitation of the sun.

(4) Finally, we consider the case in which the masses of the particles, numbering more than seven, in an " isolated " system do not vary widely, as in the case of a gas or a mixture of gases. If we are presented with the knowledge of the motion of each particle it would be

quite impossible for us to determine the ratios of the masses of the particles or the forces between them from a complete knowledge of the motions.

It is apparent, therefore, that though the ratios of the masses of the members of a system of bodies (particles) may be conceptually perfectly definite when they are interpreted in terms of the second and third laws of motion and the corollary to the second law, according to Mach's ideas, it is impossible for a Newtonian observer to determine uniquely and exactly the ratios of the masses of the members of a system—an " isolated " system—of particles (as well as the reactions between them) from a knowledge of the motions of the particles :—

(i.) if the system has more than four particles, and in a limited number of cases if the system has three or four particles, in case the observer considers their accelerations at one instant only, and

(ii.) if the system has more than seven particles in case the observer utilizes the accelerations of the particles at as many instants as he chooses.

I wish to thank Professor L. N. G. Filon, who kindly read critically a preliminary draft of this note, and made valuable suggestions for its improvement, for his interest in this note. I wish to thank also Professor H. F. Baker and Dr. W. M. Smart for their sympathetic interest.

Appendix.

We mention here some points to which there was no occasion to refer in the main part of the paper.

1. In the opinion of the writer the rule $m_{13}=m_{12}\times m_{23}$, stated in §2 above, is not contained, either explicitly or implicitly, in the laws of motion, nor is it self-evident. It is an independent axiom.

2. The observer can determine the interactions between the particles in case (I.) in §4 above, when the ratios of the masses of the particles can be uniquely determined. The process is in the following sequence :—

(i.) He has to find $\phi_{\lambda\mu}/\phi_{\mu\lambda}$ for all pairs and to verify that the ratios are constant in time.

(ii.) He has to verify that $m_{13}=m_{12}\times m_{23}$ for all groups of three particles.

(iii.) He has to choose one of the particles to be of unit mass, and to find the masses of the other particles by

means of the known ratios and the rule $m_{13}=m_{12}\times m_{23}$. Then the force on the particle P_λ due to the particle P_μ is $m_\lambda\phi_{\lambda\mu}$ in the direction $P_\lambda\to P_\mu$, m_λ being the mass of the particle P_λ as defined above.

3. In case (I.) of § 4 above the limiting value of n is 4. In case (II.) of the same section, putting $r=1$ in the inequality $n>7-\frac{12}{rn+2}$, the limiting value of n is found to be a number between 5 and 6, *i. e.*, effectively 5, since it is a whole number. The discrepancy between the two limitiug values of n is more apparent than real; for, in case (I.), there are $n(n-1)$ unknowns and not more than $3n$ independent linear equations, while in case (II.), for $r=1$, there are $n-1+\frac{1}{2}n(n-1)=\frac{1}{2}(n+2)(n-1)$ unknowns and not more than $3n$ linear algebraic equations. Now, $n(n-1)-\frac{1}{2}(n+2)(n-1)>0$, when $n>2$. Thus, in case (I.) there are more unknowns than those in case (II.), for $r=1$, while the number of equations does not exceed $3n$ in each case, provided $n>2$. Hence the difference between the limiting values in the two cases.

4 The rule $m_{13}=m_{12}\times m_{23}$ is contained implicitly in the method followed in case (II.).

References.

(1) Ernst Mach :
(i.) ' The Science of Mechanics,' ed. 4 (1919), chapter ii.; and Supplement to the Third English Edition, 1915.
(ii.) ' Conservation of Energy ' (1911). (Chicago and London : The Open Court Publishing Co.)
The latter book contains a reprint of Mach's article (1868) on the definition of mass, and information about other writings on this topic.
(2) Karl Pearson, ' The Grammar of Science,' ed. 2, 1900, chapter viii.
(3) L. N. G. Filon, " Some Points on the Teaching of Rational Mechanics," ' The Mathematical Gazette,' xiii. pp. 146–153 (July, 1926).

c/o Downing College,
Cambridge.

OBITUARY.

ERNEST LORD RUTHERFORD OF NELSON.

By Sir Oliver Lodge.

In the closing years of last century a young student, the son of a New Zealand farmer, was sent over to this country with a scholarship derived from the funds of the 1851 Exhibition, to try his fortune at Cambridge; a place which was bubbling with excitement at the discovery of the electrical constitution of matter, with its unit the electron. He came to work

under the distinguished Professor of Physics, the discoverer of the electron, Sir J. J. Thomson, having already begun to specialize in the subject of physics. This young man Rutherford was well received at Cambridge with immediate recognition of his ability, and was destined to have an unexampled career, being first made Macdonald Professor of Physics at Montreal, then Langworthy Professor at Manchester, and finally was appointed to succeed his master as Cavendish Professor of Physics in the University of Cambridge. He also became Professor of Natural Philosophy at the Royal Institution, in time President of the Royal Society, before long was made a peer, and when he died was buried in Westminster Abbey.

Rutherford gathered round him in the Cavendish Laboratory at Cambridge a host of distinguished workers, who carried on the work there initiated by Sir J. J. Thomson, and continued under the enthusiastic guidance of the new Professor, so that a series of discoveries emanated from the laboratory; and Cambridge became the centre to which the whole of Europe looked for the discoveries of the new physics. Many of these were initially published in 'The Philosophical Magazine' through the early years of this century, and often bore the name Rutherford, usually in association with other collaborators. A great number of practical applications resulted from the new view of matter and the extraordinary mobility and consequent docility of the electron—the valves for telephonic speech, the photoelectric cell leading to television, and the other inventions with which this present generation has been astonished.

Rutherford's great treatise on 'Radioactivity,' of which the first edition was published in 1904, was followed by a second and much enlarged one within two years. His researches began, in conjunction with Professor Soddy, with the disintegration of matter and the emission of alpha, beta, and gamma rays, with a demonstration that alpha rays were atoms of helium ejected at the enormous speed of ten thousand miles in a second; this was followed by the observation that the other initial product from radium drifted about and clung on to surfaces like a heavy gas of remarkable radioactive power. A view of atomic disintegration, with some idea of the production of other substances, I gave in a review of his book 'Radioactivity' in 'The Electrician' for 27 May, 1904, which can still be referred to as a summary of what was then known.

But recently it is not so much the splitting up of an atom, which is now ancient history, that attracts attention, but the use of the projectiles from it to bombard other atoms and effect changes which can reasonably be regarded as a fulfilment of the dream of the alchemists, viz., the transmutation of one species of matter into another. Rutherford began this alchemical research in 1919 at Manchester, when he bombarded

the nitrogen atom and knocked hydrogen out of it (Phil. Mag., June 1919). Subsequently, with the aid of protons as projectiles, he not only knocked elements down the series but built them up; so that fluorine and an isotope of oxygen was got from nitrogen, while aluminium was converted into radioactive phosphorus and ultimately into silicon.

The nuclear theory of the atom, in the hands of Rutherford and others, has had a great number of chemical applications: and they have introduced refinements into the ordinary equations of chemistry which have almost revolutionized that science, and must be perturbing to old-fashioned chemists. An account of all these advances was given by Rutherford himself in a Henry Sidgwick memorial lecture at Newnham College in November 1936, and is published this year by the University Press as a small book with the title 'The Newer Alchemy.' The publication of this book renders unnecessary any further reference to atomic transmutation, which is here recorded with full appreciation of the diverse workers who have followed his lead.

The nuclear theory of the atom with the inverse square law, a hypothesis abundantly justified by direct experiment (Phil. Mag., May 1911), was treated in an astronomical manner with the help of Professor Planck's quantum by Professor Bohr, then a student at Manchester, and it was found able to explain quantitatively every detail of the bright-line spectra of hydrogen in the most precise manner. Indeed, reinforced by mathematical treatment by continental theorists, the whole complicated subject of spectrum analysis has been revolutionized and made quantitatively definite, until it has become a subject allied to astronomy for the precision of its complete agreement with observation.

Rutherford's friendly breezy manner, characteristic of a colonial, and his quick comprehension of recondite hypotheses, made him an ideal leader in laboratory research and gave abundant justification for the affectionate esteem in which he was held. And so it happens that from the Cavendish Laboratory has spread a brilliant succession of teachers and workers who all own allegiance to him, so that in the twentieth century a new physics has begun, and has almost excluded the memory of the old physics; moreover, it has carried with it a revolution in chemistry, so that, it may be, future generations will speak of Rutherford as the father of the new atomic chemistry and physics.

The Editors regret that the obituary notice of the late Dr. J. R. Airey, M.A., has not been received in time for publication this month.

FIG. 6.

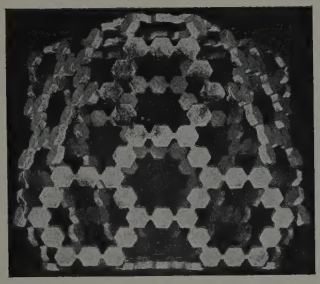

a

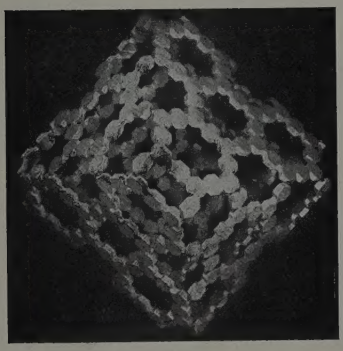

b

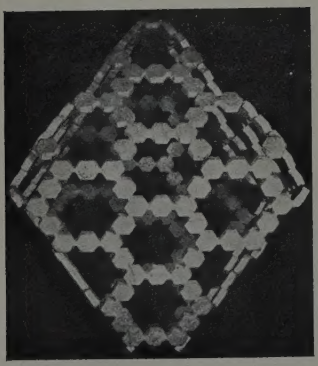

c

The C_2 molecule comprising 288 residues.

Crystal growth in wires of nickel and tungsten.